DEPARTMENT OF THE AIR FORCE

AIR UNIVERSITY

AIR FORCE INSTITUTE OF TECHNOLOGY

Wright-Patterson Air Force Base, Ohio

AFIT/GE/ENG/88D-31

ANALYSIS AND SIMULATION
OF A
PSEUDONOISE SYNCHRONIZATION SYSTEM

THESIS

Fernando A. Morgan, B.S.E.E.
Captain, USAF

AFIT/GE/ENG/88D-31

Approved for public release; distribution unlimited

AFIT/GE/ENG/88D-31

ANALYSIS AND SIMULATION
OF A
PSEUDONOISE SYNCHRONIZATION SYSTEM

THESIS

Presented to the Faculty of the School of Engineering
of the Air Force Institute of Technology
Air University
In Partial Fulfillment of the
Requirements for the Degree of
Master of Science in Electrical Engineering

Fernando A. Morgan, B.S.E.E.
Captain, USAF

December 1988

Acknowledgements

I would like to thank my advisor and committee chairman, Major Glenn Prescott, for his professional guidance and instruction during the preparation of this thesis and throughout my time at AFIT. I am also thankful for the support and interest I received from my committee members, Major David Meer, Major David Norman, and Mr. James Stephens. I would like to extend a special note of appreciation to Mr. Dan Zambon-he was always there to guide me and keep me out of trouble with the computer facilities.

But above all else, I am grateful to my wife, [redacted] for her unselfish support and love that motivates me through every new experience. The joys and frustrations we have shared will long be remembered.

Fernando A. Morgan

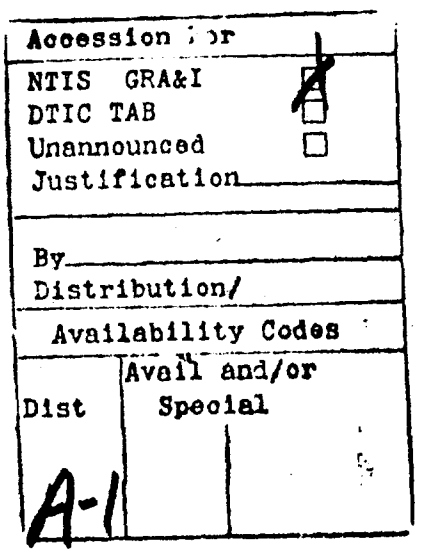

Table of Contents

List of Figures

List of Tables

Abstract

The purpose of this study was to investigate the performance characteristics of a synchronization system that uses an auxiliary matched filter channel to speed acquisition time. The study entailed a quantitative analysis and simulation of the matched filter channel. Following a presentation on computer simulation of communication systems, the investigation took the following approach: (1) Perform a quantitative analysis to characterize mean acquisition time under varying conditions of matched filter length, noise levels, and number of users in the system. (2) Build and validate a simulation model of the synchronization system using the Block Oriented Systems Simulator (BOSS). (3) Test the matched filter channel against the analytic expectations for false alarm performance via the simulation model.

The quantitative results indicate that the matched filter channel improves acquisition time. For signal-to-noise ratios above 0dB and a particular matched filter length, the mean acquisition time was directly a function of the number of users in the system. For a matched filter of length of 128 stages and 64 users in the system, the matched filter channel provides a gain in acquisition time of 156 over the active correlator device operating alone. As signal-to-noise ratios decreased below 0dB, the variation in

mean acquisition time caused by the number of users declines and the additive white Gaussian noise becomes the dominant influence. Mean acquisition time asymptotically approaches a doubling in time for each 1.5 dB decrease in the signal-to-noise ratio.

The simulation results confirmed the analytic expectations for false alarm performance. The simulated probability of false alarm (P_{fa}) was restricted to 10^{-3}. All single-pulse detection requirements at the specified P_{fa} were favorably confirmed. Multiple-pulse detection requirements were favorably validated with shorter simulations. Exceptions to the multiple-pulse detection results were noted due to the high correlation noise produced by the selected synchronization codes.

The BOSS provided a highly flexible simulation environment. The system model included flexibilities to adjust matched filter lengths, noise levels, and threshold levels. Confirmation of the analytic expectations provides a proven simulation model to accurately simulate dynamic applications of system.

ANALYSIS AND SIMULATION OF A PSEUDONOISE SYNCHRONIZATION SYSTEM

I. Introduction

Computer simulation provides a flexible and accurate method for performance evaluation and trade-off analysis in the design of digital communication systems. Recent advances in simulation techniques and advances in computer software and hardware technologies have merged to provide intelligent, user friendly and flexible simulation environments. Recently, there has been a growing interest in the use of simulation-based techniques for the analysis and design of communication systems (1:36.1.1).

In order to design and analyze complex spread spectrum systems effectively and continue to meet the stringent performance requirements, design techniques have evolved that combine traditional analysis with simulation. In fact, simulation has almost become the standard tool for communication system analysis and design (2:1).

Problem Statement

In spread spectrum communication systems, a basic task to be performed at the receiving end is the synchronization of the pseudonoise (PN) signal generated locally at the receiver with the PN signal contained in the receiver input

signal. The problem addressed in this thesis is to analyze and simulate a synchronization scheme that uses an auxiliary matched filter channel to speed synchronization and evaluate the initial acquisition characteristics. Such a synchronization system has been described by Smirnov (3).

Scope

The Block-Oriented Systems Simulator (BOSS) will be used to simulate the synchronization system. The simulation models will include flexibilities to vary the matched filter length, adjust threshold detection levels, and specify the number and noise levels of transmitted signals. Once the system model is validated, further simulations will exercise the system parameters to fully characterize acquisition performance and confirm analytic expectations. The key performance factor is the mean acquisition time as impacted by the matched filter length and the number of users in a code division multiple-access (CDMA) environment.

Materials

- BOSS User's Manual (4)
- BOSS Software Version: ST*AR 1.2
- DEC VAXstation II

Approach

The overall design philosophy is to implement the synchronization system incrementally in the simulation environment. Each system module is implemented, tested

against analytic expectations, and stored in the simulation module library. The complete synchronization system is then constructed and analyzed with a single transmitted signal. Subsequent simulation and analysis is then performed for a multiple-access environment.

Thesis Organization

In the next chapter, computer simulation is discussed. In Chapter III, the system under simulation is presented, the synchronization method is introduced, and the necessary assumptions are justified. An analysis concerning the synchronization time and the impact of the matched filter length and the number of users is given. Chapter IV is devoted to the modeling of the necessary system modules using the *BOSS*. The chapter is concluded with the integration of the modules for the complete system representation. In Chapter V, the objective and method of simulation is detailed and the simulation results are presented. Finally, in Chapter VI, conclusions on the analysis and the effectiveness of the simulation are given with recommendations for further research.

II. Communication System Simulation

Computer simulation has almost become the standard tool for communication system analysis and design (2:1). Simulation offers flexibility and insight into system performance. Although computer simulation has distinct advantages, the approach tends to be distrusted by the proponents of analytical modeling (5:89). Simulation yields answers with statistical variations, not hard results. Analytic techniques, however, are not adequate to predict the performance of systems operating in complex environments. The presence of nonlinearities, noise, and other degradations make the performance evaluation a tedious and often impossible task (6:1612). Techniques have emerged that combine simulation and analysis. "The traditional dichotomy between analysis and simulation has now been blurred" (2:1). A clear understanding of simulation techniques and methodology becomes indispensable as stringent performance requirements drive engineers to effectively design and analyze increasingly complex systems.

This chapter is a short primer on computer simulation techniques in regards to communication system simulation. The first section will look at the basic operations in communication system modeling and introduce simulation as a technique to estimate system performance. The next section will extend quantitative performance evaluation via the Monte Carlo method as the primary technique of interest. The

critical features of a communication system simulation package will be examined and finally, the methodology of the Block Oriented System Simulator (BOSS) will be explored.

Simulation Approach

There are four steps fundamental to the simulation of an elementary communication channel: 1) create and store a sequence of samples representing the modulated signal; 2) filter the sequence of samples; 3) modify the filtered signal according to channel nonlinearities; and 4) demodulate the data record to observe the effect of the channel (5:89). These four steps will be examined in terms of the elementary channel shown in Figure 1.

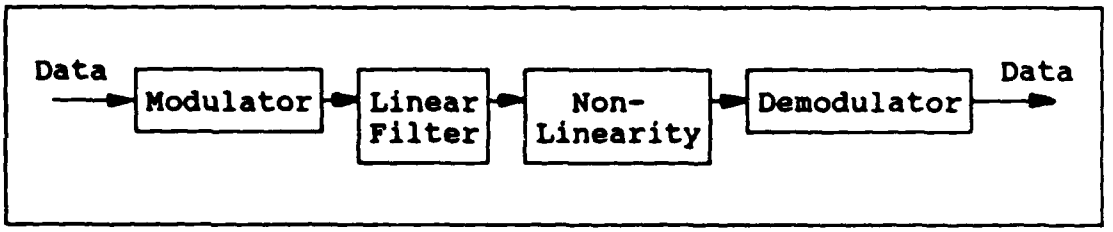

Figure 1. Elementary Communication Channel (5:90)

Signal Generation. The first step is to create a set of sampled signals. Modulated signals are generated as sampled versions of the real signal. For a sampling frequency $f_s = 1/dt$ the complex envelope representation of the k-th sample is

$$s_i(k \cdot dt) = A(k \cdot dt)\sqrt{P} \cdot \exp\left[j2\pi(f_o/f_s)k + j\theta(k \cdot dt)\right] \qquad (1)$$

where $A(k \cdot dt)$ represents the amplitude modulation, and $\Theta(k \cdot dt)$ represents the phase modulation of the signal, with power P and (f_o/f_s) as the relative carrier frequency (5:90).

The prime consideration in selecting f_s is the total bandwidth about the channel carrier frequency. In spread spectrum systems, this bandwidth is determined by the frequency of the spreading waveform. The sampling rate is expressed as a multiple N of the spreading code chip rate:

$$f_s = N/T_c \tag{2}$$

or

$$dt = T_c/N \tag{3}$$

The number of samples per chip period is usually selected as an even integer between 8 and 16. For values less than 8 samples per chip period, accuracy is sacrificed at the folding frequencies due to aliasing (5:90).

Filtering of Signals. Filtering tends to be the most CPU-intensive activity in channel simulations. There are two popular techniques to simulate filtering: 1) multiply the discrete Fourier transform (DFT) of the signal by the filter function and return to the time domain by implementing the inverse DFT; and 2) operate on the sampled signal using a digital filtering algorithm (5:91).

In the first technique, the signal data record is segmented into conveniently sized blocks (512, 1024, etc.) of data. A DFT of these smaller blocks of data is then synthesized and multiplied by the filter function. Once this

operation is performed on the total data record, an inverse DFT is performed to yield the filtered time domain waveform.

In many applications, the filters are classical types such a Butterworth, Chebyshev, or Bessel. To simulate these filters and those in which pole-zero descriptions are available, it is convenient to synthesize a recursive digital filter to implement a time domain filtering algorithm.

Channel Nonlinearities. When the channel model contains nonlinearities, analytical approaches become complex, and simulation is often the only practical approach to performance evaluation (5:92). The general approach to simulating channel nonlinearities involves the use of measured data of representative nonlinear devices. The measured data is used to generate a function for mapping input to output values. For abrupt nonlinearities, table lookup procedures are used to define nonlinear characteristics.

Receiver Structures. The first element of the receiver structure is the receiver front-end filter. At this point, the method of adding thermal noise at the input to this filter distinguishes two approaches to channel simulation. In the hybrid simulation/analysis approach, the simulation is used only to obtain the statistics of all other sources and interference. The effect of thermal noise is then added analytically (5:93).

In the simulation approach of interest, thermal noise is added at appropriate points in the channel. This approach,

direct channel simulation, is the only choice when the demodulation and detection process in nonlinear (5:93). The demodulation and detection process is followed by quantitative evaluation where bit error rate (BER) is the most often used performance characteristic for digital communication systems (7:153).

The demodulation and detection process output is compared to a decision threshold. The threshold comparison depends on the conditional probability density functions $p(z|s_1)$ and $p(z|s_0)$. Figure 2 shows representative densities that in general, need not be identical (7:154). An error will occur when either: 1) a "zero" is sent and the channel noise results in z(T) being greater than the threshold β_o or 2) a "one" is sent and the channel noise results in z(T) being less than β_o. The probabilities of these errors are given by

$$\text{Prob}(\text{error}|s_1) = p_1 = \int_{-\infty}^{\beta o} p(z|s_1)dz \tag{4}$$

and

$$\text{Prob}(\text{error}|s_0) = p_0 = \int_{\beta o}^{\infty} p(z|s_0)dz \tag{5}$$

The total probability of error is $P(s_1)\cdot p_1 + P(s_0)\cdot p_0$ where $P(s_1)$ and $P(s_0)$ are the a priori probabilities of symbols "one" and "zero" respectively.

Techniques for estimating the BER in the direct simulation approach include: 1) Monte Carlo simulation,

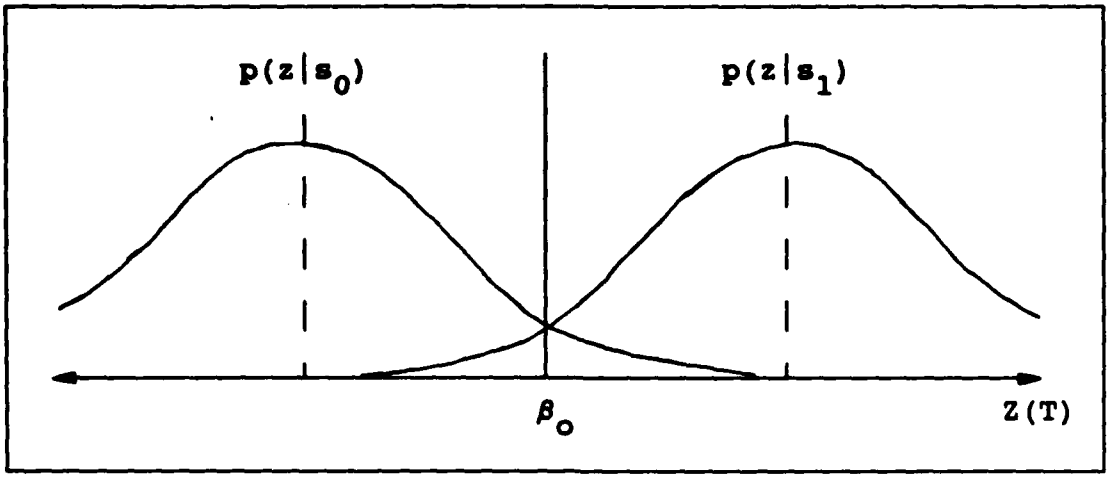

Figure 2. Conditional Probability Density Functions

2) importance sampling (modified Monte Carlo simulation), 3) extreme value theory, and 4) tail extrapolation. The four techniques differ in the way the probability density functions are handled. The Monte Carlo method is the most general and uses an empirical determination of the distribution functions evaluated at a single point. Importance sampling biases the distribution functions to cause errors to occur more often. The BER is then found by unbiasing the results. This method can substantially reduce the simulation time. The extreme value theory and tail extrapolation operate under the principle that the distribution of the extreme-value (large in magnitude) samples is the only information necessary to calculate the BER (7:154-155). Of these techniques, only the Monte Carlo method will be discussed. The BOSS in essence uses the Monte Carlo method.

Monte Carlo Simulation

Basically, the Monte Carlo method is an error counting technique. In other words, the BER can be estimated by observing the number of error occurrences. Suppose that a "zero" is sent. Then the conditional probability of error, Eq (5), can be expressed as (7:156):

$$p_0 = \int_{-\infty}^{\infty} h_0(z)p(z|s_0)dz \tag{6}$$

where $h_0(z)$ is basically an error detector:

$$h_0(z) = \begin{cases} 1, & z \geq \beta_o \\ 0, & z < \beta_o \end{cases} \tag{7}$$

Recognizing that Eq (6) expresses the expected value of $h_0(z)$, the conditional probability of error can be estimated with a sample mean of $h_0(z)$. In other words, $p_0 = E[h_0(z)]$ can be estimated by counting the number of error occurences over N observations as given by:

$$\hat{p}_0 = \frac{1}{N} \cdot \sum_{i=1}^{N} h_0(z_i) \tag{8}$$

The above equation defines the Monte Carlo method. An estimate of the BER is given by counting the error occurences over a set of observations. Simplifying Eq (8) for "n" bit errors out of "N" bits processed by the system gives an unbiased Monte Carlo estimate of the BER:

$$\hat{p} = \frac{n}{N} \tag{9}$$

In the limit, as N approaches infinity, "$\hat{p}$" will converge to the true value "p" (7:156). Obviously, it would take an infinite amount of computer time for the estimate to converge to the true value. However, for a finite number of observations, the reliability of the estimate can be quantified in terms of confidence levels. The confidence level is often specified as

$$\text{Prob}(h_2 \leq p \leq h_1) = (1-\alpha) \tag{10}$$

where $(1-\alpha)$ is the probability that the true value is bracketed by h_1 and h_2.

The two-sided confidence interval is plotted in Figure 3 for confidence levels of 90 percent, 95 percent, and 99 percent. The "rule of thumb" is that the number of observations should be on the order of $10/P_e$ where P_e represents the probability of error. This coincides with a vertical slice at $N = 10^{k+1}$ on Figure 3. For a mildly distorted communication system, this level of uncertainty corresponds to ± 0.5 dB on the signal-to-noise ratio (E_b/N_o) scale of a typical BER curve. This level of uncertainty is generally considered reasonable (7:157).

When simulating a system, a number of BER estimates are made at discretely spaced values of E_b/N_o. A best fit curve is taken to represent the characteristic behavior of the

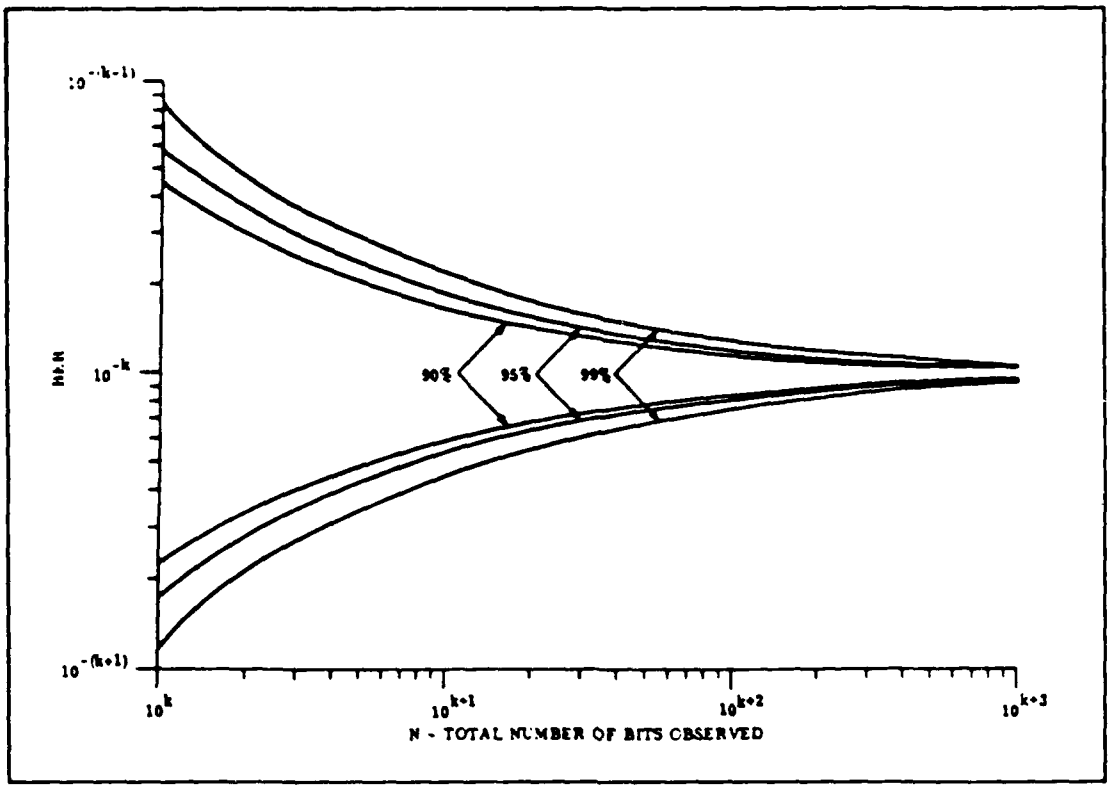

Figure 3. BER Confidence Bands (7:158)

system. This curve will take into account the relative reliability of the individual points and provide a somewhat better confidence than predicted from the single point confidence intervals of Figure 3.

Software Structure

A number of software packages have been developed for simulation-based analysis and design of communication systems. Most of these software packages were developed during the seventies and their design and implementations are based on older technologies. Advances in computer hardware technology, software technology and simulation techniques offer a totally new computing environment (4:36.1.1).

The main goal in developing a simulation software package is to provide an integrated computing environment that will allow a communication system engineer to design models, configure and execute simulations, review the results and perform design iterations. While there is no industry standard, a software simulation package should include a modular structure and a user-friendly interface (8:2).

A modular structure provides maximum flexibility in the design and analysis of communication systems. Most of the software packages now in use are made up of four major components: a system configurator, a model library, a simulation exerciser, and a post-processor (9:324).

The system configurator is used to select a set of pre-programmed models of functional blocks from the model library. These functional blocks are then connected in the desired topology as specified by the block diagram of the system being designed. Parameters of various functional blocks are specified either when the system is being configured or during the execution of the simulation. The simulation exercisor supervises the execution of the simulation (9:324).

Time histories of events or waveforms at various points in the system are generated and stored during the simulation. These time histories or waveforms are examined by the post-processor at the conclusion of the simulation run and performance measures are computed from the time histories. The post-processor also provides graphic displays of

waveforms, spectra, and histograms of signals at various points in the system. At the end of a simulation, the design engineer uses the post-processor output to verify if the performance requirements and design constraints are met. If design objectives are not met, several iterations are made until a suitable design is found (9:324).

Several software packages are presently available for simulating communication systems. The state-of-the-art features and capabilities of the Block-Oriented Systems Simulator (BOSS) are ideally suited for simulating spread spectrum systems.

BOSS Methodology

The Block-Oriented Systems Simulator (BOSS) is an interactive environment for time-domain (waveform level) analysis and design of communication systems. The user interface controls all design capabilities through the use of interactive graphics. Capabilities are provided to design models using block diagrams, configure and execute a simulation, review the results of the simulation, and perform design iterations (1:36.1.1,36.1.6).

The BOSS provides for simulation of any system which can be represented in block diagram form. Complex communication systems are synthesized in a hierarchical fashion using simple building blocks at the lowest levels, and increasingly complex modules and subsystems at subsequent higher levels.

Each block of the simulation model performs a signal processing operation (4:11,13).

During the initial model construction phase, BOSS requires the designer to provide complete descriptions of signals and parameters such as data types, ranges, and default values. Error checking is automatically performed by BOSS on all input data. The use of menus for entering data, type and range checking, and other consistency checks reduce input errors and minimize confusion (4:47).

Displays of simulation results are provided by the Post Processor. Multiple windows for display as well as multiple displays within a window are standard features. Automatic scaling of plots, labeling, pan and zoom are all built-in features (4:13).

BOSS allows flexible interactive simulation of a variety of design problems. This flexibility is fundamental for performance evaluation and trade-off analysis in the simulation and design of digital communication systems.

III. Problem Analysis

The purpose of this chapter is to present in detail the system to be simulated. Prefaced with a background on the synchronization of spread spectrum systems, an outline of the general concepts of signal flow and operation of the circuit of interest is presented. An analytic evaluation of the system is then performed to present the performance characteristics and to facilitate the proper structure and evaluation of the simulation effort.

Synchronization of Spread Spectrum Systems

For military radio communications, communication security consists of preventing signals from being detected or jammed by an adversary. Spread spectrum signals meet both of these goals and also offer the possibility of multiple-access and range measurement. To qualify as a spread spectrum system, a communications link must meet two criteria. First, the link must transmit signals using a much wider bandwidth than is required to send the information of interest. Second, an independent function other than the information being sent is used to determine the resulting modulated bandwidth. The information independent technique used to spread the bandwidth of a transmitted signal is also used to despread the received signal (10:855).

The two primary techniques used to accomplish the signal bandwidth spreading and subsequent despreading are direct

sequence modulation and frequency hopping. Direct sequence modulation causes rapid phase transitions in the carrier frequency to spread the overall signal. The individual transitions are randomly controlled by a pseudorandomly generated sequence. When frequency hopping is employed, a pseudorandom or pseudonoise (PN) code is also used, but in this case the code is used to shift the entire carrier frequency and not just its phase. In both cases, the objective is to randomize the modulated waveform so the transmitted bandwidth depends almost entirely on the pseudorandom code used. If properly coded, the transmitted signal is very difficult to acquire and despread without knowledge of the code.

In order to despread the received signal, the spread spectrum receiver generates a replica of the PN code and then synchronizes this local PN sequence to the one used to spread the incoming signal. Multiplication of the incoming signal by the synchronized local PN sequence produces the desired despreading process. The problem of synchronization is that of aligning the receiver's locally generated waveform with the spreading waveform superimposed on the incoming signal (11:3).

Classically, the synchronization process is accomplished in two phases. Initially, the PN code acquisition phase brings the two codes into coarse alignment. Once the incoming PN code has been acquired, the PN tracking phase maintains waveform alignment with a closed loop operation.

There are two widely used techniques for detection of known input signals. The first is based on active correlation where for acquisition, the local PN sequence generator is clocked in such a way that its sequence is shifted continuously or in discrete steps relative to the sequence contained in the received signal. The instants of synchronism are detected by the acquisition circuit which in turn activates the control loop provided for tracking. The second technique is based on the principle of passive correlation. The acquisition circuit has the task of detecting the instant at which the received PN sequence attains a predetermined state. In the case of passive correlation, the basic component of the acquisition circuit is typically a matched filter. Matched to a predetermined section of the received signal, the matched filter outputs periodic amplitude peaks indicating the occurrence of a subsequence of the desired code. At this moment the local PN sequence generator is started from the corresponding initial state. At the same instant the tracking loop is activated (12:5.9.2).

Matched filters in this application typically employ surface acoustic wave (SAW) technology. SAW devices are ideal choices for use in spread spectrum communication systems which must process high data rate signals. The SAW-tapped delay line matched filter is a passive correlation technique which maximizes the filter output peak signal-to-mean noise ratio. However, the length of SAW matched filters

is limited by propagation losses and the filter cannot be implemented to match the length of typical PN code sequences (13:230).

The system of interest presents a combined matched filter/serial search rapid acquisition strategy in a direct sequence, multiple-access environment. A commonly used method for PN code acquisition in direct sequence spread spectrum systems is the serial search of the relative positions of the received signal and the locally generated reference waveform in discrete steps of a fraction of a code chip. If no a priori timing information is available to the receiver, uniform search over the long pseudonoise code periods lead to acquisition times that are prohibitive. Prior information about the approximate position of the received code leads to a decrease in the mean acquisition time by several orders of magnitude over a wide range of the receiver input signal-to-noise ratios (14:157). In this system, the initial uncertainty is reduced with matched filter detection of shorter code segments of the received PN sequence. Attention is focused on initial acquisition. In other words, the initial establishment of timing synchronization from total timing uncertainty.

Signal Flow and Operation

The most straightforward acquisition strategy for long pseudonoise sequences uses active correlation and a simple serial search algorithm to determine the correct code epoch.

This method is the standard for comparison of a system that augments this technique with an auxiliary matched filter channel to speed code acquisition. A block diagram of the receiver synchronization section is shown in Figure 4. The major components of the system are the pseudonoise sequence generator, the matched filter channel, and a quadrature correlator as the active correlation device.

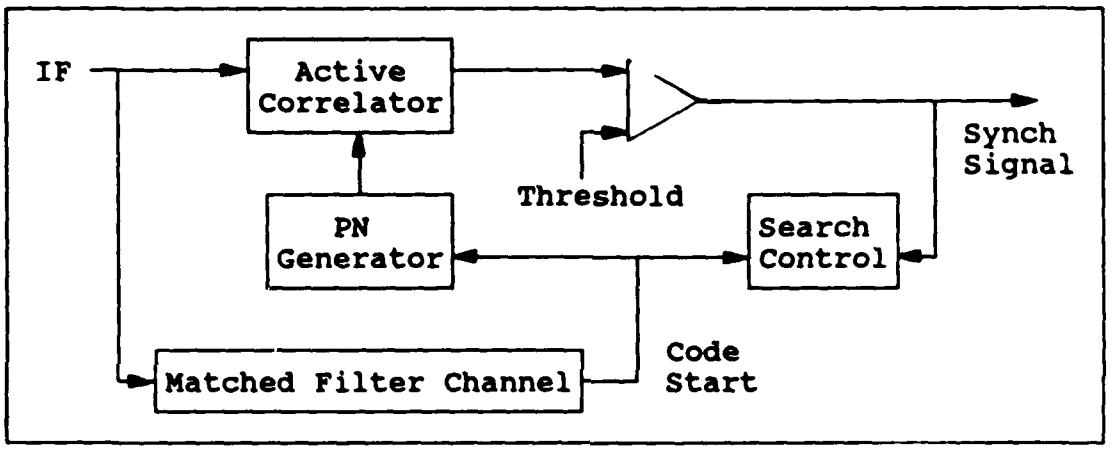

Figure 4. Synchronization System

The matched filter channel shown in Figure 5 consists of the matched filter, envelope detector, accumulator device, and a threshold detector. The matched filter can be implemented with the aid of tapped delay lines. The most suitable IF devices for use in tapped delay line correlators tend to be the surface acoustic wave type as discussed earlier. Figure 6 shows a schematic of a tapped delay line for use as a matched filter in spread spectrum receivers-a usable filter would contain many delay elements.

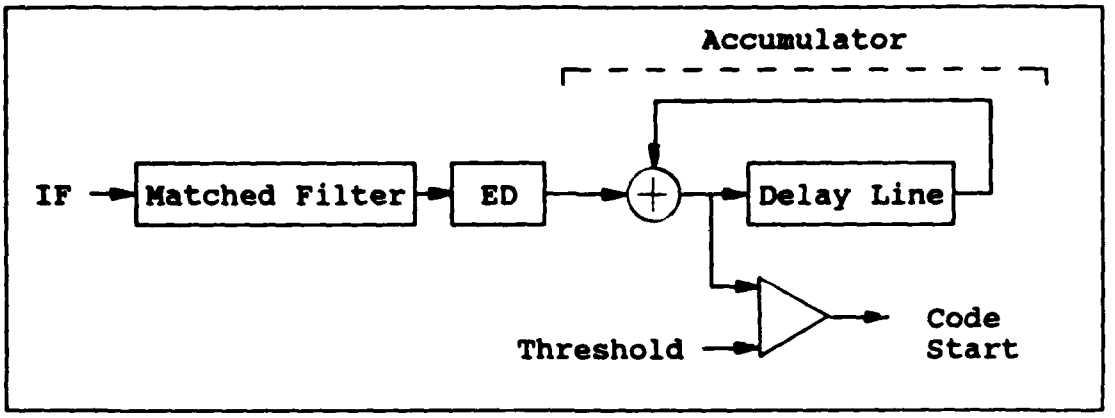

Figure 5. Matched Filter Channel

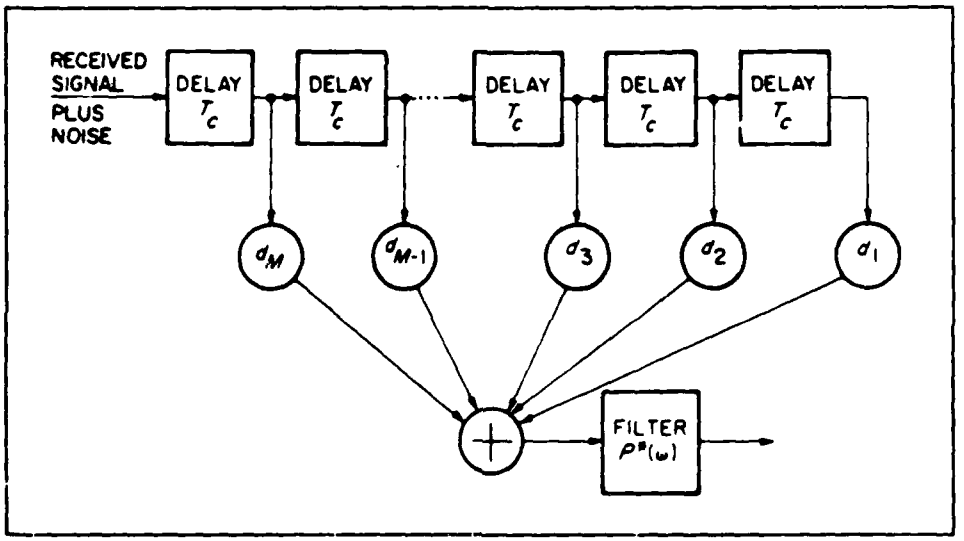

Figure 6. Tapped Delay Line Matched Filter (11:70)

If the interference and the narrow-band data modulation is initially ignored, the input QPSK signal is given as:

$$r(t) = \sqrt{2P} \cdot PN_I(t) \cdot \cos(w_o t) + \sqrt{2P} \cdot PN_Q(t) \cdot \sin(w_o t) \qquad (11)$$

where r(t) has a carrier angular frequency of w_o and an amplitude $\sqrt{2P}$. The carrier phase is reversed at the rate of the binary PN sequence where $PN(t) \in \{-1,+1\}$ with clock frequency of $f_c = 1/T_c$.

The sequence PN(t) is a maximal length sequence whose autocorrelation function $R_{PN}(\tau)$ at $|\tau| \geq T_c$ is very low. The chip period T_c is selected in such a way that it is an integer multiple of the carrier period. The delay line has M taps spaced at time intervals of T_c. The delay intervals must accurately represent the clock period of the code sequence to be detected (12:5.9.2).

The taps of the delay line matched filter are programmed such that the matched filter will recognize a particular subsequence of length M of the incoming PN sequence. The tap values will pass the signal unaltered or with a phase reversal in accordance with the desired section of sequence PN(t). With a length of M chips, k_H of the M output signals of the delay line are fed directly to the adding network and the remainder $k_L = M - k_H$ after a phase reversal of 180°. Most of the time, assuming the PN code sequence signal levels are equally probable, the amplitude of the summation is on the order of $\sqrt{2P}$. When the phase reversals of the input signal match those reversals programmed into the delay line, the output summation is on the order of $M \cdot \sqrt{2P}$ since M signals having the same phase are added (12:5.9.2).

The rectified and filtered periodic peaks at the output of the envelope detector mark a certain state of the received PN sequence. This signal is therefore suitable as a synchronization pulse for setting and starting of the local PN generator. There is, however, more to consider.

The subsequence of PN(t) programmed into the tapped delay line must be chosen such that the main correlation peak exceeds the partial autocorrelation characteristics. In practical systems, the input signal to the matched filter contains a narrow-band data modulation. This impairs the operation of the matched filter. The impairment can be made negligibly small as long as the bandwidth of the data modulation is relatively narrow. The signal-to-noise ratio (SNR) of an interfering signal at the output of the delay line is higher by about a factor M as compared to its input SNR. The setting and starting accuracy is impaired by this interference. The interference can offset synchronization epochs and prevent detection of correct synchronization pulses. The rate of false alarms and loss of correct synchronization pulses become greater as the input SNR of the target transmitter becomes smaller and as the input deviates from the desired code due to data modulation (12:5.9.3).

In order to ensure acceptable values in the probability of detection (P_d) and the probability of false alarm (P_{fa}), the accumulator circuit processes a designated number of main correlation peaks prior to threshold detection and initiation of the PN generator. The number of correlation peaks processed is based on the peak SNR at the output of the matched filter. The threshold detect circuit is set to initiate the PN generator such that the active correlator will synchronize in the first dwell period for given probabilities of false alarm and detection.

Analytical Evaluation

The analysis of the quadrature correlator and the matched filter channel serves two purposes: 1) the output signals must be characterized in order to verify the simulation models, and 2) the mean acquisition time performance must be assessed to gauge the accuracy of the simulation results.

The first objective is to establish the performance of the quadrature correlator. To assess the improvement in synchronization time provided by the auxiliary matched filter channel, the performance of the quadrature correlator as a stand-alone synchronization circuit is analyzed. This will serve as the standard to judge improvement in acquisition time via the auxiliary matched filter channel. The performance due to inclusion of the matched filter channel will then be determined.

Quadrature Correlator. The quadrature correlator shown in Figure 7 is a coherent single dwell acquisition system. It is assumed that the receiver is capable of determining good estimates of the carrier phase produced by the propagation delay and Doppler. The received signal plus noise is demodulated by in-phase and quadrature carrier reference signals whose frequency is equal to that of the transmitter carrier frequency but with an arbitrary phase. The demodulated and despread signals are passed through integrators with identical dwell times. It is assumed that the rectifiers are square-law devices to remove the unknown

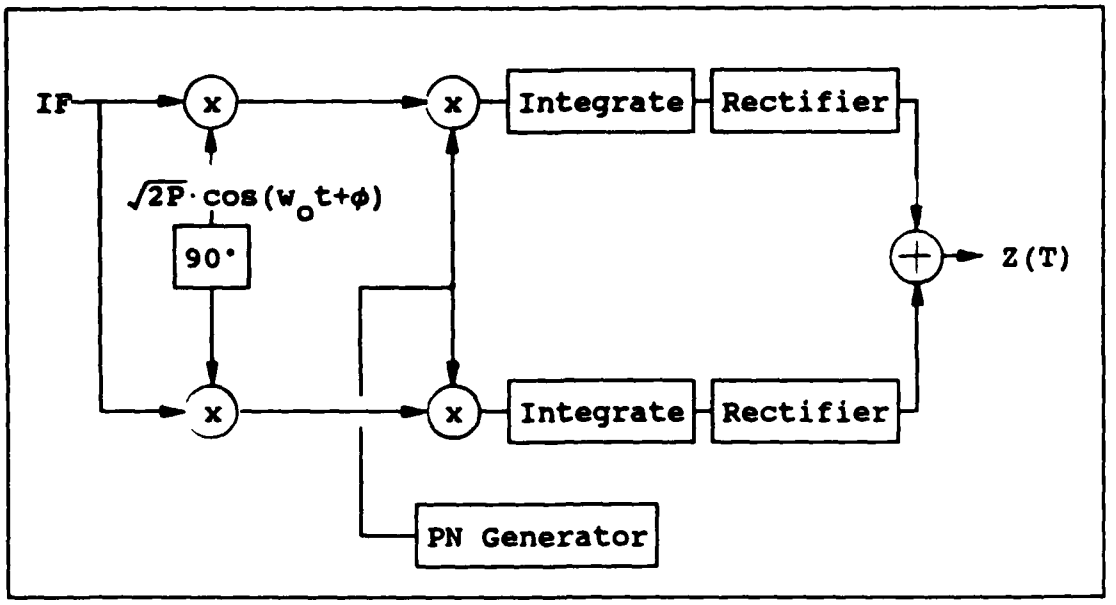

Figure 7. Quadrature Correlator

data modulation and unknown carrier phase (11:67). It is also assumed that the output of the correlator is fed to a simple threshold device controlling an implementation of a serial search strategy. The evaluation will proceed with a characterization of the quadrature correlator output signal.

Correlator Output Signal. The received modulated signal, in the absence of noise, is of the form

$$r(t) = \sqrt{2P}\cdot d_I(t)PN_I(t)\cos w_o t + \sqrt{2P}\cdot d_Q(t)PN_Q(t)\sin w_o t \quad (12)$$

where $d_I(t)$ and $d_Q(t)$ are the in-phase (I) and quadrature (Q) data streams, and $PN_I(t)$ and $PN_Q(t)$ are the pseudonoise sequences with the I signals on a carrier shifted 90° from the Q carrier (15:347).

A conventional QPSK signal is assummed. The PN code epoch times are common to both the I and Q signals and

without indication otherwise in the Smirnov description, the I and Q pseudonoise sequences are assumed identical. The receiver's replica signals are:

$$s_I(t) = \sqrt{2P}\cdot PN_I(t+\tau)\cos(w_o t+\phi) \tag{13}$$

$$s_Q(t) = \sqrt{2P}\cdot PN_Q(t+\tau)\sin(w_o t+\phi) \tag{14}$$

where τ is the time offset of the PN replica sequence and ϕ is the carrier reference offset. The received signals are modulated by the replica signals and input to the integrate and dump circuits. The input to the in-phase integrator is

$$\begin{aligned} x_I(t) &= r(t)\cdot s_I(t) \\ &= 2P\Big[d_I(t)PN_I(t)PN_I(t+\tau)\cos w_o t\cdot\cos(w_o t+\phi) \\ &\quad + d_Q(t)PN_Q(t)PN_I(t+\tau)\sin w_o t\cdot\cos(w_o t+\phi)\Big] \end{aligned} \tag{15}$$

Given the period of integration is over a complete PN sequence and assuming the data rate is low enough relative to the chip rate that $d_I(t)$ and $d_Q(t)$ are constants over this period, the output of the in-phase integrator channel is

$$\begin{aligned} \int_0^{nT_c} x_I(t)dt &= P\cdot d_I(t)\int_0^{nT_c} PN_I(t)PN_I(t+\tau)\cos\phi[1+\cos 2w_o t]dt \\ &\quad + P\cdot d_Q(t)\int_0^{nT_c} PN_Q(t)PN_I(t+\tau)\sin\phi[1-\cos 2w_o t]dt \end{aligned} \tag{16}$$

Since the period of integration is an integral multiple of the period of the carrier, the integrate and dump circuit

acts as a low pass filter. The result is as follows:

$$\int_0^{nT_c} x_I(t)dt = P \cdot nT_c \cdot R_{PN}(\tau)\left[d_I(t)\cdot\cos\phi + d_Q(t)\cdot\sin\phi\right] \qquad (17)$$

Similiarly, for the quadrature channel:

$$\int_0^{nT_c} x_Q(t)dt = P \cdot nT_c \cdot R_{PN}(\tau)\left[d_I(t)\cdot\sin\phi + d_Q(t)\cdot\cos\phi\right] \qquad (18)$$

Assuming the rectifiers are square-law devices, the data modulation and the unknown carrier phase is effectively removed and the output of the correlator is:

$$Z_c(t) = 2\left[P \cdot nT_c \cdot R_{PN}(\tau)\right]^2 \qquad (19)$$

With the bit energy as unity,

$$Z_c(t) = 2\left[n \cdot R_{PN}(\tau)\right]^2 \qquad (20)$$

When τ equals zero, the reference PN sequence is synchronized with the received PN sequence and $Z_c(t)$ achieves its maximum value; in other words, a main correlation peak occurs at the output of the correlator.

Correlator Acquisition Time Performance. It is assumed that the correlator output signal is applied to a simple threshold device which in turn drives a serial search strategy. If the correlator output is above the threshold level, then the search algorithm enters the code tracking loop mode. The threshold indication is verified in the tracking mode with an extended dwell time. The extended

dwell time is an integral multiple of the dwell time, where the dwell time is the correlator period of integration. If the verification is successful, then the true code phase position has been acquired and the search comes to an end. If not, the search continues and the time penalty for the false alarm is the extended dwell time of the verification process. If the correlator output is below the threshold value, the local PN generator is stepped to its next position and the search proceeds (11:17).

It is typical practice to require the alignment between the received and local PN codes be within one-half of a code chip period before entering the tracking mode. The PN code generator is stepped in one-half chip periods over the uncertainty region. In the absence of a priori information concerning the code phase position, the uncertainty region between the received PN code and the local PN code could be as much as the entire code period (11:18).

Smirnov defines the region of uncertainty as the entire code period. Smirnov presents Eq (21) as the time for entry into synchronization for the quadrature correlator (3:68).

$$T_{sc} = T_c n^2 E \tag{21}$$

where n is the number of chips in a full PN code sequence, T_c is the chip duration, and E is the number of frequency intervals in the region of uncertainty. This result is taken as the average time for acquisition for complete timing uncertainty and the simple case where probability of

detection is unity, probability of false alarm is zero, and the dwell time (as it turns out) is for full period correlation.

This result can be verified using the mean acquisition time of a serial direct sequence search system (11:22). The expression given below assumes the search is performed in half-chip increments (cells) and in the absence of code Doppler and carrier instabilities.

$$T_{acq} = \frac{(2 - P_d)(1 + K \cdot P_{fa})}{2P_d} \cdot q \cdot \tau_d \qquad (22)$$

As stated above, the case given by Smirnov sets the probability of detection (P_d) to unity and the probability of false alarm (P_{fa}) to zero. With the dwell time set for full period correlation, the number of cells to search is $q = 2 \cdot n$ where $n = M$, the total number of chips in a full period. It follows that the integration time for a full period is $\tau_d = n \cdot T_c$ and the result of Eq (21) is repeated:

$$T_{acq} = n^2 T_c \qquad (23)$$

This result is the mean acquisition time for searching the frequency interval in which the code is located (E = 1).

Before proceeding with the analysis of the matched filter channel, the standards for correlator performance must be expressed in terms of receiver operating characteristics. When the matched filter initiates the PN generator, it does so such that for given probabilities of false alarm and

detection, the quadrature correlator will synchronize upon detection of a single pulse in the first dwell period. The ability of the quadrature correlator to successfully indicate synchronization, as specified by the above probabilities, is a function of its output SNR. This data is tabulated for single and multiple pulse detection of signals and will be the standard to determine the required matched filter output SNR (16:205,248-261). If the matched filter initiates the PN generator with the specified output SNR, the correlator will synchronize with the same probabilities.

Figure 8 specifies average output SNR requirements for single pulse detection over a wide range of P_{fa} and P_d. All further analysis will develop with the peak SNR rather than the average SNR. The values provided will be scaled by +3dB.

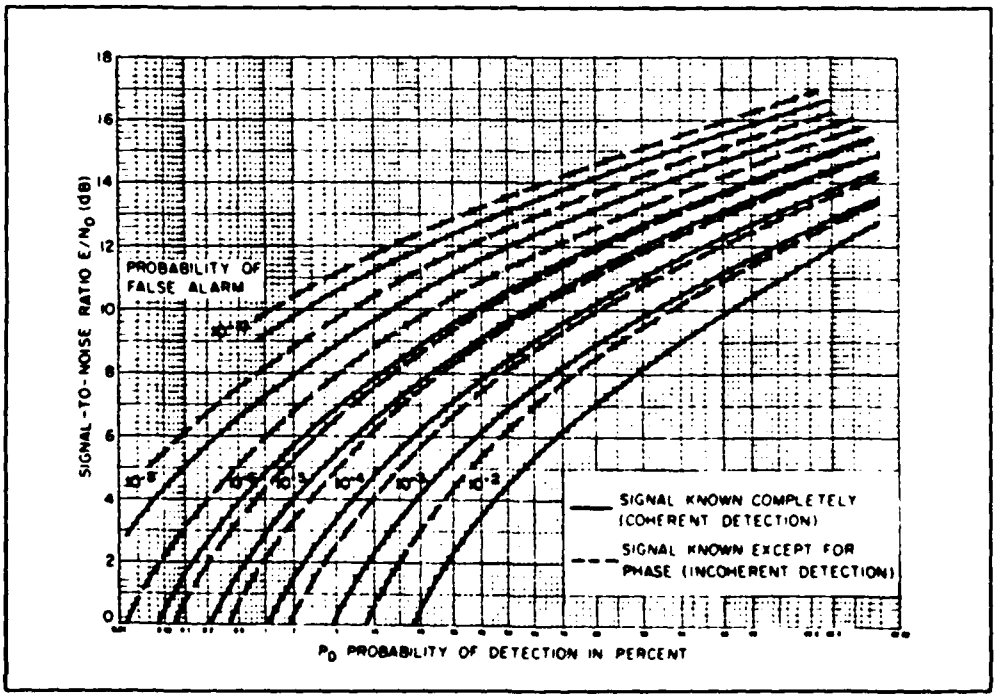

Figure 8. Single-Pulse Detection Requirements (16:205)

Matched Filter Channel. The main advantage of matched filtering in a synchronization circuit is the potential of very fast acquisition times. The IF matched filter placed in an auxiliary channel continuously correlates a subsequence of the incoming signal with that of the reference subsequence of the filter. A correlation peak appears at the output of the matched filter when the epoch of the incoming signal matches with that of the filter. The timing signal is obtained by rectifying the matched filter output and accumulating a number of successive correlation peaks until a threshold level is crossed. The timing signal, initiated at the instant of the threshold crossing, sets the epoch of the local PN generator and receiver synchronization is achieved.

Matched Filter Output Signal. As given in Eq (12), the received modulated signal, in the absence of noise, is of the form:

$$r(t) = \sqrt{2P}\cdot d_I(t)PN_I(t)\cos w_o t + \sqrt{2P}\cdot d_Q(t)PN_Q(t)\sin w_o t \quad (12)$$

where $d_I(t)$ and $d_Q(t)$ are the I and Q data streams, and $PN_I(t)$ and $PN_Q(t)$ are identical pseudonoise sequences with common epoch times for the I and Q channels. The pseudonoise signals have a clock frequency $f_c = 1/T_c$ with a period equal to $n\cdot T_c$ where n is the total number of chips in a full sequence.

Assuming additive white Gaussian noise at the input to the receiver, the impulse response of the matched filter is

$$h(t) = \begin{cases} \sqrt{2P}\cdot PN_I(MT_c - t)\cdot \cos w_o t & 0 \le t \le MT_c \\ 0 & \text{otherwise} \end{cases} \qquad (24)$$

The output of the matched filter is the convolution of the received signal and the impulse response of the filter as given by $u(t) = r(t) * h(t)$. Assuming the data rate is low relative to the chip rate, $d_I(t)$ and $d_Q(t)$ are constants over the period of integration for the convolution and the output is:

$$u(t) = P\cdot d_I(t)\int_0^{MT_c} PN_I(\tau)\,PN_I[\tau+(t-MT_c)]\cos w_o t[1+\cos 2w_o\tau]d\tau$$

$$+ P\cdot d_Q(t)\int_0^{MT_c} PN_Q(\tau)\,PN_I[\tau+(t-MT_c)]\sin w_o t[1-\sin 2w_o\tau]d\tau \qquad (25)$$

Assuming the period of integration is much greater than the period of the carrier, u(t) is given by

$$u(t) = P\cdot MT_c\cdot R_{PN}(t-MT_c)\left[d_I(t)\cos w_o t + d_Q(t)\sin w_o t\right] \qquad (26)$$

The output of the matched filter is passed through an envelope detector consisting of a square-law device and a low pass filter. The data modulation is effectively removed through the square-law device with the following output:

$$[u(t)]^2 = \left[P\cdot MT_c\cdot R_{PN}(t-MT_c)\right]^2\cdot[1 + 0.5\sin 2w_o t] \qquad (27)$$

With the bit energy as unity, the input to the threshold detector is given by

$$\mathrm{LPF}[u^2(t)] = \begin{cases} \left[M \cdot R_{PN}(t-MT_c)\right]^2 & |t| \le MT_c \\ n_p(t) & |t| > MT_c \end{cases} \qquad (28)$$

When $|t| \le MT_c$, the reference PN sequence is synchronized with the received PN sequence and the output of the matched filter channel achieves its maximum value, in other words, a full correlation peak occurs. At all other times, $n_p(t)$ represents the output of partial autocorrelation peaks that occur due to the correlation characteristics of subsequences of the selected PN code. This value cannot be determined analytically but will be quantified via simulation.

Matched Filter Acquisition Time Performance. In addition to the main correlation peak and the partial autocorrelation peaks due to the PN synchronization waveform, additional signals appear at the output of the detector. The IF bandwidth includes thermal noise, the data waveform of the desired signal, and in a multiple-access environment-the data and PN code waveforms of other users. These additional signals contribute to the partial autocorrelation output and collectively degrade the output signal-to-noise ratio.

As stated previously, the driving performance characteristic is the matched filter peak output signal-to-noise ratio (δ_{MF}). To determine δ_{MF}, the average signal power for each of the above interfering signals and the peak

power of the desired PN code sequence must be determined. The performance of the matched filter channel can be characterized in terms of the first two moments of the probability density function for the amplitude of the matched filter output. The partial correlation output of the matched filter is treated as a Gaussian random variable at the input to the square-law detector. The basis for the Gaussian assumption is the relationship between the matched filter length and the overall PN code length. Because the correlation time of the matched filter ($M \cdot T_c$) is much less than the PN code time period ($n \cdot T_c$), the correlation output amplitude has a binomial distribution. With the additional relationship that the correlation period is much greater than unity, the binomial distribution behaves like a Gaussian distribution (11:78).

The PN code correlation function is triangular over an interval of plus and minus one code chip ($-T_c, T_c$). Let H_1 denote the hypothesis that the received code waveform and the reference waveform of the matched filter are misaligned by less than one code chip. The alternate hypothesis H_0, denotes that the relative alignment is greater than or equal to a code chip period (11:61).

The input chip waveform, $\sqrt{2P} \cdot r(t+\tau)$, correlated by the matched filter reference, $c(t+\tau')$ over the period MT_c is given by (11:77):

$$C = \sqrt{2P} \int_0^{MT_c} r(t+\tau) \cdot c(t+\tau')dt \qquad (29)$$

The expected value of the correlation conditioned upon whether the incoming chip waveform is correlated with the reference waveform (H_1) or uncorrelated (H_0) is given by (11:77):

$$E\{C|H_i\} = \begin{cases} \sqrt{2P}\cdot MT_c\cdot(1-|\Omega|) & i = 1 \\ 0 & i = 0 \end{cases} \tag{30}$$

where Ω is the fractional timing offset with respect to a chip between the two code waveforms as given by,

$$\Omega = \left[\frac{\tau - \tau'}{T_c}\right] \pm N_\Omega \cdot T_c \tag{31}$$

and N_Ω is the smallest integer such that Ω lies in the interval (-1,+1). It is apparent that the expected value reaches a peak value of $\sqrt{2P}\cdot MT_c$ when the codes are correlated (Ω=0). Since partial correlation is a Gaussian random variable with zero mean, the expected value of uncorrelated code segments is zero.

The power of the uncorrelated waveforms is expressed by the variance given below (11:77):

$$var\{C|H_i\} = 2P\cdot MT_c^{\,2}\cdot G_i(\Omega) \tag{32}$$

where

$$G_i(\Omega) = \begin{cases} \Omega^2 & i = 1 \\ 1 - 2|\Omega| + 2\Omega^2 & i = 0 \end{cases} \tag{33}$$

The normalized mean and variance of the partial correlation as a function of the relative timing offset between the incoming chip waveforms and the reference waveform is shown in Figure 9 for a normalized chip interval of (-3,+3).

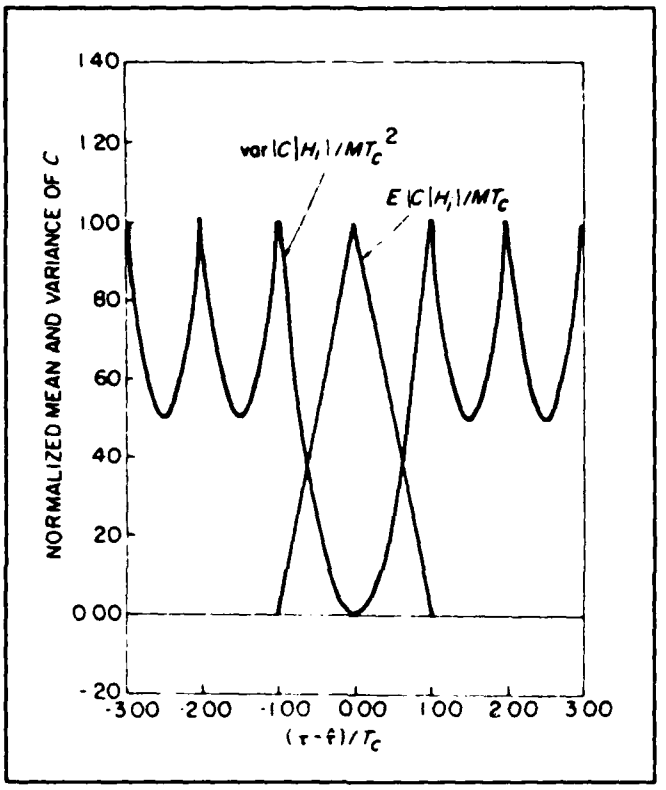

Figure 9. Normalized Mean and Variance For Partial Correlation (11:78)

The power of the interfering waveforms can now be determined. The data waveform of the desired signal will be synchronized with its associated PN code waveform and will therefore have no offset (Ω=0) with the reference waveform. The power is therefore equal to $2P_D \cdot MT_c^2$ where P_D represents the power in the data waveform. The average power is $P_D \cdot MT_c^2$. The data and PN code waveforms associated with

other users will occur with an offset outside the correlation interval. As seen in Figure 9, the variance for an uncorrelated waveform repeats every chip period outside the correlation interval. Assuming that the timing offset for these waveforms is uniformly distributed over a chip period, the average offset will be $\Omega = 2/3$ as shown below:

$$\Omega = \int_0^1 (1-2|\alpha|+2\alpha^2)\,d\alpha = 2/3 \tag{34}$$

The average power for the data waveforms associated with other users is therefore $2/3 \cdot P_{D'} \cdot MT_c^2$. The average power for the PN code waveforms associated with other users is $2/3 \cdot P_{C'} \cdot MT_c^2$.

With thermal noise at the input to the matched filter expressed as $N = N_o \cdot BW_{IF}$ and no correlation with the reference signal (Ω=1 or -1), the noise power at the output of the matched filter channel is $N \cdot MT_c^2$. The total average power of interfering sources can now be expressed:

$$\sigma_{tot}^2 = MT_c^2\left[N + P_D + 2/3 \cdot K(P_{D'} + P_{C'})\right] \tag{35}$$

where $K \geq 0$ is the number of interfering users.

The peak signal power of the desired PN code waveform is the square of the peak (Ω=0) expected value for a correlated waveform and is equal to $2P_C \cdot (MT_c)^2$. The peak SNR at the output of the matched filter channel can now be expressed:

$$\delta_{MF} = \frac{2P_C \cdot M}{N + P_D + 2/3 \cdot K(P_{D'} + P_{C'})} \qquad (36)$$

This signal-to-noise ratio will determine the number of correlation peaks that must be processed to achieve synchronization with given probabilities of false alarm and detection. To achieve synchronization in the first code period, the matched filter ouput signal-to-noise ratio must meet the same single-pulse detection requirements given in Figure 8 for the quadrature correlator. For a probability of detection equal to 0.9 and selected values for probability of false alarm, the peak output signal-to-noise ratio requirements are summarized below in Table 1.

Table 1. Single-Pulse Detection Requirements

P_{fa}	Peak Output SNR Requirements
10^{-3}	13.7 dB
10^{-5}	15.5 dB
10^{-6}	16.2 dB

As evident in Eq (36), the matched filter output signal-to-noise ratio is dependent on the length of the filter, the number of users in a multiple-access system, and the level of thermal noise. Given these factors, the matched filter may not achieve the required output signal-to-noise ratios required for single-pulse detection. At lower output signal-

to-noise ratios, several correlation spikes must be processed prior to threshold detection and initiation of the local PN generator. Requirements for multiple pulse detection of signals are tabulated (16:248-261) and are summarized below. Figure 10 gives the number of pulses required for detection at specified probabilities of false alarm and detection over a range of peak output signal-to-noise ratios.

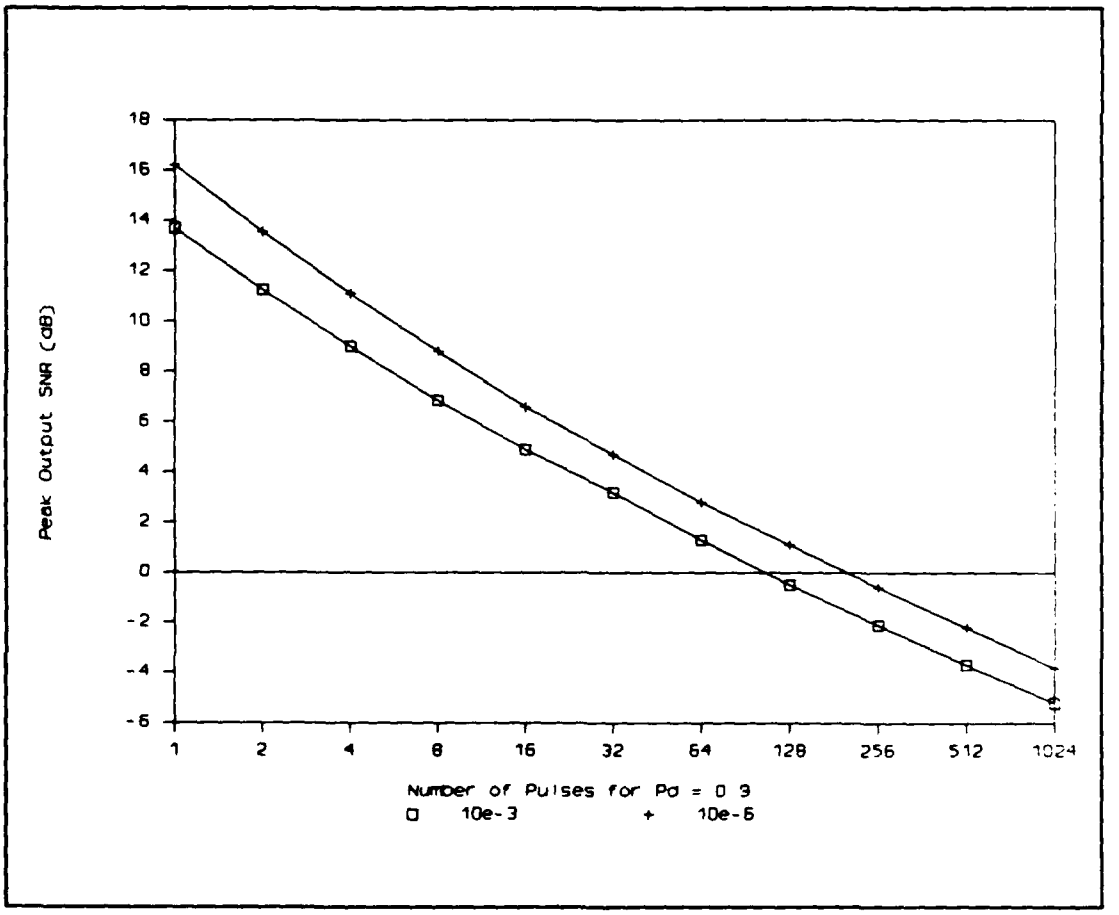

Figure 10. Multiple-Pulse Detection Requirements (16:248-261)

The threshold level at the output of the accumulator controls the number of pulses processed by the matched filter

prior to the initiation of the local PN generator. At the end of each PN code period, the matched filter outputs a main correlation peak of amplitude on the order of the length of the filter. This main correlation spike and the associated noise throughout the remaining PN code period is squared through the envelope detector and input to the accumulator. Dependent on the noise level accompanying the main correlation peak, the threshold level is set to require the specified number of pulses to accumulate prior to threshold crossing. If the threshold requirements are met, the local PN generator will be initiated such that the quadrature correlator will indicate synchronization in the first dwell period with corresponding probabilties of false alarm and detection.

Acquisition Time Performance

The matched filter output SNR and therefore the acquisition time of the matched filter channel is influenced by the length of the filter, the number of interfering users, and the level of thermal noise. In this section, each of these influences will be examined in order to characterize the acquisition time performance of the system. A comparison will then be performed to highlight the improvement in acquisition time offered by the auxiliary matched filter channel against the quadrature correlator alone.

The first step is to simplify the equation describing the peak output SNR of the matched filter. In Eq (36), the

power of the data and PN code waveforms will all be set equal such that $P_C = P_D = P_{C'} = P_{D'}$. Allowing the combined power of the data and PN code waveforms of a particular transmitted signal to be represented as $S = P_C + P_D$, the matched filter peak output SNR reduces to:

$$\delta_{MF} = \frac{M \cdot \delta_i}{1 + \delta_i(1/2 + 2/3 \cdot K)} \tag{37}$$

where $\delta_i = S/N$ is the matched filter input SNR of a single transmitted signal and K is the number of other users.

As stated previously, for output signal-to-noise ratios less than the requirements for single-pulse detection, the matched filter channel must process a number of pulses to meet a particular false alarm rate and probability of detection. Recognizing that each pulse the matched filter channel processes equates to a PN code period, the requirements for multiple-pulse detection given in Figure 10 can be used to evaluate acquisition time performance.

Acquisition time performance in terms of code periods is specified by the number of pulses processed prior to initiation of the local PN generator and the length of code. The length of a code period is equal to the code chip time multiplied by the number of chips in the code sequence or $n \cdot T_c$. Letting N_p represent the number of pulses processed according to the multiple-pulse detection requirements of Figure 10, the mean acquisition time is given by:

$$T_{MA} = N_p \cdot n \cdot T_c \tag{38}$$

Acquisition time performance for a range of input signal-to-noise ratios, matched filter lengths, and number of other users is given below. Figures 11 through 15 show performance characteristics for an ideal false alarm rate $P_{fa} = 10^{-6}$ and detection probability $P_d = 0.9$ while Figures 16 through 20 show performance characteristics at $P_{fa} = 10^{-3}$. A probability of false alarm at 10^{-3} can be simulated in reasonable time frames and the expected values in Figures 16 through 20 are provided to highlight the performance characteristics that will be simulated.

Improvement in acquisition time offered by the matched filter channel is evident in the ratio of the mean acquisition times for the correlator and that of the matched filter given in Eq (39). Recalling Eq (22) and recognizing that $K \cdot P_{fa} << 1$ for the case of interest ($P_{fa} = 10^{-6}$), the mean acquisition time for the correlator acting alone is:

$$T_{acq}(C) = 1.22 \cdot n^2 \cdot T_c \tag{39}$$

where n is the number of code chips in the PN code period. The acquisition time is improved by a factor (I) expressed in the following ratio:

$$I = 1.22 \cdot \frac{n}{N_p} \tag{40}$$

As shown in Figures 11 through 15, for signal-to-noise ratios in the range above 0 dB, a variation of the input SNR has no effect on the acquisition times. In this range, the

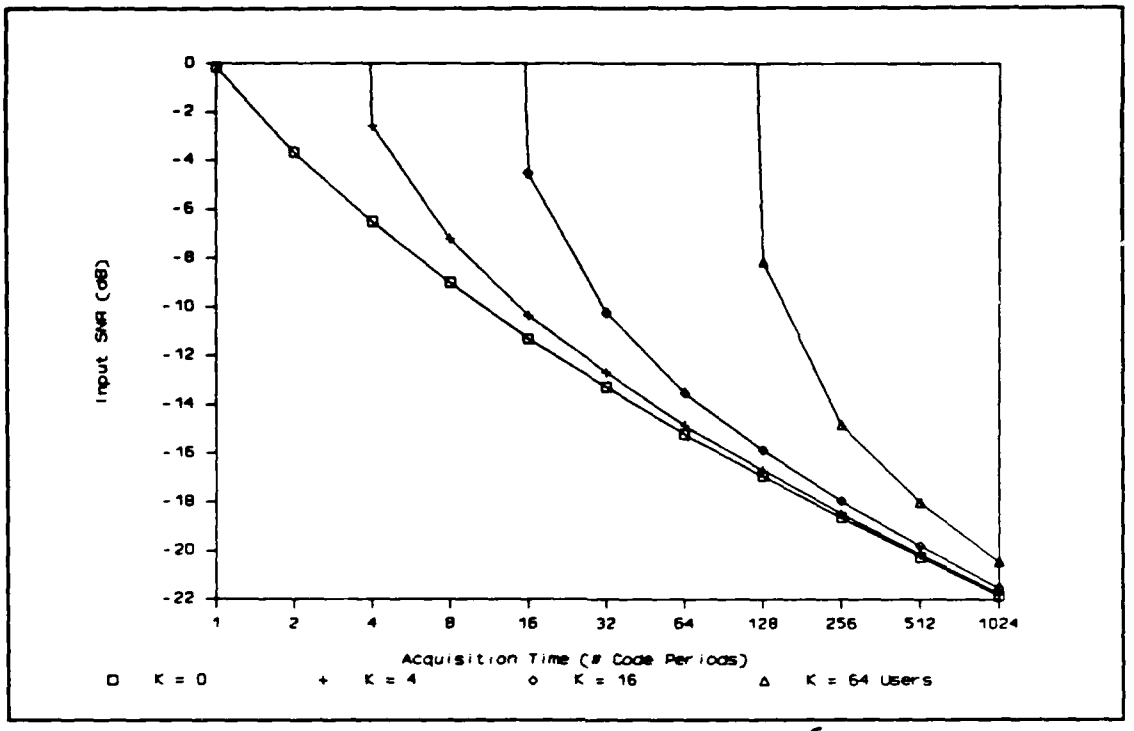

Figure 11. MF Length = 64 ($P_{fa} = 10^{-6}/P_d = 0.9$)

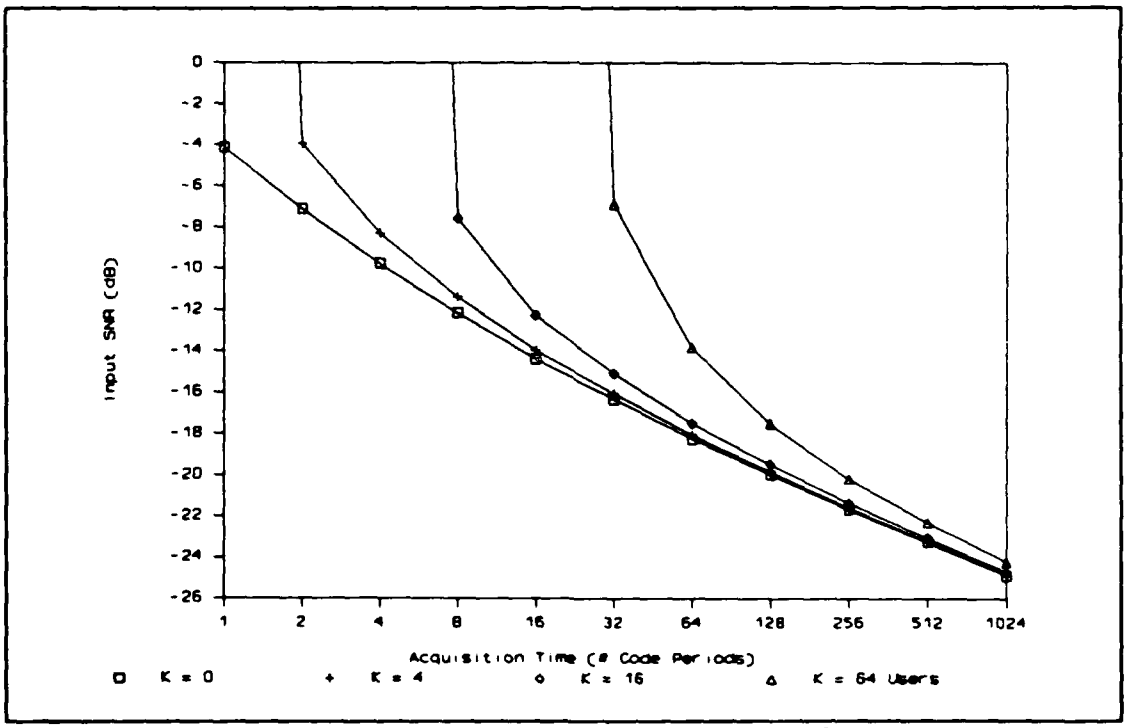

Figure 12. MF Length = 128 ($P_{fa} = 10^{-6}/P_d = 0.9$)

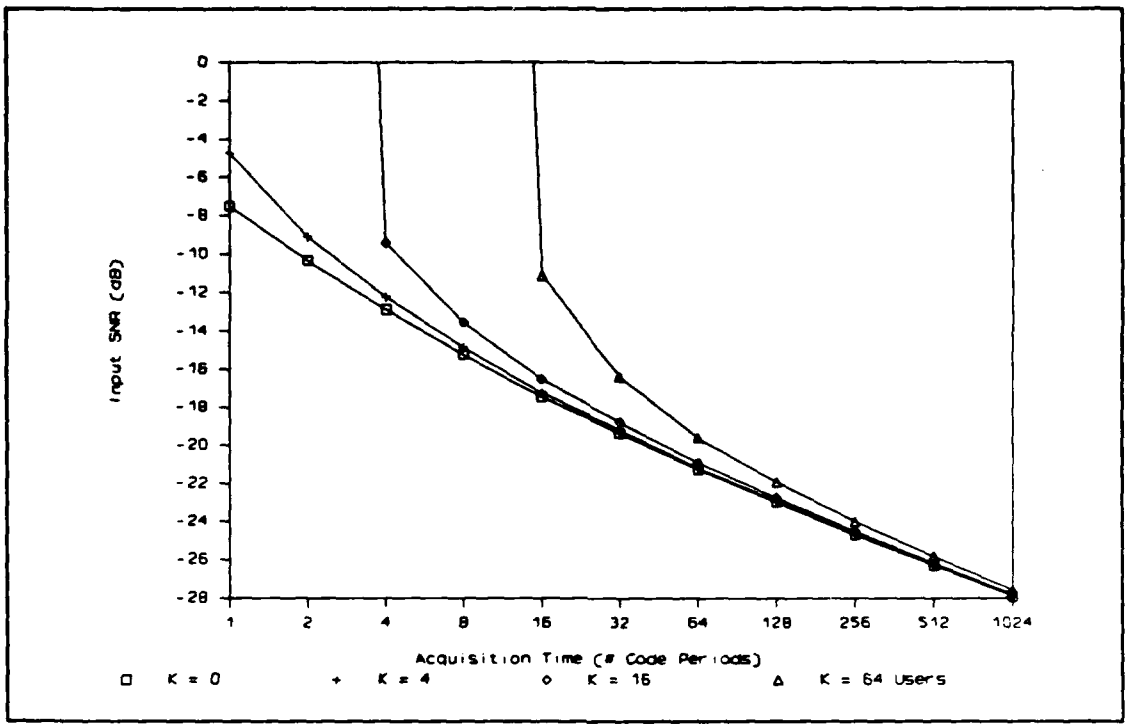

Figure 13. MF Length = 256 ($P_{fa} = 10^{-6}/P_d = 0.9$)

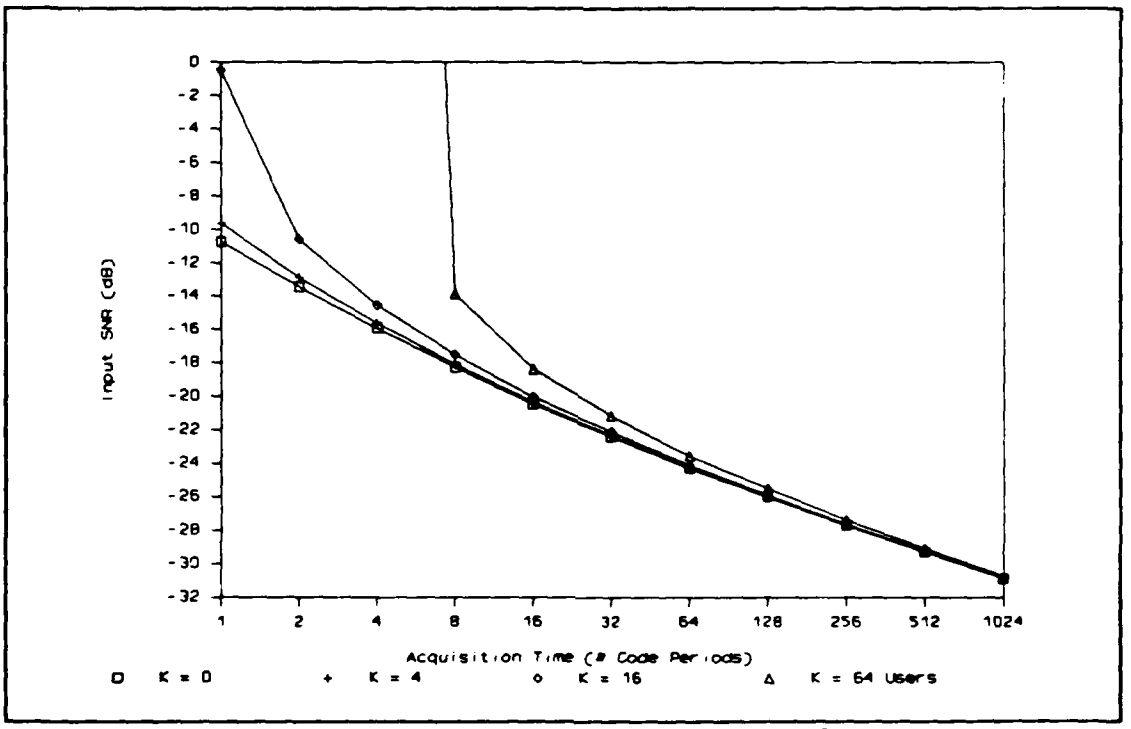

Figure 14. MF Length = 512 ($P_{fa} = 10^{-6}/P_d = 0.9$)

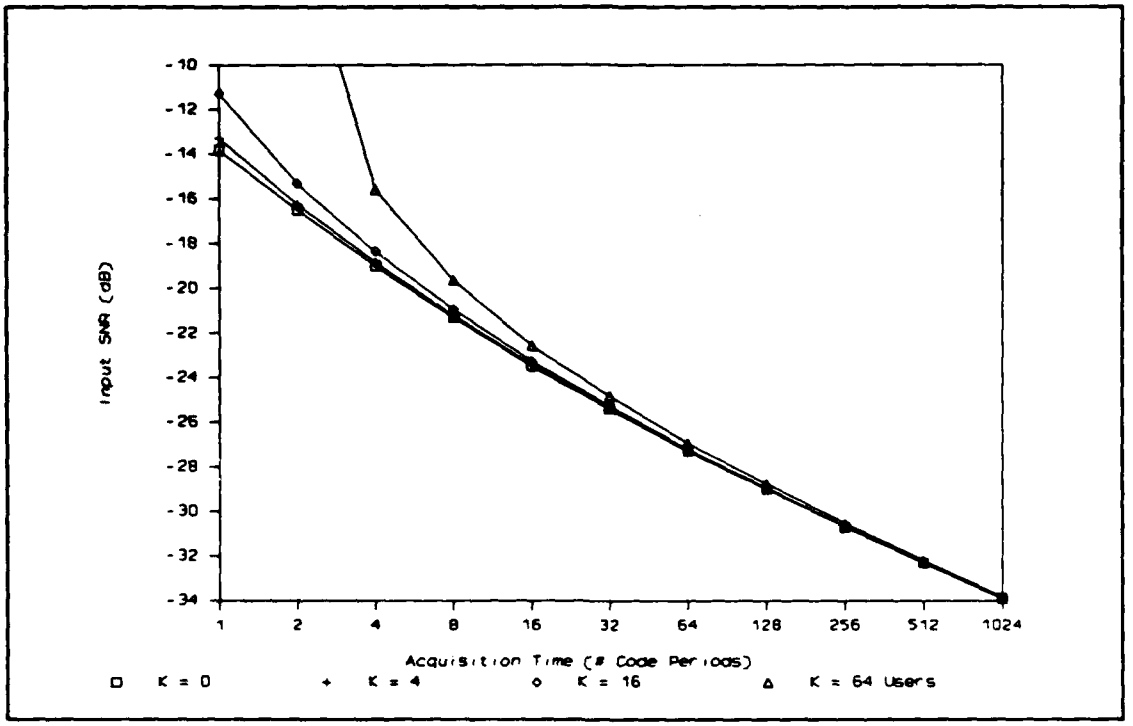

Figure 15. MF Length = 1024 ($P_{fa} = 10^{-6}/P_d = 0.9$)

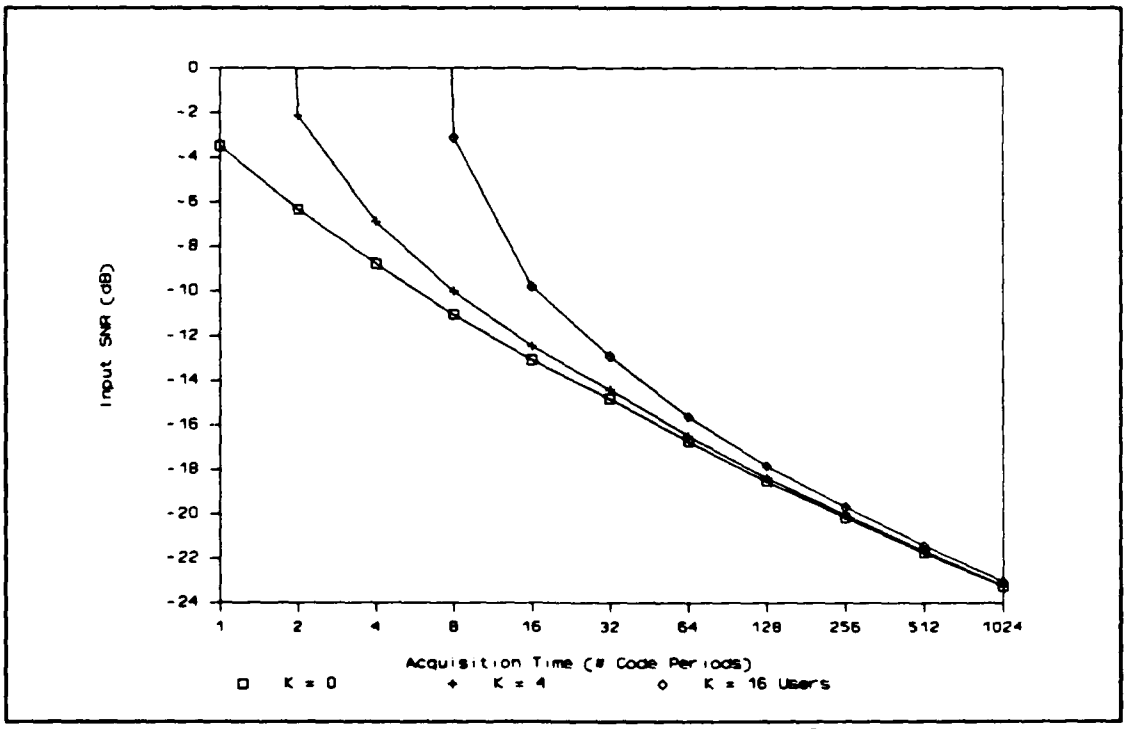

Figure 16. MF Length = 64 ($P_{fa} = 10^{-3}/P_d = 0.9$)

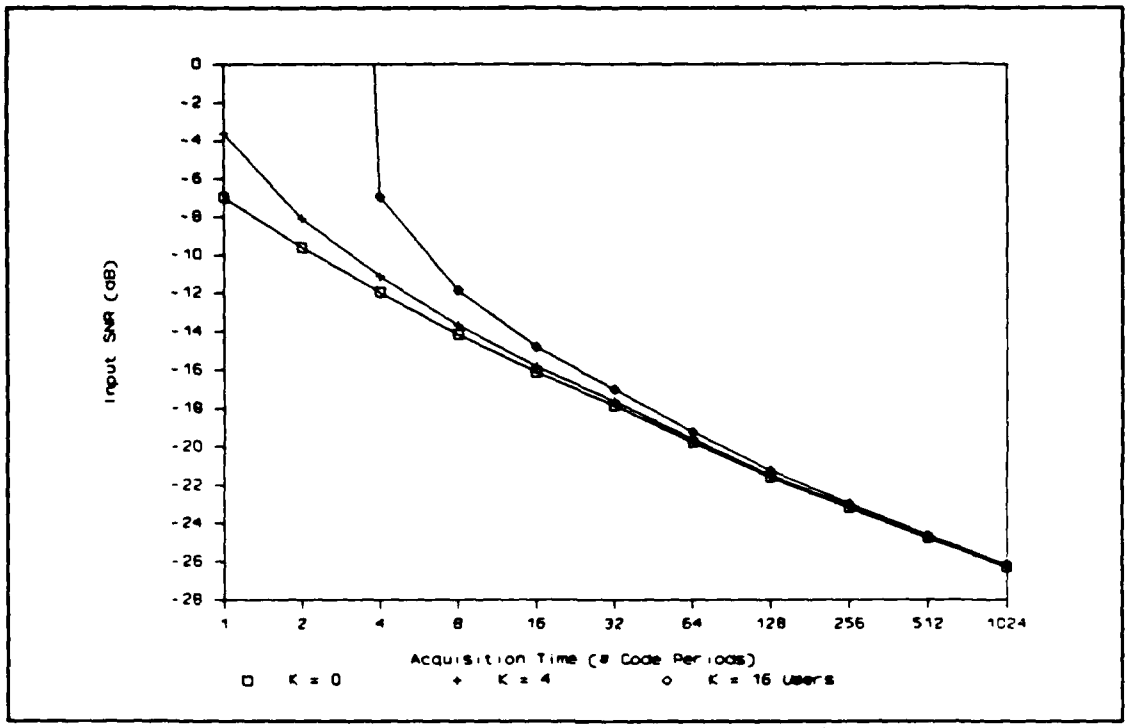

Figure 17. MF Length = 128 ($P_{fa} = 10^{-3}/P_d = 0.9$)

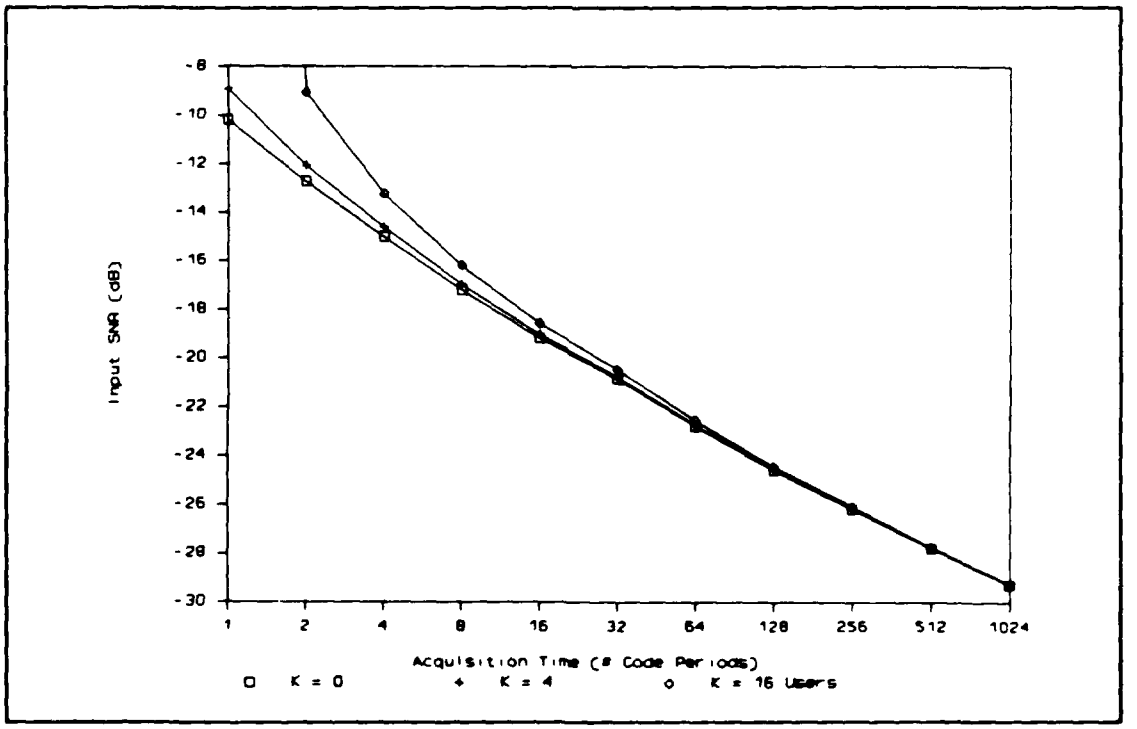

Figure 18. MF Length = 256 ($P_{fa} = 10^{-3}/P_d = 0.9$)

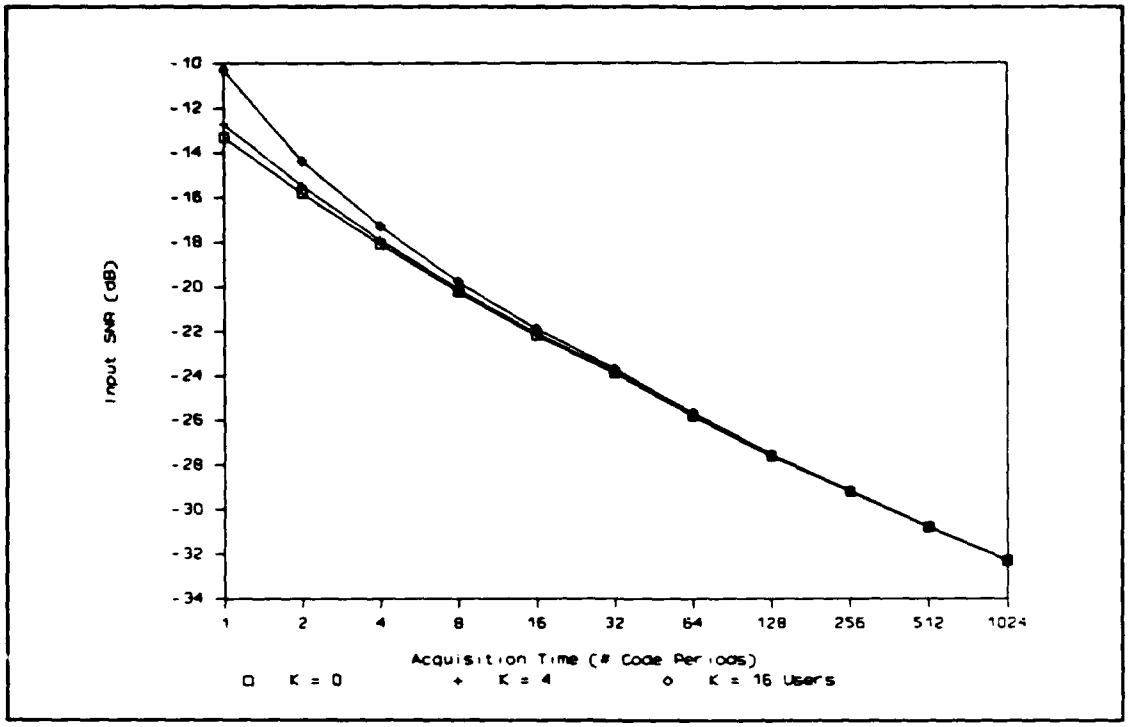

Figure 19. MF Length = 512 ($P_{fa} = 10^{-3}/P_d = 0.9$)

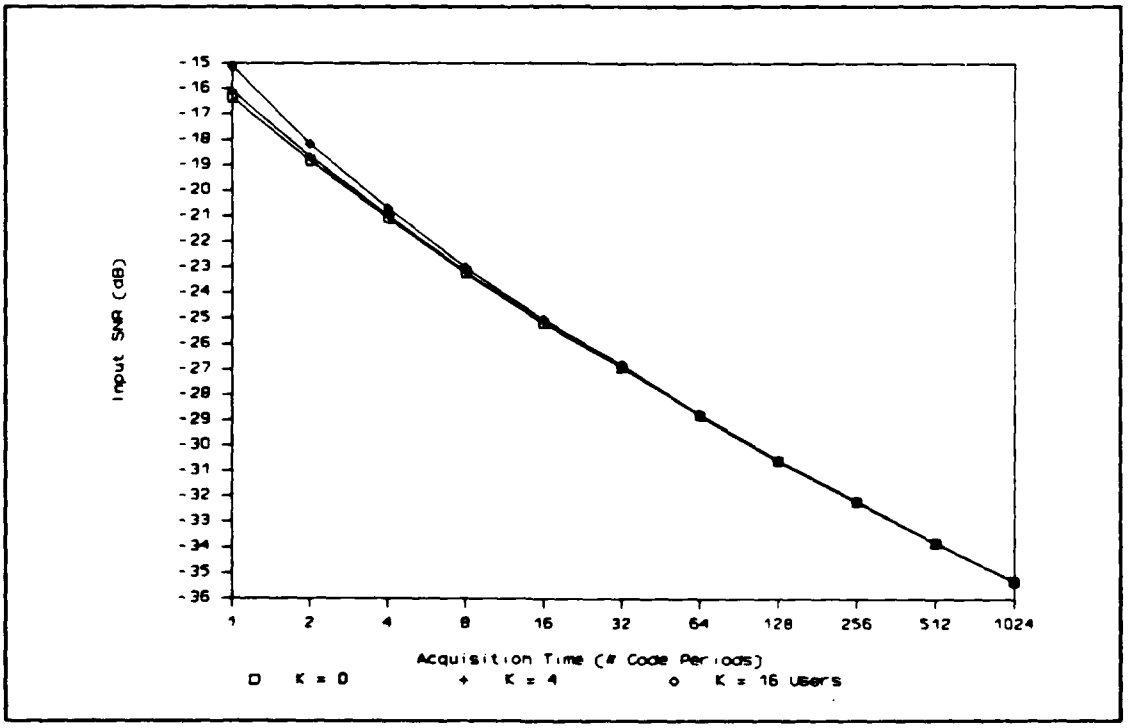

Figure 20. MF Length = 1024 ($P_{fa} = 10^{-3}/P_d = 0.9$)

primary influence on acquisition time performance for a given matched filter length is the number of users in the system. Improvement in the acquisition times over this range of input signal-to-noise ratios is shown in Figure 21 for a code length of n = 2047 chips.

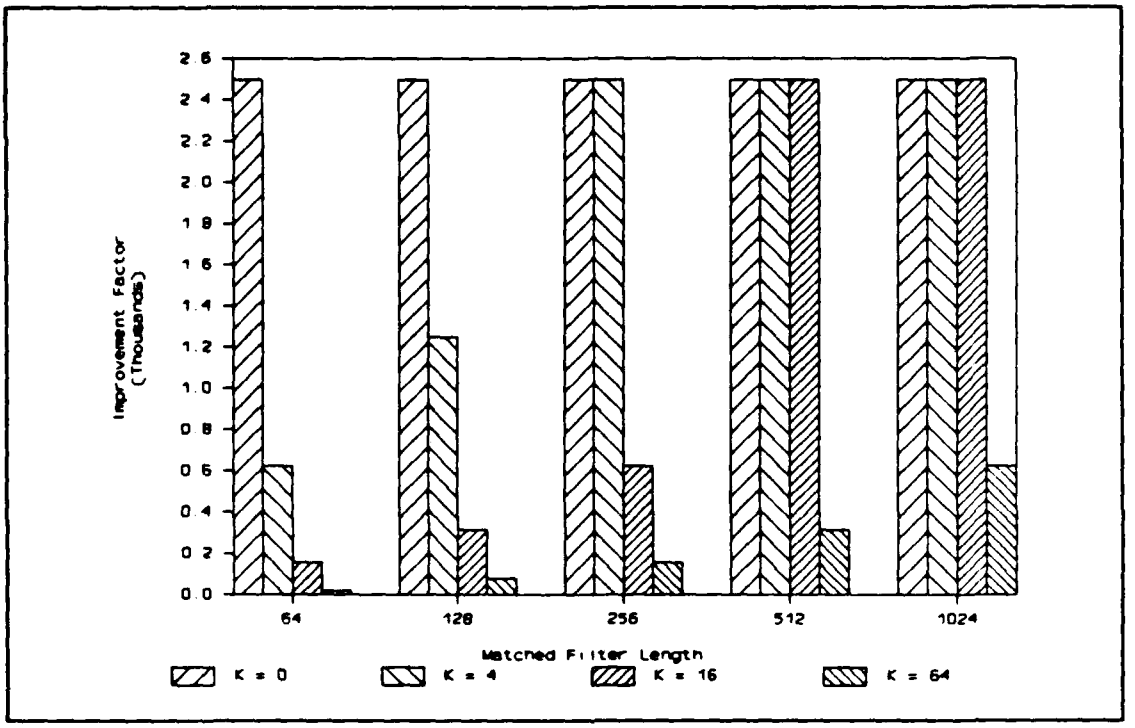

Figure 21. Acquisition Time Improvement (Input SNR $\geq$ 0dB)

As the input signal-to-noise ratio decreases below 0 dB, the number of users in the system becomes less of an influence on the acquisition times. For further decreases in the input signal-to-noise ratio, the curves presented in Figures 11 through 15 asymptotically approach a doubling in the acquisition time for each 1.5 dB decrease in the input SNR (16:262). For the input SNR range below -20 dB, noise is the dominant influence on acquisition time. To demonstrate

this trend, the improvement in acquisition time for an input SNR of -10 dB is given in Figure 22.

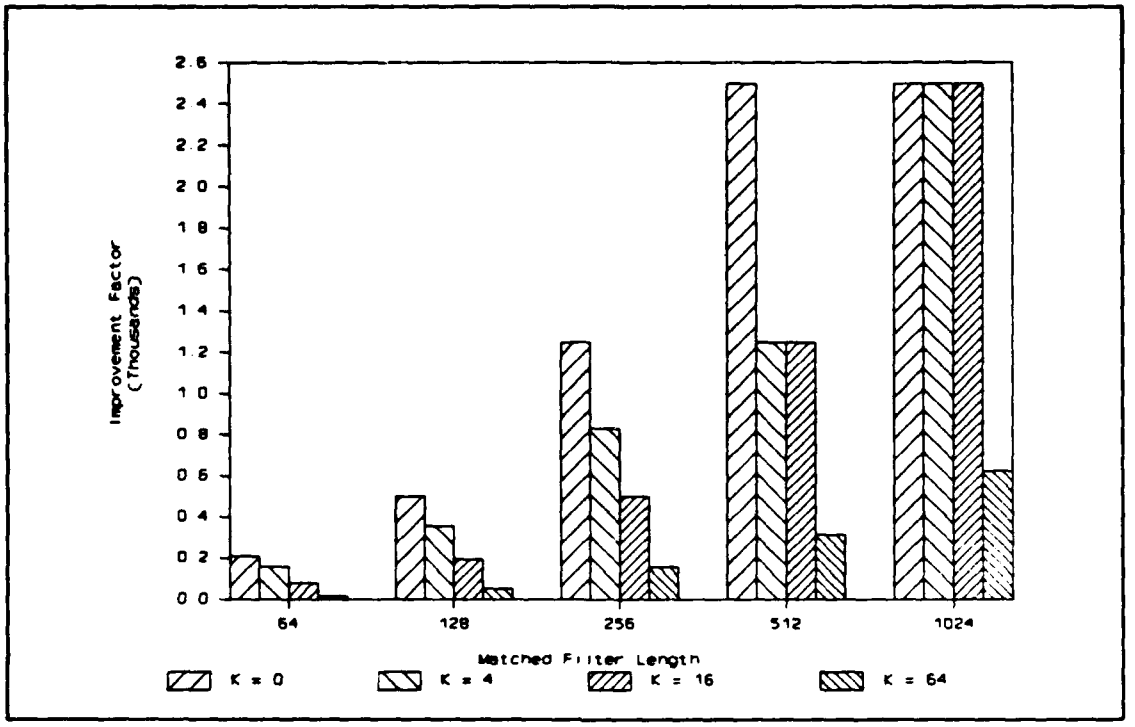

Figure 22. Acquisition Time Improvement (Input SNR = -10 dB)

As evident in Figure 22, increasing the number of users does not produce the degree of variation in the improvement factor that is seen at higher input signal-to-noise ratios. In addition, the improvement levels are significantly reduced to due the high AWGN noise levels.

To summarize, it is the peak output SNR of the matched filter that determines acquisition time performance. A number of factors influence this system parameter. First of all, the partial autocorrelation of the PN code of interest outputs correlation noise. Other influences on the output SNR include the cross-correlations of the data waveform of

the signal of interest, the data and PN code waveforms of the other users, and thermal noise. The amplitudes of these signals are assumed to have a Gaussian distribution. The influences of the Gaussian signals and the length of the matched filter are quantified in Eq (36) for the matched filter peak output SNR.

For a selected P_{fa} and P_d, the peak output SNR determines whether a signal can be detected within the tabulated single-pulse or multiple-pulse detection requirements. If the output SNR does not meet single-pulse detection requiremets, the number of pulses that must be processed to meet the multiple pulse detection requirements determines the acquisition time. The time between successive pulses is equal to a full PN code period. Therefore, the acquisition time performance is directly related to the matched filter output SNR as a function of the matched filter length, the number of other users in the system, and the AWGN level.

The next chapter proceeds with modeling the system components using the Block-Oriented Systems Simulator. The output signal analysis in this chapter will be used to validate the simulation models for the matched filter channel and the quadrature correlator. The single and multiple-pulse detection requirements will be used to select simulation times and associated threshold detection levels to test performance of the matched filter via simulation.

IV. BOSS Modeling of the System

The Block Oriented Systems Simulator (BOSS) provides for simulation-based analysis and design of any system which can be represented in block diagram form. Simulation models of systems are constructed using a heirarchial block diagram approach where each block performs a signal processing operation. Once a correct description of the system is expressed in block diagram form, BOSS supports a time-domain (waveform level) simulation (1:36.1.1). The pseudonoise (PN) synchronization system to be simulated is composed of a single dwell quadrature correlator augmented by a matched filter channel to speed PN code acquisition. The simulation model will be configured to analyze the initial acquisition characteristics of the matched filter channel.

The chapter begins with the approach to modeling the synchronization system. The second section is dedicated to the successive steps and analysis to perform a bottom-up modeling of the individual subsystem components using BOSS functional modules. The final section will discuss integration of the simulation models for a single user system and a multiple-access system.

Top-down Decomposition

The first step in the BOSS modeling process is to perform a top-down decomposition of the system. The major components of the system, the (1) Pseudonoise Sequence Generator, the (2) Matched Filter Channel, and the

(3) Quadrature Correlator consist of the block diagram representations shown below in Figure 23.

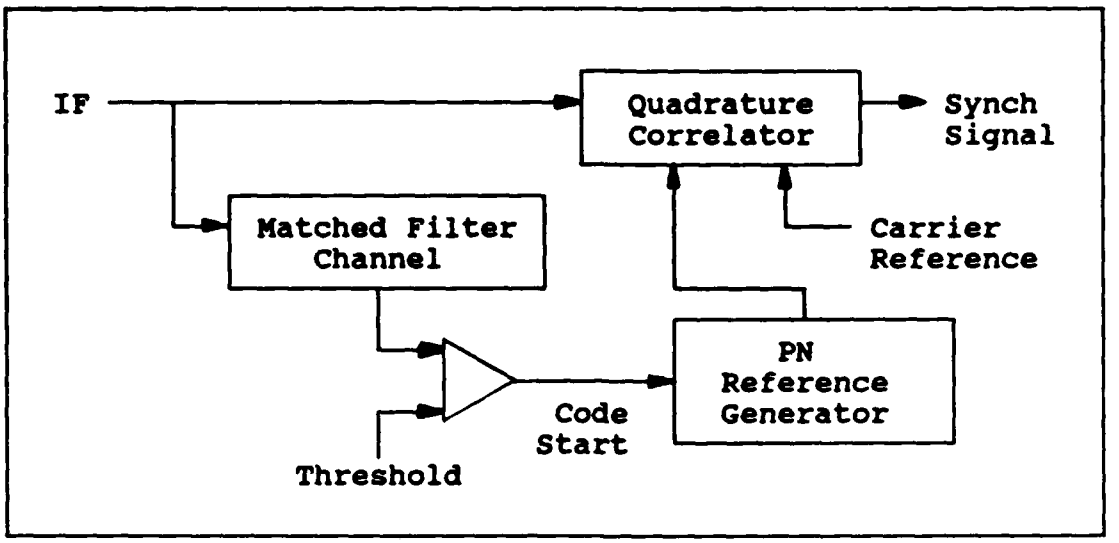

Figure 23. Synchronization System (3:68)

Further decomposition of the functional blocks is necessary to suppport BOSS's bottom-up hierarchial concept of system design. BOSS supplies a library of low-level modules called primitives to construct more complex modules. Modules of increasing complexity can in turn be used in higher level modules in a bottom-up hierarchial fashion until the visual representation of the simulation matches the high-level system block diagram of Figure 23.

The first simulation model will be the PN sequence generator. The generator will then be used in the construction of the QPSK direct sequence transmitter. Once the transmitter has been successfully tested, it will be used as the signal source to test the implementation of the matched filter. The matched filter requires the loading of a

reference code sequence. A reference code generator will be implemented to perform this function and is basically a PN sequence generator and timing control elements. The envelope detector, accumulator, and decision circuit at the output of the matched filter will be modeled separately. At this point, the modules will be integrated for implementation of a single user system. The additional transmitters necessary to construct a multiple-access system will then be modeled.

Pseudonoise Sequence Generator. The code sequence produced by the generator depends on the number of stages of linear shift registers, the feedback connections, and the initial conditions. For this system, the code sequence will be generated by an 11-stage linear simple shift register (SSRG) with appropriate feedback to produce a maximal length sequence. To produce the maximal length sequence, the feedback connections are determined by the selection of a primitive 11th degree polynomial over a Galois field of two. The polynomial selected,

$$p(x) = x^{11} + x^2 + 1 \tag{41}$$

will produce a pseudonoise sequence with a repetition period of $2^{11} - 1 = 2047$ code symbols (chips). Code sequences with long repetition periods are typically selected as they result in code sequences that are virtually decorrelated for a shift of a single chip. A high degree of correlation between an undesired code and a receiver reference will cause an increase in the receiver's false alarm rate and possibly,

false receiver synchronization. The block diagram representation of the PN sequence generator to be modeled is shown below in Figure 24.

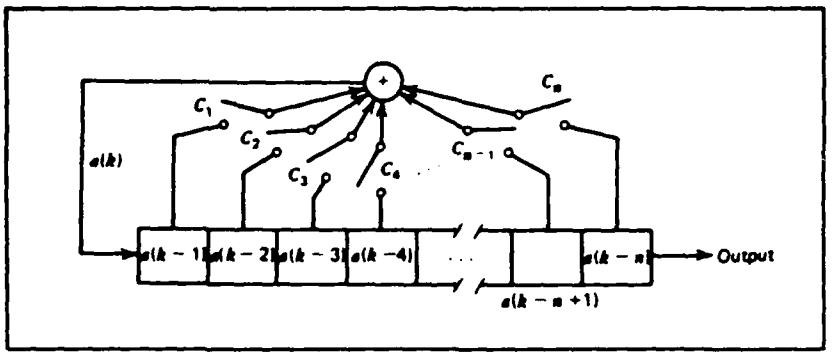

Figure 24. Linear SSRG Model (15:310)

For efficiency in terms of simulation, the PN sequence generator will be implemented with a reset capability for consistent and accurate initiation of the PN sequence. This will eliminate the timing uncertainty of initiating the generator by closing the feedback loop and loading initial conditions as described by Smirnov (3:68).

The fundamental cell used in the construction of the generator is the SSRG Cell with a reset capability as shown in Figure 25. The cell provides the signal and the running sum inputs and outputs necessary for the multistage implementation. The initial condition for each stage is set at the Reset Unit Delay module and the feedback connection is established by setting a logical true condition at the Constant Generator. The reset signal is propagated through the logical AND gate for a simultaneous reset of the cascaded cells. The complete implementation of the Resetable PN

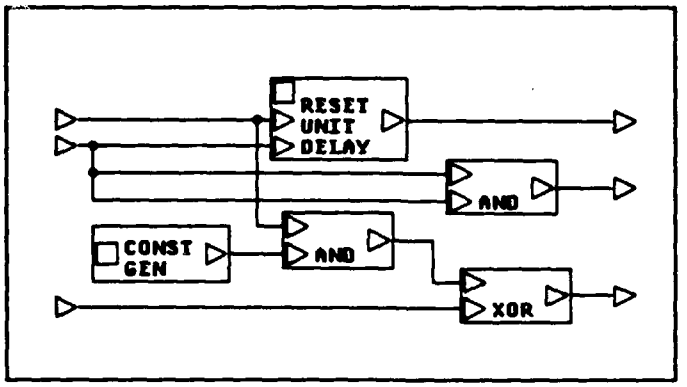

Figure 25. SSRG Cell

Generator is shown below in Figure 26. The tap weights are set according to the polynomial selected and initialized with a logical true in the low order register.

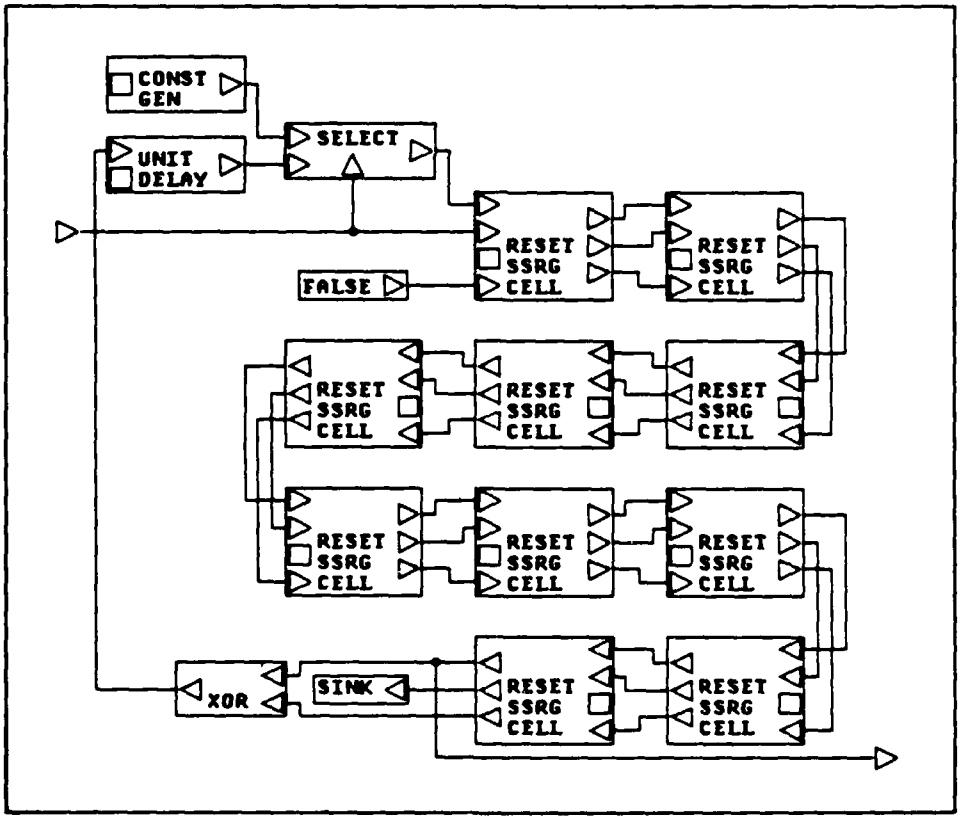

Figure 26. Resetable PN Generator

As implemented at this point, the generator module uses the simulation clock and only generates one sequence value per sample interval. In order to increase flexibility at simulation time, an impulse train is used to drive the chip rate rather than the simulation clock.

QPSK Direct Sequence Transmitter. The quadriphase modulation scheme for this implementation is straightforward as shown in Figure 27. The single Resetable PN Generator is used to modulate both the in-phase and quadrature channels. The logical true and false outputs of the generator are converted to numerical signal levels of +1 and -1 respectively. Operation of the PN generator is controlled by the enable signal from the Impulse Train module. The parameter that establishes the rate of the impulse train is exported for specification at simulation time. This parameter is termed CHIP RATE and establishes chip rate of the PN generator in units of Hertz. The logical false input to the PN generator disables the reset feature of the generator.

The data sources for modulation are independent random sources into each channel. The numerical signal levels are +1 and -1 and the signal rate is identical for each source. The signal rate is controlled by the single exported parameter DATA RATE. The random sources are initialized with different seeds.

The channel outputs are combined into a complex number and modulated on a complex carrier. The frequency produced

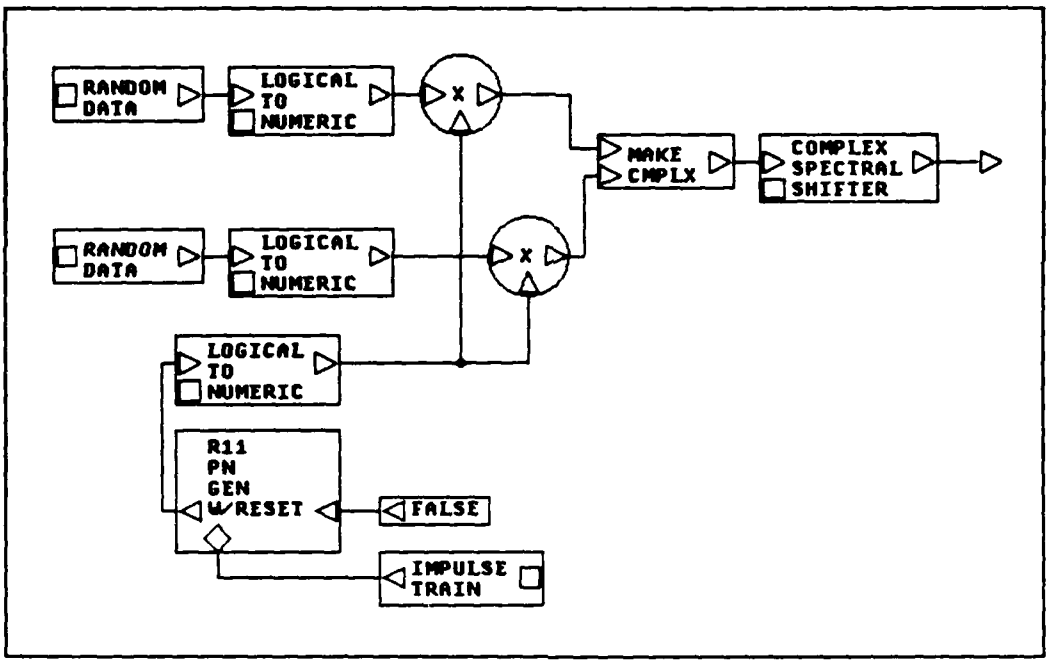

Figure 27. QPSK Direct Sequence Transmitter

by the Complex Spectral Shifter module is controlled by the exported parameter, CARRIER FREQUENCY, which sets the transmitter output frequency in units of Hertz.

Matched Filter Channel. As shown in Figure 28, the matched filter channel consists of a tapped-delay line matched filter, envelope detector, accumulator device, and a threshold detector.

Matched Filter Module. Conceptually, the implementation of the matched filter is in the form of a tapped delay line followed by a passive filter matched to a single PN chip waveform. Figure 29 illustrates the delay line matched filter configuration for this channel. The delay line matched filter is configured to recognize a particular code sequence of finite length and that sequence

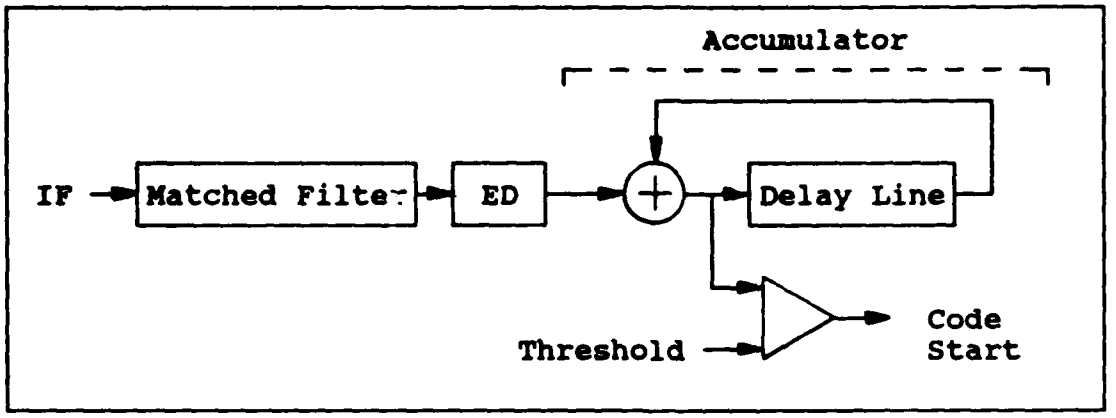

Figure 28. Matched Filter Channel

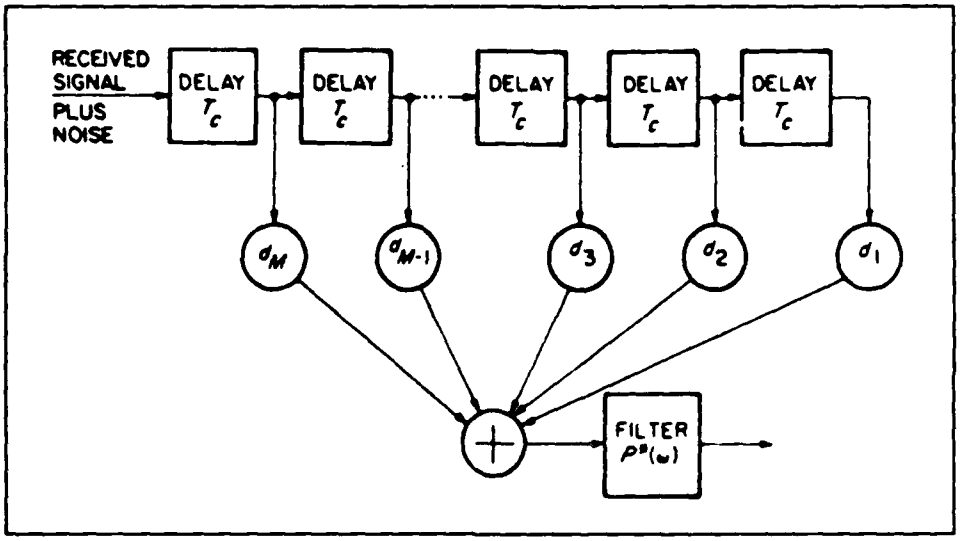

Figure 29. Tapped Delay Line Matched Filter (11:70)

only. Each delay element has a delay equal to the period of the expected code clock so that each element contains energy corresponding to only one code chip at any one time (13:30).

The matched filter is a passive device that maximizes the output peak signal-to-mean noise ratio. The signal to be detected is a segment of the input signal r(t) of length T_o that is a function of the PN code modulation only. The impulse response of the filter is a time-reversed form of the

signal as given by (11:69):

$$h(t) = \begin{cases} r(T_o - t) & 0 \le t \le T_o \\ 0 & \text{otherwise} \end{cases} \tag{42}$$

or in terms of Fourier transforms,

$$H(w) = R^*(w) \cdot e^{-jwTo} \tag{43}$$

Expressing the segment length as $T_o = M \cdot T_c$, the encoded PSK signal takes the form,

$$r(t) = \sum_{n=1}^{M} d_n \cdot p[t-(n-1)T_c] \tag{44}$$

where $d_n \in \{-1,+1\}$ is the polarity of the n-th chip and p(t) is the chip pulse shape for a bandpass implementation,

$$p(t) = \begin{cases} \sqrt{2P} \cdot \cos w_o t & 0 \le t \le T_c \\ 0 & \text{otherwise} \end{cases} \tag{45}$$

Taking the Fourier transform of r(t) and substituting its complex conjugate into the equation for H(w) results in the implementation of Figure 29 and the following expression (11:71):

$$H(w) = P^*(w) \cdot \sum_{n=1}^{M} d_n \cdot e^{-jw(M-n+1)Tc} \tag{46}$$

The simulation model takes a modified form of the matched filter described above. Taking the inverse Fourier transform of the matched filter impulse response gives,

$$h(t) = \sum_{n=1}^{M} d_n \cdot p^*[(M-n+1)T_c - t] \tag{47}$$

Recognizing that d_n is real, an equivalent form for h(t) is,

$$h(t) = \sum_{n=1}^{M} \left[d_n \cdot p[(M-n+1)T_c - t] \right]^* \tag{48}$$

The simulation model establishes the tap values as the complex conjugate of d_n, given below and eliminates the filter shown in Figure 29.

$$d_{n'} = d_n \cdot p[(M-n+1)T_c - t] \tag{49}$$

The modules to implement this filter are provided by BOSS. A sirgle stage of the matched filter is shown in Figure 30. The reference sequence is loaded into the top delay channel of the single filter cell. A load enable signal controls the sample and hold module and locks in the reference code for that particular matched filter cell at the end of the load sequence. The complex conjugate of the reference code is multiplied with the incoming signal of the bottom delay channel. The output of the multiplier is added to the running sum output of the set of cascaded cells that comprise the complete matched filter.

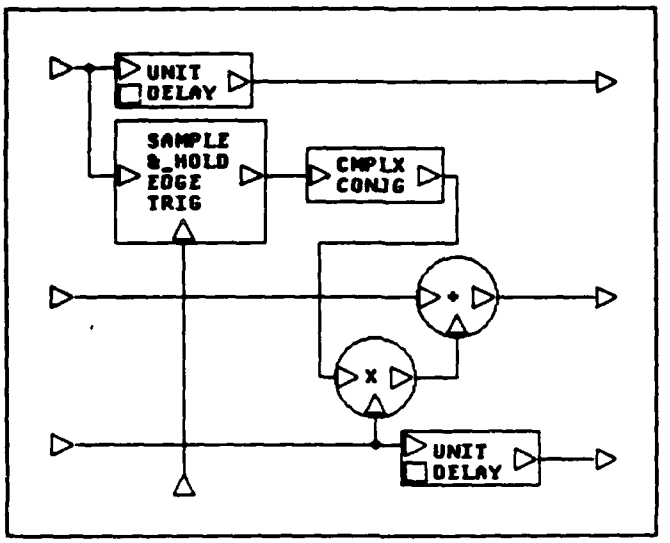

Figure 30. Correlate Single Stage

The complete matched filter is implemented using the Correlate Multi-Stage module supplied by BOSS as shown in Figure 31. The dashed lines indicate use of the replicate function. The replicate function allows user-specification of the number of individual stages. The length of the filter is set at simulation time with the parameter # OF STAGES. The maximum length of the filter is 2047 stages. The initial running sum input is initialized to zero and the delay line outputs are terminated with sink modules.

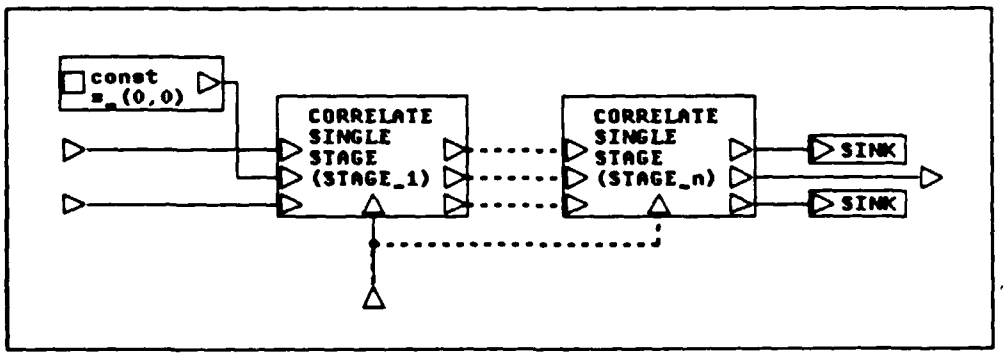

Figure 31. Correlate Multi-Stage

Envelope Detector. As described earlier, the envelope detector consists of a square-law device followed by a low-pass filter. A simpler implementation for the simulation model will provide an equivalent output.

The sinusoidal output of the matched filter is amplitude-modulated by the correlation of the reference sequence and the incoming signal. As expressed in Eq (26), the matched filter output is

$$u(t) = P \cdot MT_c \cdot R_{PN}(t-MT_c)\left[d_I(t)\cos w_o t + d_Q(t)\sin w_o t\right] \qquad (26)$$

The desired output of the envelope detector given in Eq (28) can also be achieved by multiplying the incoming signal by its complex conjugate and reducing the gain by half. This will be the method of simulation as justified in the following development.

The incoming signal multiplied by its complex conjugate gives

$$u(t) \cdot u^*(t) = [P \cdot MT_c \cdot R_{PN}(t-MT_c)]^2 \cdot |d_I(t)\cos w_o t + d_Q(t)\sin w_o t|^2$$

where $|d_I(t)\cos w_o t + d_Q(t)\sin w_o t| = \sqrt{2}$. With the bit energy as unity, it follows that

$$u(t) \cdot u^*(t) = 2 \cdot [M \cdot R_{PN}(t-MT_c)]^2 \qquad (50)$$

This result is twice the value of the expected signal derived in Eq (28). It is therefore valid to model the envelope detector as shown in Figure 32.

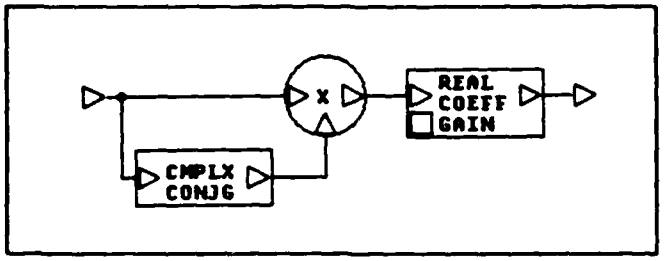

Figure 32. Envelope Detector

Accumulator. The accumulator circuit performs a running sum of the incoming signal over the period of the PN code. As shown in Figure 33, a cascade of delay elements produce the necessary delay. The size of both multi-stage delays is specified by the parameter 0.25*SAMPLES/PN PERIOD.

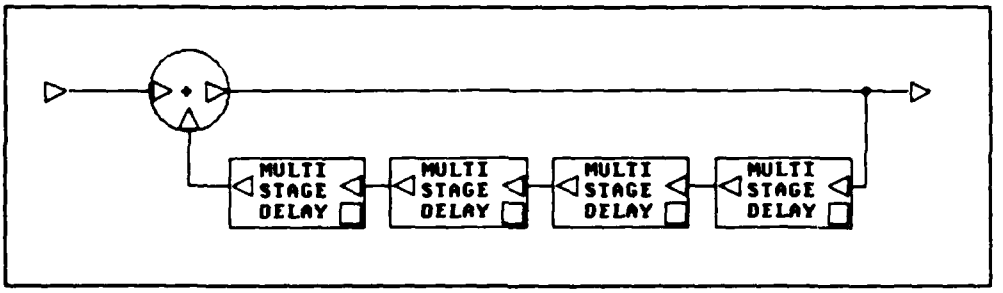

Figure 33. Accumulator

Threshold Detector. The threshold detector must continuously compare the input signal to a specified threshold. When the threshold is exceeded, the detector must transition to a logical true condition in order to initiate the reset function in the PN Sequence Generator. As shown in Figure 34, the comparison value is produced by the Constant Generator module with the parameter THRESHOLD. When the threshold value is exceeded, the comparator circuit transitions to a logical true condition for one sample

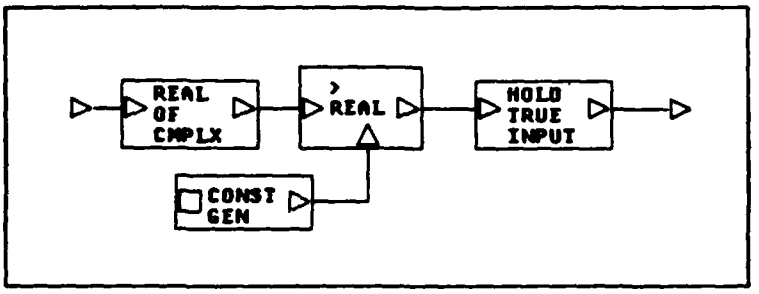

Figure 34. Threshold Detector

period. The Hold True Input module maintains the logical true condition through the remainder of the simulation as required by the PN Sequence Generator.

Quadrature Correlator. The implementation of this simulation model follows directly from the block diagram model presented in Figure 7. The inputs to the simulation model shown in Figure 35 consist of the received signal and the local PN code-modulated carrier.

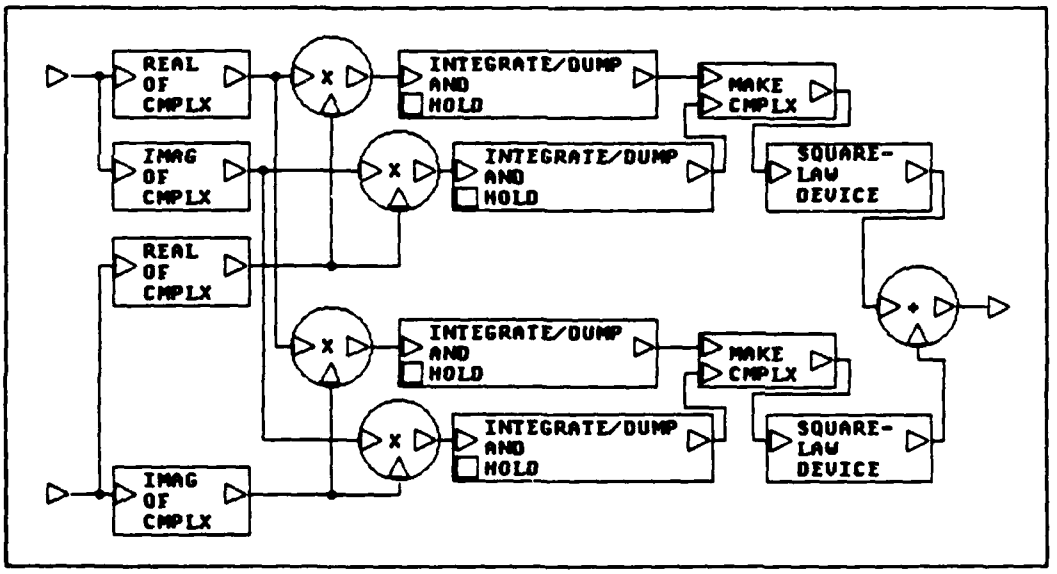

Figure 35. Quadrature Correlator

The real and imaginary components of the received signal are individually multiplied by the real and imaginary outputs of the local PN code-modulated carrier. The local PN code-modulated carrier is a complex signal with the real and imaginary components corresponding to the required replica signals for the in-phase and quadrature channels as given below:

$$s_I(t) = \sqrt{2P} \cdot PN_I(t+\tau)\cos(w_o t+\phi) \tag{51}$$

$$s_Q(t) = \sqrt{2P} \cdot PN_Q(t+\tau)\sin(w_o t+\phi) \tag{52}$$

The integrate-and-dump circuit is a modified version of the Integrate And_Dump module provided by BOSS. The modification shown in Figure 36 provides the necessary gain and the control elements to output the integration value at the end of a every PN code period. The output of the integrator circuits is given by Eq (16) and repeated below:

$$\int_0^{nT_c} x_I(t)dt = P \cdot d_I(t) \int_0^{nT_c} PN_I(t)PN_I(t+\tau)\cos\phi[1+\cos 2w_o t]dt + P \cdot d_Q(t) \int_0^{nT_c} PN_Q(t)PN_I(t+\tau)\sin\phi[1-\cos 2w_o t]dt \tag{16}$$

The gain of integrator circuits is the power given by P. With the bit energy as unity, this gain is equal to 1/Tc. This gain is provided by the Gain module and set at simulation time by the CHIP RATE parameter specified also for the PN Sequence Generator. The Impulse Train module selects

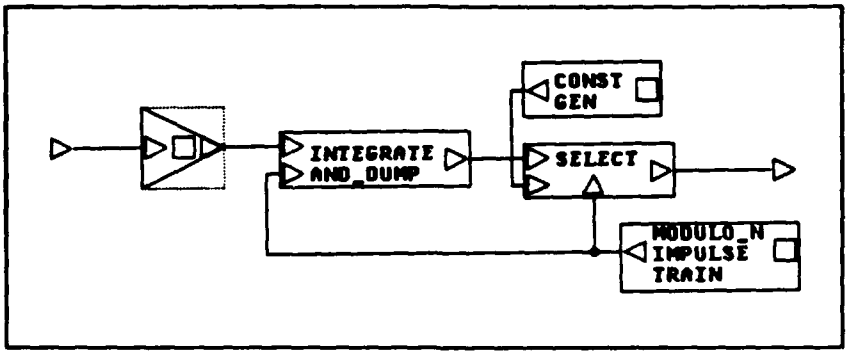

Figure 36. Integrate/Dump and Hold Circuit

the integrator output at the end of the PN code period and also resets the integrator for the start of the next period. At all other times, the output of the module is zero.

Additional System Requirements. Before the subsystem modules can be integrated, some additional modules are necessary. A module to generate the sequence for the reference channel of the matched filter is required as well as a module to generate the local reference for the quadrature correlator.

Matched Filter Reference Generator. This module loads a subsequence of the pseudonoise code into the reference channel of the matched filter. The strategy is to use the last M code chips as the reference sequence where M is the length of the filter. There are two benefits to this method: 1) the matched filter generator is enabled for one full code period and the appropriate values are loaded regardless of the filter length selected, and 2) by using the last M code chips, the correlation peak occurs at the instant of the start of a new PN code period. This prevents

initializing the local PN code generator with different initial conditions for different matched filter lengths. The correlation peak always signals the start of a new period.

The reference generator must produce a replica of the PN code-modulated carrier. To accomplish this, the locally generated reference PN sequence will modulate a carrier with the same timing epoch as accomplished in the transmitter. This method is necessary in order to produce an exact reference sequence in the alternate form taken for the matched filter.

The matched filter generator is shown in Figure 37. The load sequence takes place in the first PN code period of the simulation. The PN generator is driven by the impulse train at the specified chip rate and then modulates a carrier at the specifed frequency. At the end of the code period, the reference generator output is disabled. The reference signal is loaded in the matched filter in a time-reversed orientation and locked in the reference channel.

The reference generator has two output signals. The REFERENCE OUTPUT signal is the desired reference sequence. The REFERENCE LOAD ENABLE signal is a logical output that enables the sample-and-hold modules of the matched filter. The timing of the enable signal is controlled by the RESET SAMPLE # parameter and is set for the end of the code sequence. The CHIP RATE and CARRIER FREQUENCY parameters are set to match the parameters of the transmitter.

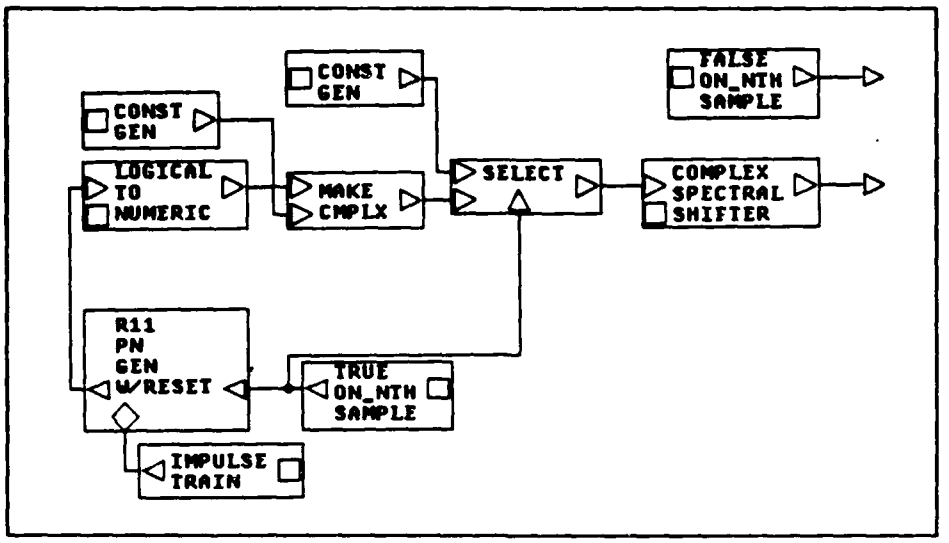

Figure 37. Matched Filter Reference Generator

Local Reference Generator. This module produces the local reference required at the input to the quadrature correlator. This module is similar to the Matched Filter Reference Generator described above. The reference signal for the quadrature correlator must be a complete complex signal. The real and imaginary parts provide reference signals for the in-phase and quadrature channels of the correlator. The real part provides the PN code-modulated cosine signal while the imaginary part provides the modulated sine function. This requirement necessitates the structure shown in Figure 38. The PN code generator feeds both sides of the Make Complex module. In the matched filter case, only the real signal is required and the PN code generator must only feed the real side of the Make Complex module (see Figure 37). The reset signal to the Local Reference Generator is used to produce a reset strobe to the PN

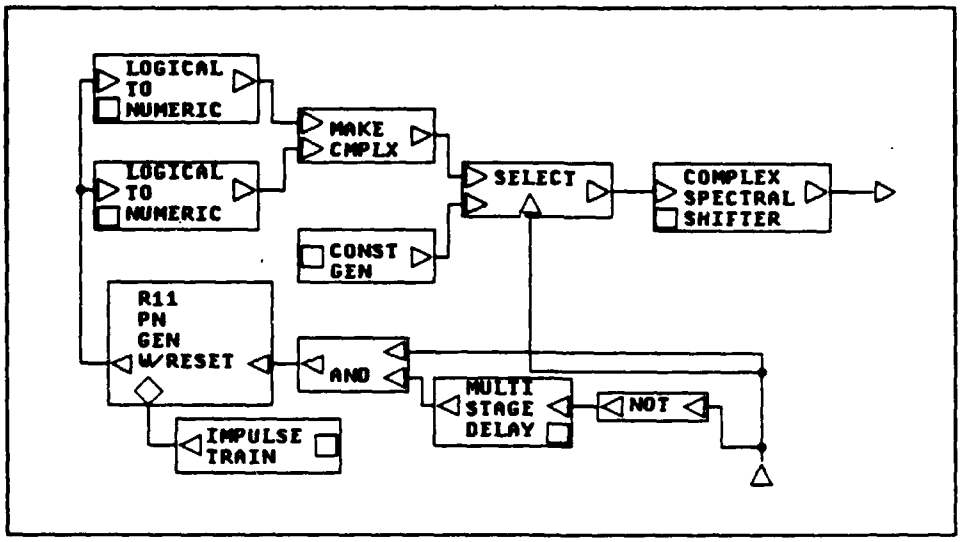

Figure 38. Local Reference Generator

Sequence Generator and select the PN code-modulated carrier for output. Once again, the CHIP RATE and CARRIER FREQUENCY parameters match the parameters of the transmitter.

Single-User System Model

The single-user system, shown below in Figure 39, is an integration of the subsystem models presented so far. The single-user system is discussed in further detail during the simulation and analysis of the next chapter.

Multiple-Access System Model

In code-division multiple-access (CDMA) all transmitters operate at the same nominal frequency and simultaneously use the entire bandwidth. The important feature of CDMA is the absence of time coordination needed between the various users in the system. Each user is assigned a unique PN code as its spreading function. Assuming synchronization at the

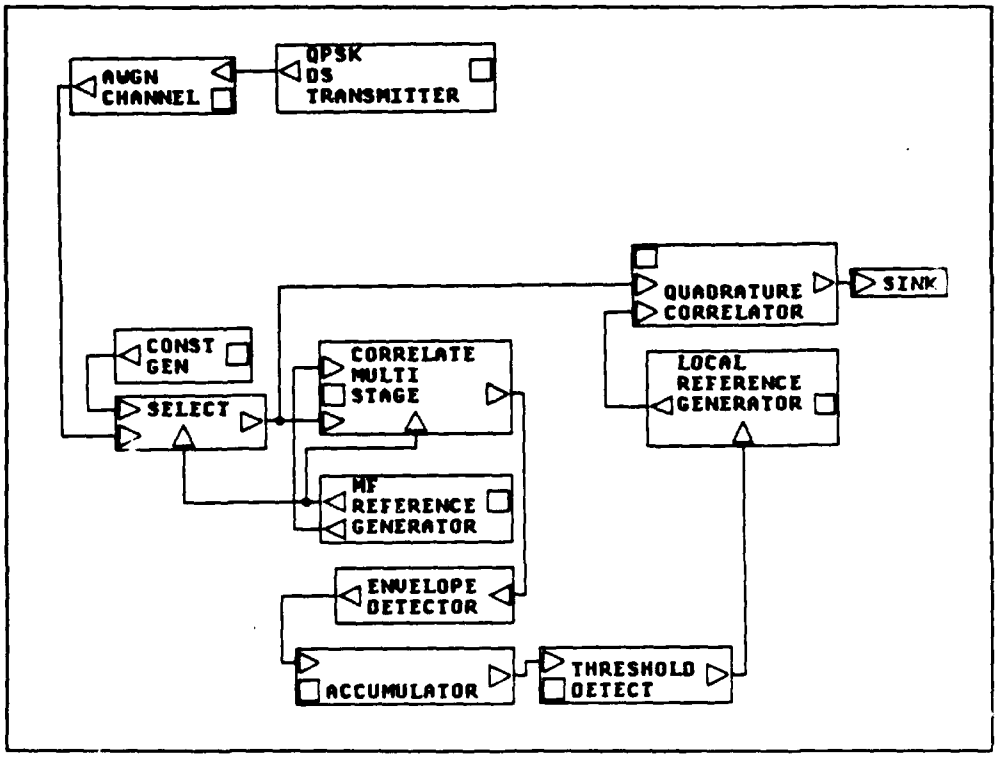

Figure 39. Single-User System

receiver, the intended user's spreading function will correlate with the identical despreading function of the receiver. Following this correlation, only the original, modulated waveform remains. Other transmitted waveforms appearing at this receiver will not be correlated and are effectively spread and appear as noise to the demodulator (17:268-271).

The correlation noise is minimized with the utilization of sets of PN sequences with low cross-correlation properties. As seen in the analytic evaluation, the reduction of the cross-correlation noise power and associated increase in the output signal-to-noise ratio of the correlation receiver is an important factor in maximizing the

total number of simultaneous users. For maximal length sequences, as used in this system, only small sets (five or less) can have good cross-correlation properties. Large sets of maximal length sequences generally have poor cross-correlation properties and are typically not suitable for a large number of users in a CDMA system (17:281).

For the multiple-access simulation model, the number of other users is set at four. The QPSK Direct Sequence Transmitter will act as the target transmitter. The spreading code for the target transmitter is the maximal length sequence generated by the PN Sequence Generator. The transmitter model for the other users is shown in Figure 40.

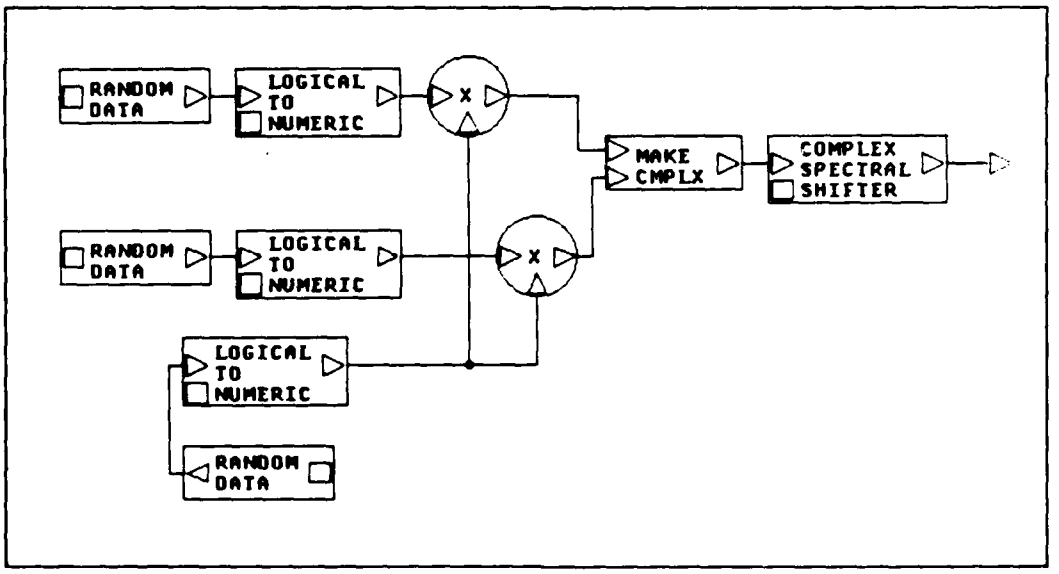

Figure 40. Multiple-Access Transmitter

This transmitter is identical to the QPSK Direct Sequence Transmitter shown in Figure 27 with the exception of the source for the spreading code. For the Multiple-Access

Transmitter, the Random Data module provides a random data stream as the spreading function. It has been shown that purely random sequences provide slightly better CDMA performance than maximal length PN codes. This difference can be made negligibly small by a judicious selection of the PN sequences used (18:33.3.1). Since the simulation effort is to distinguish the target transmitter only, use of the random data spreading codes is further justified.

The transmitter set for the multiple-access system is shown in Figure 41. Carrier frequencies for all four transmitters are set to the same frequency by the single parameter TARGET CARRIER FREQUENCY. The seeds for the random spreading codes of each Multiple-Access Transmitter are

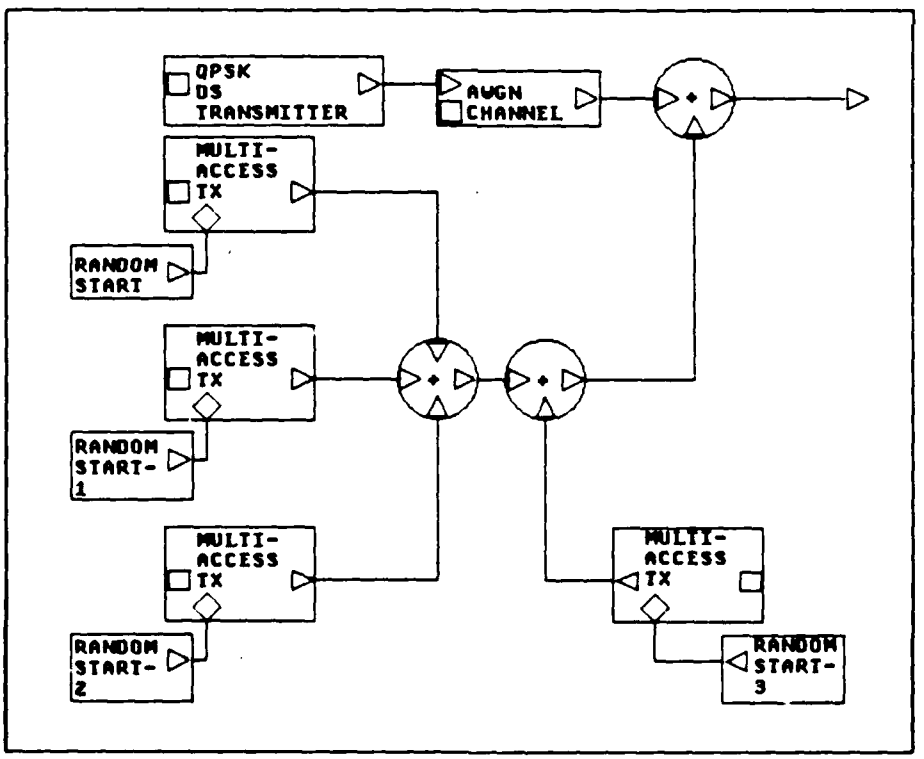

Figure 41. Multiple-Access Transmitter Set

different and preset. The DATA RATE and CHIP RATE parameters for each Multiple-Access Transmitter are available for specification as are the TARGET DATA RATE and TARGET CHIP RATE parameters for the target transmitter. Additive white Gaussian noise (AWGN) is specified with two parameters. The one-sided bandwidth is set with the parameter NOISE BW and the output signal-to-noise ratio is set with the parameter SNR (DB). The Random Start modules ensure asynchronous operation of the transmitters.

The multiple-access system is shown in Figure 42. Parameter designations in the individual modules are assigned to facilitate specification at simulation time. The single specification of the parameters for the target transmitter's carrier frequency and chip rate also specifies associated parameters in other modules. The parameter TARGET CARRIER FREQUENCY sets the carrier frequencies for the other multiple-access transmitters and sets the receiver's local carrier frequency in the matched filter and local reference generators. The TARGET CHIP RATE parameter also sets the chip rate in matched filter and local reference generators as well as the gain for the quadrature correlator. Simultaneous specification of these parameters reduces the simulation effort and avoids possible input errors.

Each of the primary modules-the PN Sequence Generator, the QPSK Direct Sequence Transmitter, the Matched Filter Channel, and the Quadrature Correlator were simulated to confirm operability. These simulations also indirectly

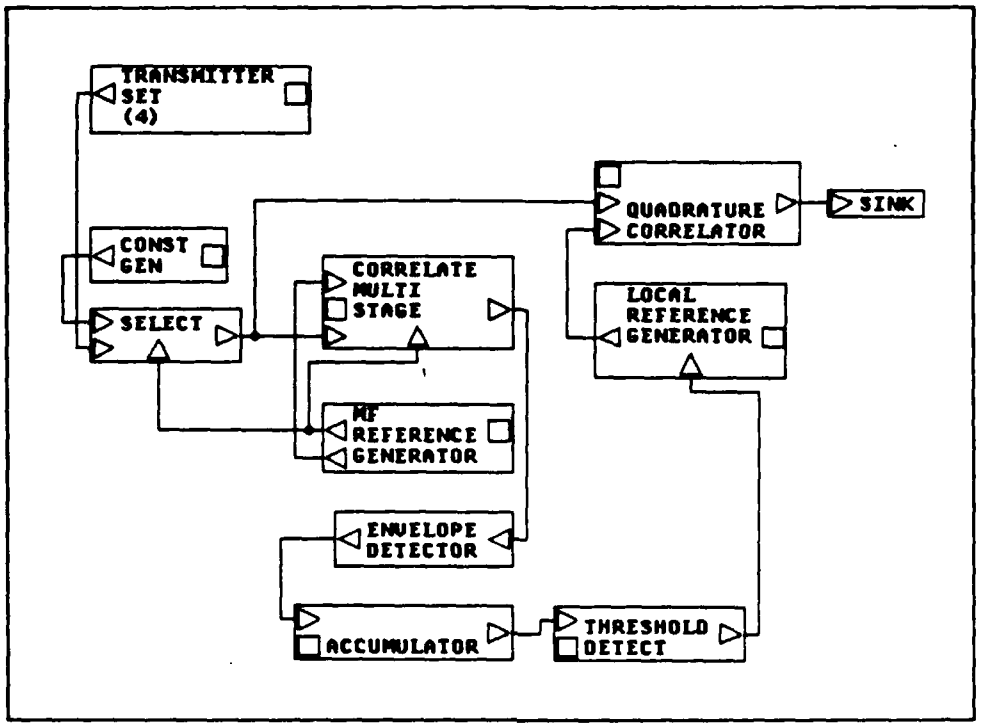

Figure 42. Multiple-Access System

confirmed operability for the Matched Filter Reference Generator and Local Reference Generator modules. The simulation results are documented in the Appendix.

In the next chapter, system operability will be confirmed through simulation of the Single-User System. Further simulations will then examine the performance characteristics of interest.

V. Simulation Results

Each of the subsystem simulation models described in Chapter IV have been validated with methods and results documented in the Appendix. The primary purpose of the validation is to verify the simulation model prior to commitment to time-consuming Monte-Carlo simulations. The length of the validation simulations are set to adequately verify the expected end-to-end behavior of a system or characterize the input/output behavior of the subsystem modules.

The validation mode of simulation is also a highly flexible and useful tool in conceptual communication system studies. It develops a useful and realistic appreciation of actual system behavior and serves as a useful adjunct to detailed analysis (8:58). Development of a model that will allow a realistic appreciation of actual system behavior under a variety of scenarios is the goal of the simulation effort. However, a simulation model must be proven against theoretical expectations before it can be freely exercised. Extensive simulation against the analytic expectations developed in Chapter III is the immediate concern. Before proceeding into extensive simulation, it is necessary to examine the system, review the analytic expectations, and determine which system performance characteristics can be effectively explored via simulation.

Simulation Approach

The mean acquisition time is the performance characteristic of interest. As shown in Chapter III, the performance of the matched filter as a function of input signal-to-noise ratios, matched filter length, and the number of other users in the system directly influences the acquisition time performance. Specifically, the matched filter output signal must be tested against the single and multiple-pulse detection requirements for a specified P_{fa}. If the matched filter output meets the specified false alarm rate, the incoming PN code will be successfully acquired in a known time frame. The accumulator threshold is set to process the required number of correlation peaks out of the matched filter prior to initiating the local PN generator. The number of correlation peaks necessary, and therefore the acquisition time, is specified by the multiple-pulse detection requirements given in Figure 10.

The first step is to confirm system operability. The single-user input is used to validate the system simulation model. Following validation, a series of simulations will characterize matched filter performance for both the single user and multiple-access inputs. Within this series of simulations, the first set will quantify the level of partial autocorrelation noise produced by the matched filter.

The next set of simulations will determine the matched filter peak output SNR over a selected range of input signal-to-noise ratios and matched filter lengths. From

these results, appropriate threshold levels will be determined for the theoretical single-pulse or multiple-pulse detection requirements. Simulations will then test the matched filter against the detection requirements for a specified probability of false alarm. The objective is to actively test matched filter performance against theoretical expectations. If successful, the simulation model is proven suitable to simulate realistic operating scenarios.

System Validation

The single-user system serves as the base simulation platform. The purpose of the validation with the single-user system is to demonstrate that the subsystem models will perform as expected in an integrated system. The single-user system is presented below in Figure 43.

A single transmitter with an additive white Gaussian noise (AWGN) channel is implemented. At the end of the initial load sequence, the Matched Filter Reference Generator sends a ready signal to select the transmitter output. The output of the Quadrature Correlator is terminated into a SINK module-the focus of the simulation effort is in examining the initial acquisition characteristics.

Simulation Parameters. In order to offer flexibility at simulation time, several key parameters are available for specification. For the transmitter, the parameters DATA RATE, CHIP RATE, and CARRIER FREQUENCY are set in units of Hertz. Note that the one-time specification of the CHIP RATE

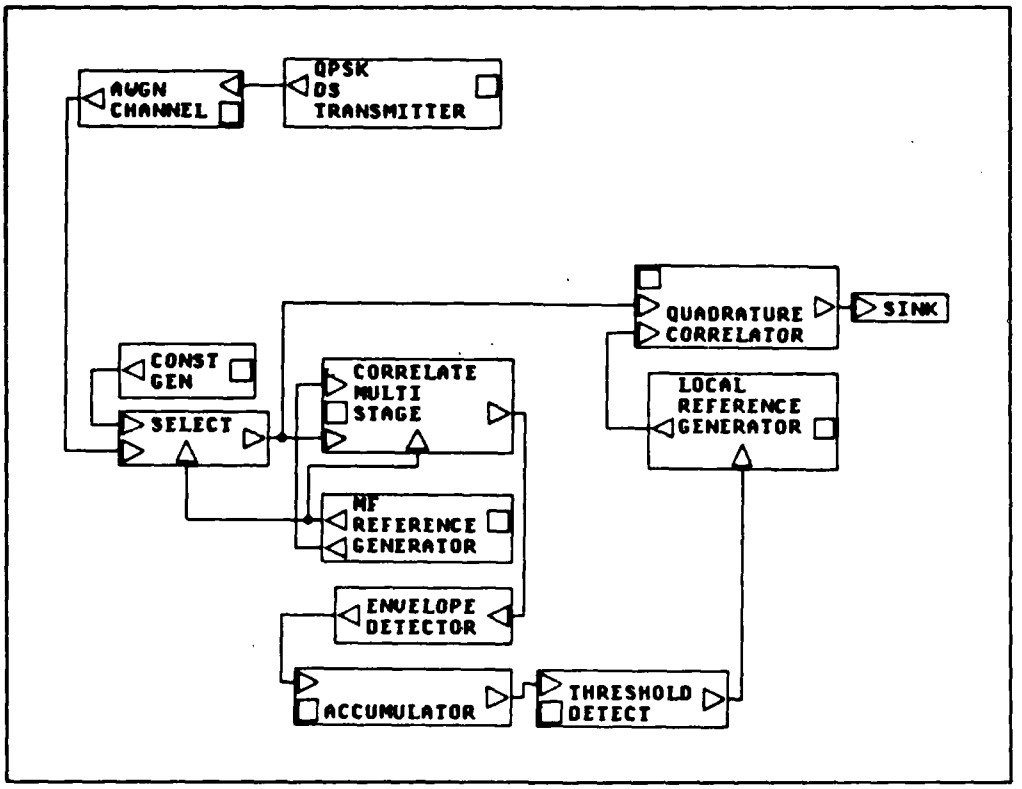

Figure 43. Single-User System

and CARRIER FREQUENCY parameters not only sets the rates for the transmitter, but also sets rates in the Matched Filter and Local Reference Generators. Additionally, the CHIP RATE parameter establishes the gain of the Quadrature Correlator. The noise channel has parameters to specify the signal-to-noise ratio (SNR), noise bandwidth (NOISE BW), and the time noise is activated (NOISE ON-TIME).

At the receiver, the matched filter is specified with the parameter # OF STAGES. The maximum length of the matched filter is 2047 stages. The remaining parameter for the Matched Filter Reference Generator specifies the number of samples in one PN code period. This parameter, #SAMPLES/PN

PERIOD, stops the load sequence of the matched filter reference channel, locks in the reference values, and selects the transmitter output.

The accumulator has four delay modules to provide a total delay equal to a full PN code period. The required input for the parameter 0.25*SAMPLES/PERIOD is one-quarter of the number of samples in a single PN period. The output of the accumulator is compared against a threshold value. The threshold is set with the parameter ACCUMULATOR THRESHOLD.

Many of the above parameters, such as RESET SAMPLE # and NOISE BW, will not change through a series of simulations. These parameters are preset. The remaining parameters are exported for specification at each simulation. In order to confirm the system model operates as intended, the exported parameters were specified as shown in Table 2.

Table 2. Validation Parameters

STOP-TIME = 6.2E-3
DT = 6.25e-8
SNR (DB) = 10
NOISE ON-TIME = 6.2E-3
ACCUMULATOR THRESHOLD = 60000.0
OF MF STAGES = 128
DATA RATE(HZ) = 1200
CHIP RATE (HZ) = 2.0e6
CARRIER FREQUENCY (HZ) = 4.0e6

Simulation Results. A matched filter length of 128 stages was arbitrarily chosen for the validation simulation. The threshold value was set to require the processing of four

correlation peaks (four PN code periods) at the output of the envelope detector output. The additive white Gaussian noise (AWGN) is disabled for the validation.

During the first PN code period of the simulation, the matched filter is loaded with the reference sequence. At the end of the next period, the matched filter output displays a full correlation peak as shown in Figure 44. With the length of the filter equal to 128, the amplitude of the main correlation peak is also this same value.

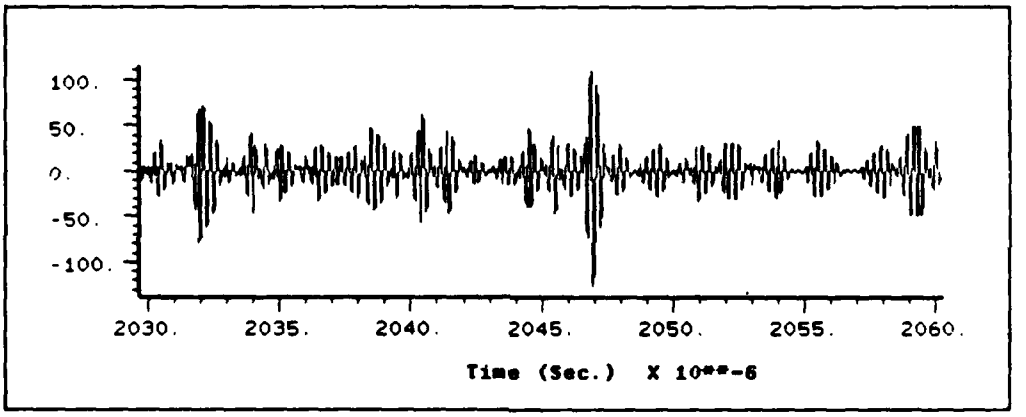

Figure 44. Matched Filter Output

The output of the accumulator exceeded the threshold value at 5.1175 milliseconds, or five PN code periods into the simulation. With the matched filter load sequence occuring in the first period, the accumulator output breaks the threshold value of 60,000 in the expected time frame as shown in Figure 45. And in response, the output of the threshold detector moves to a logical true value as shown in Figure 46. This transition initiates the Local Reference Generator as shown in Figure 47.

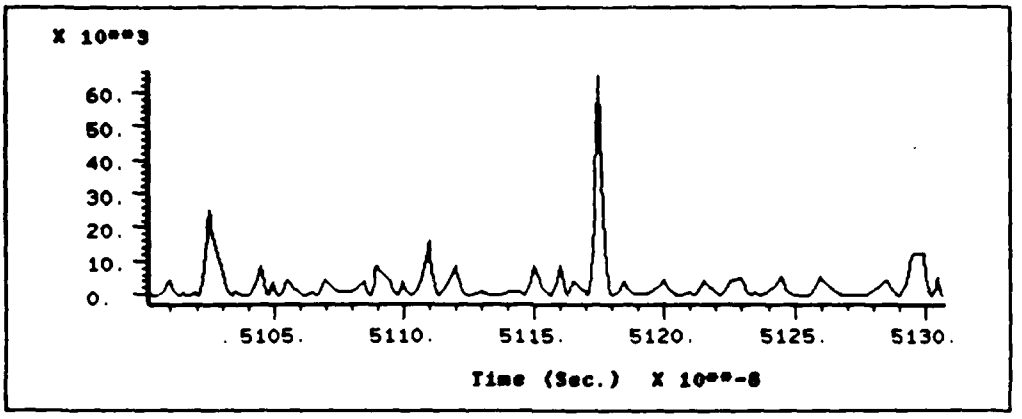

Figure 45. Accumulator Output

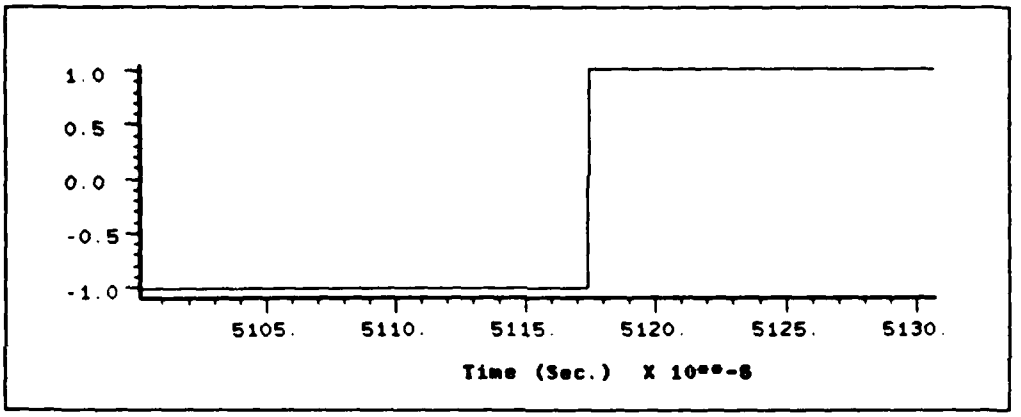

Figure 46. Threshold Detector Output

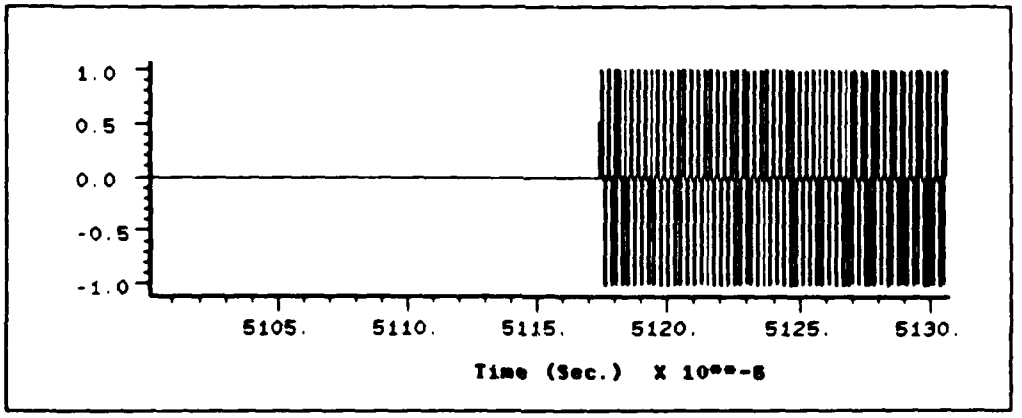

Figure 47. Local Reference Generator Output

The Quadrature Correlator is now activated for full-period correlation of the incoming signals. Figure 48 shows the

correlator output at the end of one PN code period following initiation of the Local Reference Generator. The correlation peak achieves the expected maximum value of $8.380418 \cdot 10^6$ indicating synchronization with the received signal.

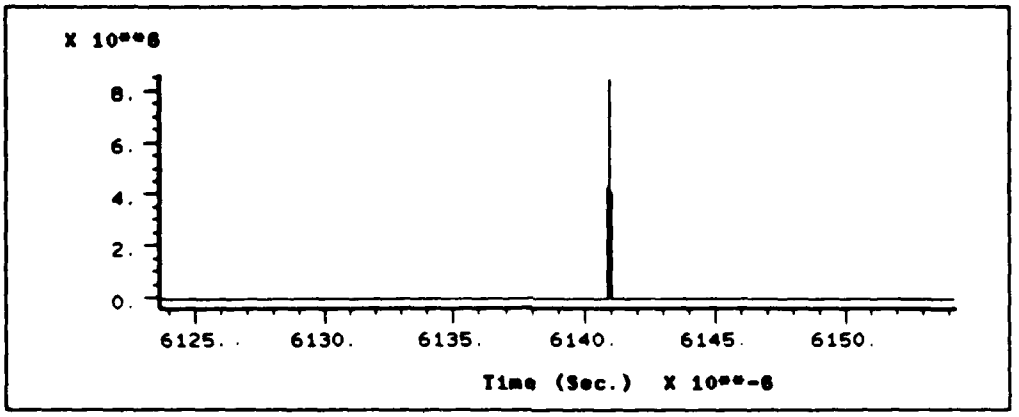

Figure 48. Quadrature Correlator Output

The results of this simulation coupled with the subsystem simulations given in the Appendix validate system operability of the model. The next task is to confirm matched filter performance.

Matched Filter Performance

The operating characteristics of the matched filter is the key to system performance. For a given signal-to-noise ratio and probability of detection, the matched filter output will be examined to determine if the correlation peaks occur at the expected value for the specified probability of false alarm (P_{fa}).

Determination of the P_{fa} via simulation is a multi-step process. First, the average noise power at the output of the

matched filter is determined via simulation over a selected range of matched filter lengths and input signal-to-noise ratios. The associated peak output signal-to-noise ratios are then determined analytically. The peak output SNR distinguishes whether the matched filter at a particular length and input SNR can perform at single or multiple-pulse detection requirements for a specified P_{fa}. Appropriate threshold values are then set to confirm matched filter performance at the specified P_{fa}.

Matched Filter Output Noise Power. The test system to determine the average noise power for the single-user system is shown in Figure 49. The test system for the multiple access system uses the same configuration as the single-user

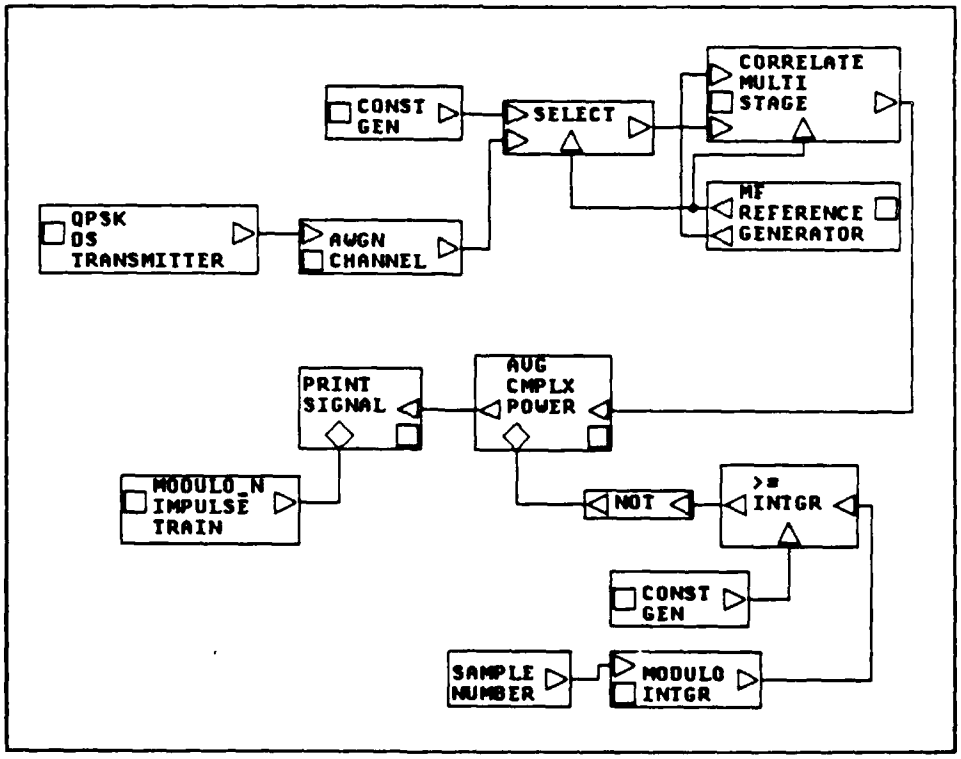

Figure 49. Matched Filter Noise Test System

system except with the multi-transmitter input. The output of the matched filter is fed to the Avg Cmplx Power module. This module computes the average output power. In order to get an accurate measure of the noise, the module is disabled while a main correlation peak occurs and is also disabled during the initial matched filter loading period.

The results of the simulations are given in Tables 3 and 4 and reflect average noise power given an input signal of unit amplitude. The lengths selected for the matched filter and the values chosen for the input signal-to-noise ratios will be consistent throughout subsequent simulations.

Table 3. Single-User Output Noise Power

MF Length	Target Transmitter SNR Levels				
	No Noise	3dB	0dB	-3dB	-6dB
64	627.3	731.4	839.0	1061.1	1497.4
128	1305.1	1515.7	1733.6	2163.4	3038.7
256	2610.9	3034.6	3478.6	4377.4	6179.1
512	5231.3	6081.7	6945.1	8675.0	11922.3
1024	9658.9	11280.4	12952.9	16314.7	22723.5

As seen in the first column of Table 3, the partial autocorrelation characteristics of the PN code introduces a significant amount of noise at the output of the matched filter. To quantify the bias introduced by this noise, the peak output SNR must be determined. The peak signal power is given by squaring the amplitude of the main correlation peak.

Table 4. Multi-User Output Noise Power

MF Length	Target Transmitter SNR Levels				
	No Noise	3dB	0dB	-3dB	-6dB
64	2754.4	2876.6	2983.1	3143.8	3528.0
128	5816.7	6043.3	6252.0	6651.5	7454.6
256	11694.6	12323.7	12822.1	13388.2	15036.9
512	24024.8	25130.7	26042.1	27076.8	30145.2
1024	44973.1	46304.1	47731.9	50623.3	56452.8

As shown in Chapter III, the expected value of this amplitude is equal to the length of the filter. This method provides the peak output SNR results given in Tables 5 and 6. Recall that the peak output SNR is the key element in determining acquisition time performance.

Table 5. Single-User Peak Output SNR (dB)

MF Length	Target Transmitter SNR Levels				
	No Noise	3dB	0dB	-3dB	-6dB
64	8.15	7.48	6.89	5.86	4.37
128	10.99	10.34	9.75	8.79	7.32
256	13.99	13.34	12.75	11.75	10.26
512	17.00	16.35	15.77	14.80	13.42
1024	20.36	19.68	19.08	18.08	16.64

The partial autocorrelation of the entire PN code against a segment of itself effectively introduces a bias to the input SNR. In other words, an input SNR equal to 3 dB

Table 6. Multi-User Peak Output SNR (dB)

MF Length	Target Transmitter SNR Levels				
	No Noise	3dB	0dB	-3dB	-6dB
64	1.72	1.53	1.38	1.15	0.65
128	4.50	4.33	4.18	3.92	3.42
256	7.48	7.26	7.09	6.90	6.39
512	10.38	10.18	10.03	9.86	9.39
1024	13.68	13.55	13.42	13.16	12.70

appears at the matched filter output as a lower input SNR due to the introduction of this partial autocorrelation noise. Determination of this bias allows accurate comparison of the simulation results to the expected performance. The bias is determined using the results listed in the first column of Table 5. The gain of the matched filter is equal to the length of the filter and is used to determine the effective input SNR. These results and the effective input SNR due to the multi-user influence are given in Table 7.

Table 7. Input SNR Bias

MF Length	Effective Input SNR (dB)	
	Correlation Noise Only	Correlation Noise w/ Multi-User Input
64	-9.91	-16.34
128	-10.08	-16.57
256	-10.09	-16.60
512	-10.09	-16.71
1024	-9.74	-16.43

These levels establish the upper bounds of input SNR levels for which the simulation results can be compared against the analytic expectations. The remaining peak output SNR levels given in Tables 5 and 6 are used to distinguish which matched filter lengths and associated input SNR levels can perform at the single-pulse detection requirements. The minimum peak output SNR levels for specified probabilities of false alarm were given in Figure 8 and summarized in Table 1 for a $P_d = 0.9$. The P_{fa} chosen for simulation is 10^{-3} and requires a minimum peak output SNR of 13.7 dB to meet single-pulse detection requirements. This false alarm rate can be simulated with reasonable time and memory requirements.

Matched Filter False Alarm Performance. The false alarm probability is the probability that a threshold crossing will occur during the interval of observation when the receiver input contains only noise. If a false alarm occurs in the matched filter channel, the local reference generator will be improperly initiated and the quadrature correlator will not indicate synchronization. The penalty for this false alarm is time-the full period correlation sequence of the quadrature correlator and the time expended by the matched filter. If the matched filter is in a multiple-pulse detection sequence, the time becomes significant.

In order to confirm P_{fa} performance, the threshold level must be accurately determined. There are two methods to confirm performance under single-pulse detection requirements. The first method sets the threshold level for

the signal directly at the output of the matched filter. The governing equation for this method is (16:204):

$$P_{fa} = \exp\left[\frac{\beta^2}{2}\right] \tag{53}$$

where $\beta = \alpha/\sigma_T$. The threshold value (α) necessary to test for a particular P_{fa} is dependent on the average noise power (σ_T^2) at the sampling instant.

The second method establishes the threshold level at the output of the envelope detector. A table of bias levels $\delta = \delta(m,p)$ corresponding to the specified probability of false alarm (10^{-p}) as a function of the number of processed pulses (m) exist for $1 \leq p \leq 12$ and $1 \leq m \leq 150$ for receivers using square-law detectors (19:38-45). Given the bias level from the table and σ_T^2, the threshold level is determined by:

$$\alpha = 2 \cdot \sigma_T^2 \cdot \delta \tag{54}$$

This method is also suitable for the multiple-pulse detection tests. For $m >> 1$ and not included in the table of bias levels, the threshold level can be computed using the following equation (16:245):

$$P_{fa} = 1 - I\left[\frac{\delta}{2 \cdot \sqrt{m}}, m-1\right] \tag{55}$$

where I(x,y) is a form of the incomplete Gamma function.

Threshold Settings. The first method will be used to set the thresholds for the single-pulse detection tests. This method is simple and direct and offers a certain clarity in terms of the threshold value against the expected peak signal value. The second method was the only method found to set threshold values for the multiple-pulse detection tests.

The computed threshold settings are given in Tables 8 and 9. The asterisk (*) indicates a threshold setting for single-pulse detection requirements. If a peak output SNR falls below the minimum required for single-pulse detection but the single-pulse detection threshold is less than the expected peak signal amplitude, a single-pulse detection test will be run. These situations are indicated by a double asterisk (**). For the multiple-pulse detection thresholds, the number of pulses necessary is indicated in parenthesis.

Table 8. Single-User Threshold Levels ($P_{fa} = 10^{-3}$)

MF Length	Target Transmitter SNR Levels				
	No Noise	3dB	0dB	-3dB	-6dB
64	18.56e3 (5)	28.71e3 (8)	32.94e3 (8)	57.36e3 (13)	113.9e3 (21)
128	24.11e3 (2)	27.99e3 (2)	38.93e3 (3)	56.52e3 (4)	109.77e3 (7)
256	189.92 *	204.75 **	219.22 **	245.92 **	138.77e3 (3)
512	268.84 *	289.86 *	309.76 *	346.19 *	405.85 **
1024	365.30 *	394.77 *	423.02 *	474.76 *	560.30 *

Table 9. Multi-User Threshold Levels ($P_{fa} = 10^{-3}$)

MF Length	Multi-User Input SNR Levels				
	No Noise	3dB	0dB	-3dB	-6dB
64	458.35e3 (57)	506.3e3 (61)	539.3e3 (63)	620.7e3 (70)	845.7e3 (88)
128	426.96e3 (20)	475.9e3 (22)	508.9e3 (23)	593.8e3 (26)	742.5e3 (30)
256	459.04e3 (8)	483.7e3 (8)	503.3e3 (8)	566.5e3 (9)	725.8e3 (11)
512	443.18e3 (2)	564.4e3 (3)	584.9e3 (3)	608.1e3 (3)	787.5e3 (4)
1024	788.24 **	799.82 **	812.10 **	836.29 **	883.12 **

The next step is to determine how long the simulations must run in order to confirm performance at a particular probability of false alarm.

False Alarm Performance Results. As stated in Chapter II, the rule of thumb is to run the simulation long enough to count at least ten errors. For a specific P_{fa}, the period of simulation is equal to $10/P_{fa}$ times the interval over which a false alarm can occur. The interval over which a false alarm can occur is different for single-pulse and multiple-pulse detection sequences.

For the single-pulse detection sequences, a false alarm can occur over any two-chip period. The matched filter continuously correlates its reference sequence with the incoming signal and the main correlation peak occurs over a two-chip period. During all other two-chip intervals, a

correlation peak exceeding the specified threshold can occur due to noise or the cross-correlation characteristics of the input signal. Therefore, the length of all simulations testing P_{fa} for single-pulse detections is set according to:

$$\text{STOP TIME} = \frac{10}{P_{fa}} \cdot DT \cdot \left[\frac{\text{Samples}}{\text{Chip}}\right] \cdot (2 \text{ Chips}) \qquad (56)$$

The time at which the simulation is stopped is designated by the parameter STOP TIME and the interval between sampling instants is DT-the discrete time interval. The discrete time interval is set such that 8 to 16 samples occur per PN code chip.

The interval over which a false alarm can occur for multiple-pulse detection sequences is the number of pulses to be processed times an entire PN code period. The threshold value for a multiple-pulse detection sequence is crossed by the accumulated amplitude of the number of processed pulses. The length of all simulations testing P_{fa} for multiple-pulse detections is set according to the equation:

$$\text{STOP TIME} = \frac{10}{P_{fa}} \cdot DT \cdot \left[\frac{\text{Samples}}{\text{Chip}}\right] \cdot \left[\frac{\text{\# Chips}}{\text{PN Period}}\right] \cdot (\text{\# Pulses}) \qquad (57)$$

Obviously, the length of simulations to characterize multiple-pulse detection requirements are excessive.

For the single-pulse detection sequences, the matched filter channel will be characterized for a P_{fa} equal to 10^{-3}. Simulations at this P_{fa} can be accomplished in 5-6 hours per table entry. Simulations at lower values of P_{fa} become excessive in terms of time and memory requirements. A validation simulation will be run for the multiple-pulse detection sequences. In other words, the simulation will verify that the specified threshold is crossed in the expected time frame. The time required to verify multiple-pulse detection performance at a reasonable P_{fa} extends well beyond the gain in terms of insight to system performance.

As discussed in Chapter II, simulations of this nature are an exercise in counting errors. The test system for the single-pulse detection requirements is shown in Figure 50. This test system simply counts the number of threshold crossings over the simulation period. Two threshold crossing counts are taken. The first count tracks the number of threshold crossings during the period which only noise is present. This count provides the numbers necessary for P_{fa} calculations. The second count provides the total number of crossings. This number is used as a check to insure the signal is detected when present.

The test system to validate the multiple-pulse detection requirements is shown in Figure 51. In this system, the threshold value is set according to values in Tables 8 and 9. When the threshold is crossed, the simulation will automatically terminate and the time at which the threshold

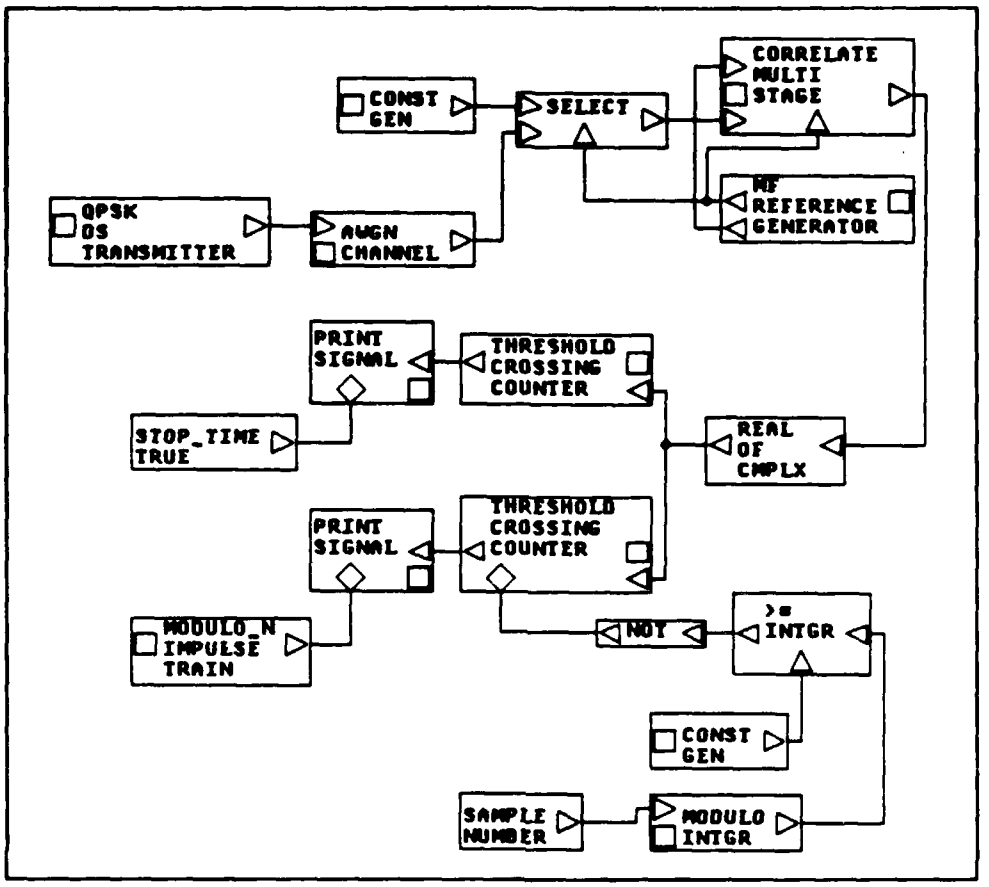

Figure 50. Single-Pulse Detection Test System

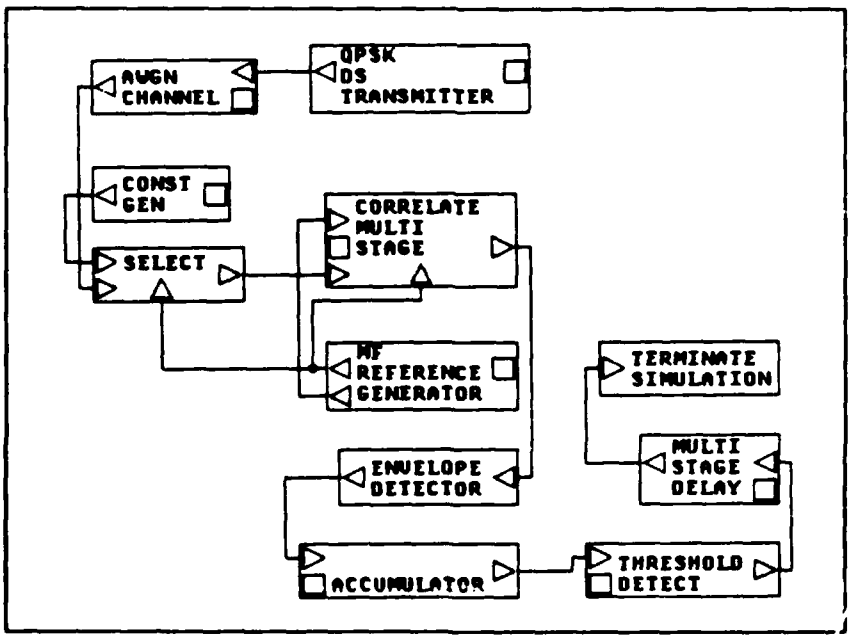

Figure 51. Multiple-Pulse Detection Test System

is crossed will be recorded. This time period is then matched against the expected time frames. The single-user input depicted in each of the above test systems is substituted with the multi-user input as necessary.

The results of the P_{fa} simulations are given in Tables 10 and 11. In the single-pulse detection tests, the result is a value for false alarm performance. The multiple-pulse detection tests are validation simulations which yield pass or fail results.

Table 10. Single-User P_{fa} Results

MF Length	Target Transmitter SNR Levels				
	No Noise	3dB	0dB	-3dB	-6dB
64	Pass	Fail	Fail	Fail	Fail
128	Pass	Pass	Pass	Pass	Pass
256	0.69e-3	0.50e-3	0.20e-3	<1.0e-3	Pass
512	1.19e-3	1.09e-3	0.89e-3	0.69e-3	0.30e-3
1024	1.39e-3	1.39e-3	1.39e-3	1.09e-3	0.89e-3

Table 11. Multi-User P_{fa} Results

MF Length	Target Transmitter SNR Levels				
	No Noise	3dB	0dB	-3dB	-6dB
128	Fail	Fail	Fail	Fail	Fail
256	Pass	Pass	Pass	Fail	Fail
512	Pass	Pass	Pass	Pass	Pass
1024	0.20e-3	0.20e-3	0.20e-3	0.20e-3	0.20e-3

For a matched filter of length equal to 64 stages, the multiple-pulse detection tests failed with the single-user input. These failures are attributed to the high level of partial autocorrelation noise produced by the selected code. These correlation peaks add linearly from period to period. This noise coupled with the AWGN consistently produced failure indications even with threshold level and time period adjustments. This filter length was therefore not simulated with the multiple-user input. At shorter matched filter lengths, performance becomes increasingly sensitive to the correlation noise produced by the selected PN code. It is reasonable to assume that a PN code with lower partial autocorrelation characteristics would produce favorable results at these matched filter lengths.

In the multi-user system, code selection is a significant consideration. Ideally, a set of orthogonal codes is used. In the simulation, the effort did not entail a code selection process for the multi-user system-detection of the single target transmitter was the objective. Therefore, random sequence generators substituted controlled code generation by the other users. The impact was increased cross-correlation noise and higher threshold levels. The effect was significant at a matched filter of length equal to 128 stages. Once again, it is reasonable to assume that careful code selection would produce favorable results at these matched filter lengths.

The remaining results confirm the expected performance characteristics. All single-pulse detection tests were successful. The validation tests for multiple-pulse detections were also successful at the longer matched filter lengths. Sensitivity to the correlation noise at these matched filter lengths was not a factor. It is highly probable that the successful validation simulations would also prove successful with the longer simulations necessary to confirm false alarm performance. Recognizing the impact of code selection and the correlation noise produced by the selected PN code, the simulation model is suitable to provide a realistic appreciation of actual system behavior under a variety of scenarios.

VI. Conclusion and Recommendations

Conclusions

The primary objective of this study has been to investigate the performance characteristics of a synchronization system that uses an auxiliary matched filter channel to speed acquisition time. A quantitative analysis was conducted to characterize mean acquisition time under varying conditions of matched filter length, noise levels, and number of users in the system. A simulation model of the synchronization system was constructed using the Block Oriented Systems Simulator (BOSS). The objective for simulation was to confirm the analytic expectations and provide a proven simulation model for further system analysis.

The quantitative results indicate that the auxiliary matched filter channel improves acquisition time. For signal-to-noise ratios above 0dB and a particular matched filter length, the mean acquisition time was directly a function of the number of users in the system. Also, mean acquisition time was significantly improved for signal-to-noise ratios above 0dB. As one example, for a matched filter length of 128 stages and 64 users in the system, the matched filter channel provides a gain in acquisition time of 156 over the active correlator operating alone. As the signal-to-noise ratio decreases below 0dB, the variation in mean acquisition time caused by the number of users rapidly

declines. For signal-to-noise ratios below -18dB, mean acquisition time is almost directly related to the noise level-irrespective of the number of users. Mean acquisition time asymptotically approaches a doubling in time for each 1.5 dB decrease in the signal-to-noise ratio.

The simulation results confirmed the analytic expectations for false alarm performance of the matched filter channel. All single-pulse detection requirements at the specified P_{fa} were favorably confirmed. Multiple-pulse detection requirements were favorably validated with shorter simulations. The false alarm interval for the multiple-pulse detection requirements was too lengthy to confirm performance at the specified P_{fa}.

Exceptions to the multiple-pulse detection results were noted due to the high partial autocorrelation noise produced by the selected PN code. The noise generated at the output of the matched filter by this correlation of the selected PN code and its reference segment was significant. The shorter matched filter lengths proved sensitive to the linearly additive qualities of the correlation noise under the multiple-pulse detection tests.

The simulated probability of false alarm was restricted to 10^{-3}. Simulation times for lower false alarm rates were excessive. The BOSS provided a highly flexible simulation environment. The system model includes flexibilities to adjust matched filter lengths, noise levels, and threshold levels. With a minimum of effort, a different pseudonoise

code may be selected, the modulation scheme adjusted, and the number of users in the system can be changed. In this effort, the simulation model was used to statically confirm the analytic expectations. The successful static tests prove suitability of the model to accurately simulate dynamic applications of system.

Recommendations

The following recommendations are proposed for further study:

1. A number of proposed systems use a similar configuration to speed code acquisition (12; 14; 20; 21; 22). None of these systems, however, implement an accumulator circuit. Additionally, Smirnov does not describe dynamic operation of the accumulator. Methods to control the accumulator should be explored. Control modules for the accumulator can be added to the present simulation model to dynamically simulate and analyze system performance.

2. A standard Monte Carlo technique was used to test false alarm performance. For probability of false alarm values below 10^{-3}, the simulation times were excessive. A modified Monte Carlo technique such as importance sampling could significantly reduce simulation times and allow performance evaluations at more desirable false alarm rates. Modified Monte Carlo techniques should be investigated and implemented for the BOSS.

Appendix: Simulation Model Validations

The purpose of this appendix is to validate the simulation models presented in Chapter III. The emphasis in the validation phase is to show that the models operate as intended. The simulation parameters are set at the minimum necessary to confirm expected input/output behavior.

Pseudonoise Sequence Generator

The first test of the PN generator confirms the length and character of the code. The reset feature of the generator is then tested. The configuration for both tests is shown in Figure 52.

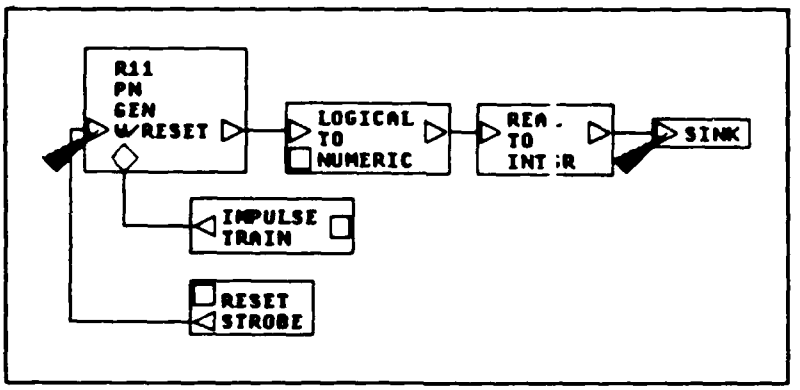

Figure 52. PN Generator Test

An impulse train controls the chip rate of the PN generator. The system parameter, CHIP RATE, is set throughout the validations at 2 MHz. The simulation is set for eight samples per chip period which requires the discrete time interval parameter, DT, to be set at $6.25 \cdot 10^{-8}$ seconds per sample. For the first test, the length of the simulation

is set to run through two complete code periods requiring a STOP TIME equal to $2.147 \cdot 10^{-3}$ seconds. The reset feature is not of interest in this test. The occurence of the reset strobe is set to the end of the simulation period. The simulation parameters are given in Table 12.

Table 12. PN Generator Validation Parameters

STOP-TIME = 2.1470001E-3
DT = 6.25e-8
RESET SAMPLE # = 17970
RESET LENGTH (#SAMPLES) = 2
CHIP RATE (HZ) = 2.0e6

The length of the code is $2^{11}-1 = 2047$ chips . At the given chip rate, the code should repeat every 1.0235 milliseconds. The signal plots of Figures 53 and 54 were taken at the probe placed at the input to the sink module.

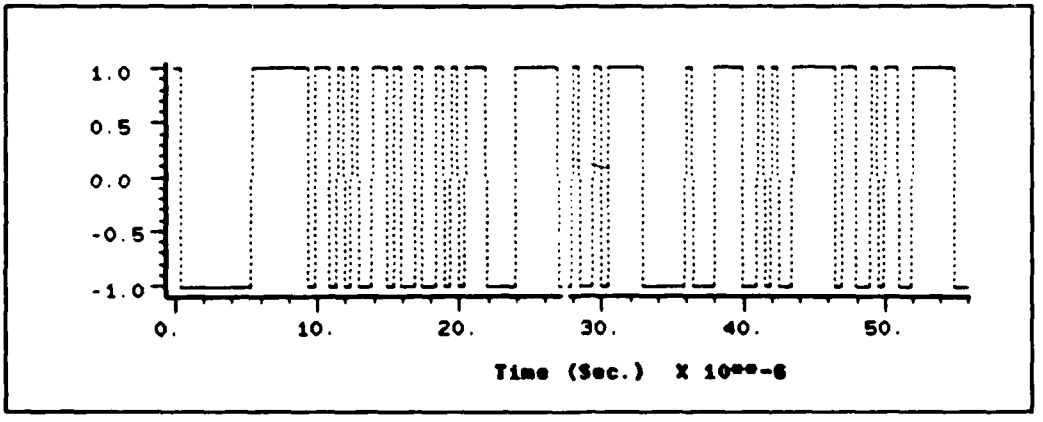

Figure 53. PN Generator Output

The signal plot of Figure 53 displays the code at the start of the simulation. The dashed presentation of the signal

plot was produced by overlaying the plot of Figure 54 which starts at 1.0235 milliseconds. The dashed line confirms that the code repeats as expected.

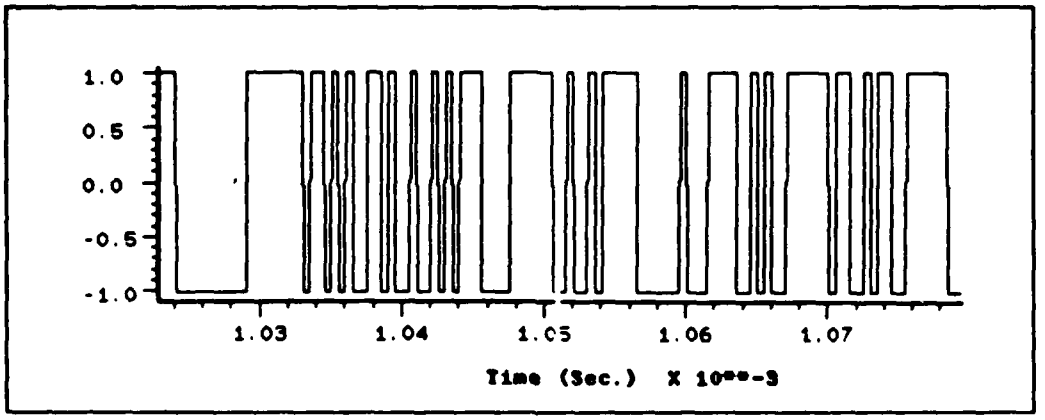

Figure 54. PN Generator Output

The autocorrelation of the PN generator output is shown in Figure 55 and at a code period later in Figure 56. As expected, the width of the autocorrelation waveform is twice the chip period and equal to one microsecond. The second correlation peak occurs at exactly one code period after the start of the sequence (1.0235 microseconds). The amplitude of the correlation peaks do not reach unity due to the sampling rate and the memory limitations of this particular post-processor function. The correlation function will correlate a maximum of 8000 samples. The plots provided use 3435 samples for the time frame to be correlated and 3435 samples for the reference sequence. The magnitude of the autocorrelation is the length of the correlation interval times the chip period which is equal to $2.146875 \cdot 10^{-4}$ as indicated.

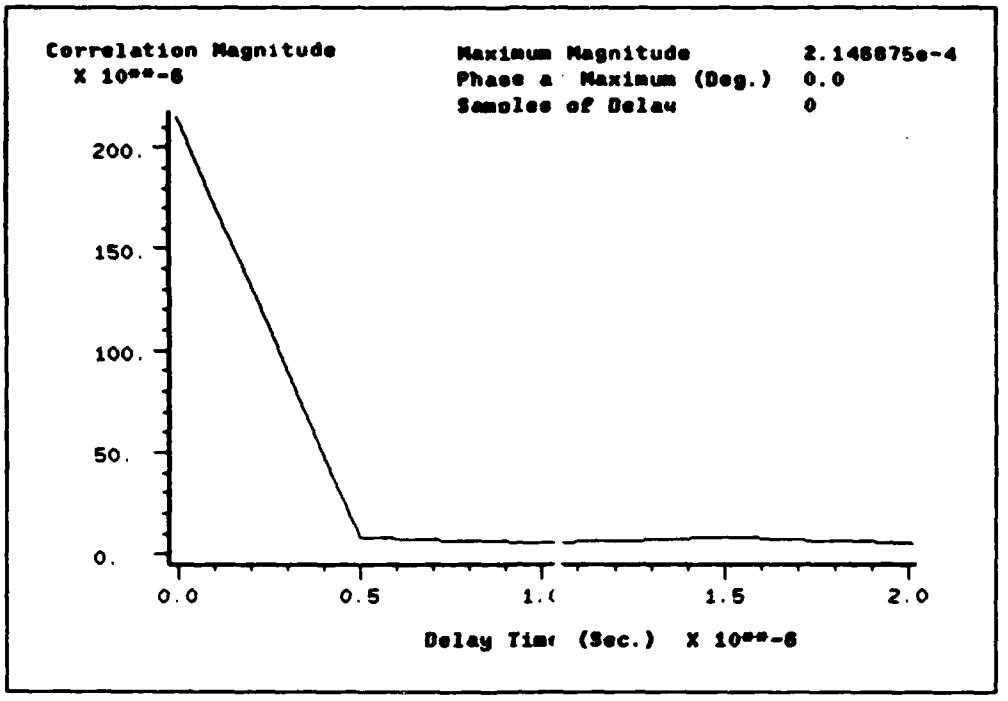

Figure 55. Autocorrelation of the PN Output

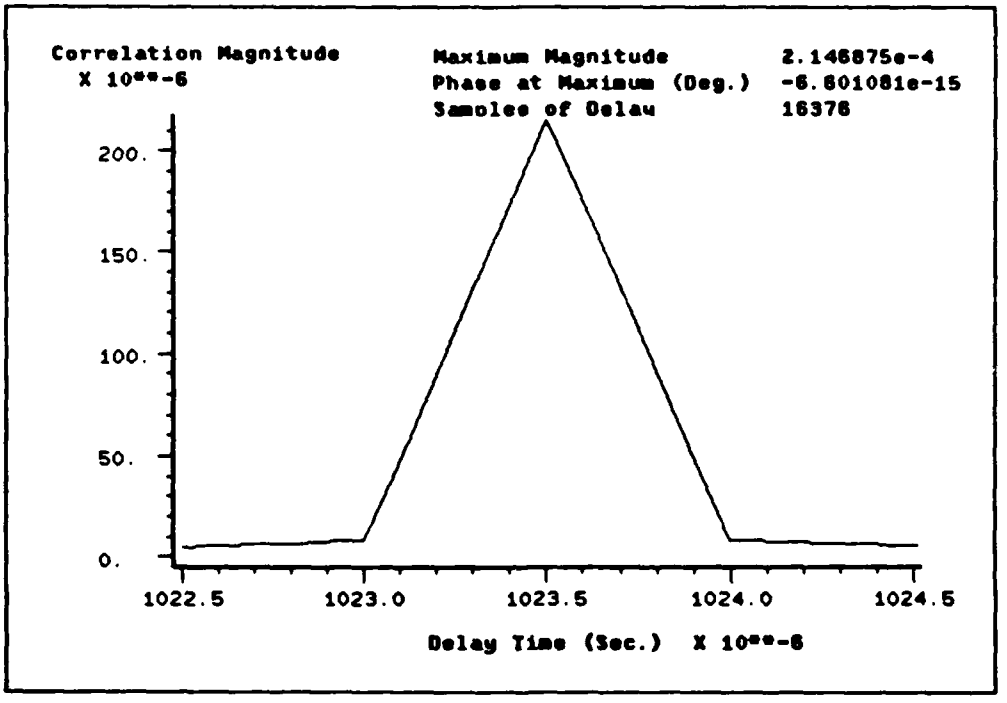

Figure 56. Autocorrelation of the PN Output

The reset feature is now tested by setting the reset strobe to occur at 250 milliseconds. As shown in Figure 57, the reset output transitions to a logical true condition for two sample periods.

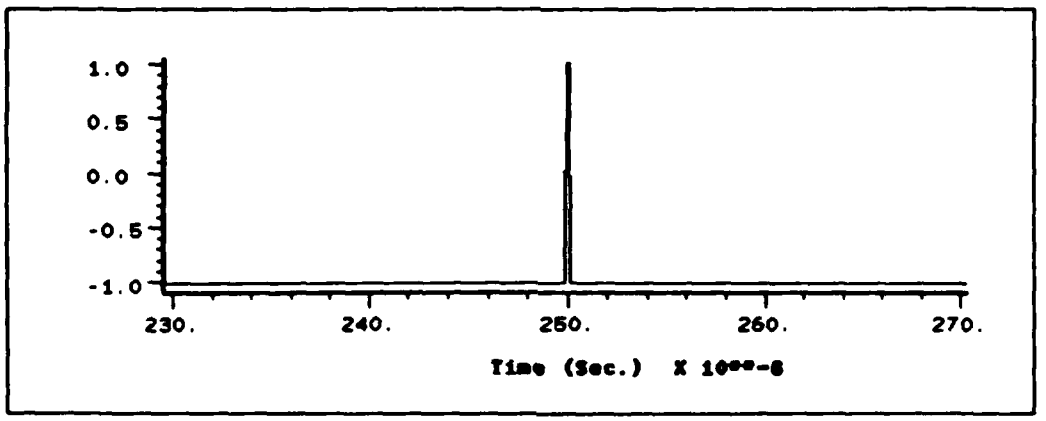

Figure 57. Reset Strobe

The strobe resets the PN Generator to the specified set of initial conditions. Figure 58 shows the initiation of a new code sequence in response to the reset signal.

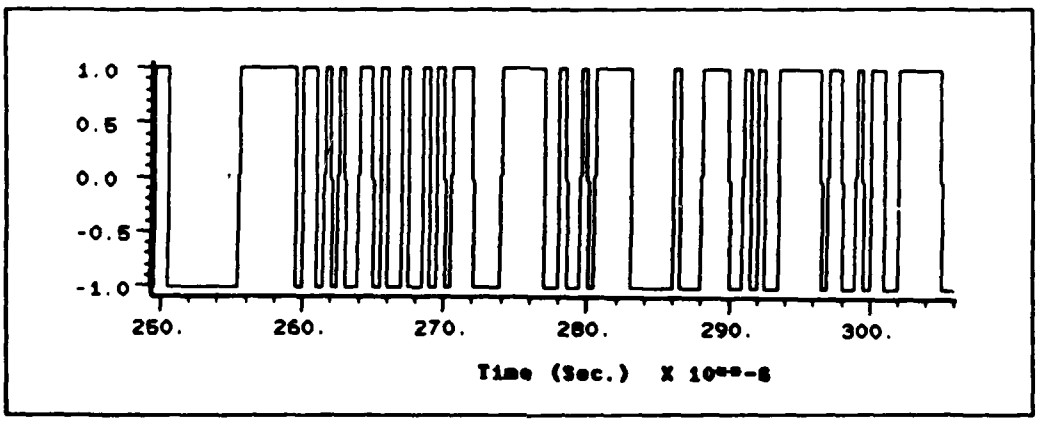

Figure 58. PN Generator Output

As a final check, the magnitude spectrum of the PN Generator output is given in Figure 59.

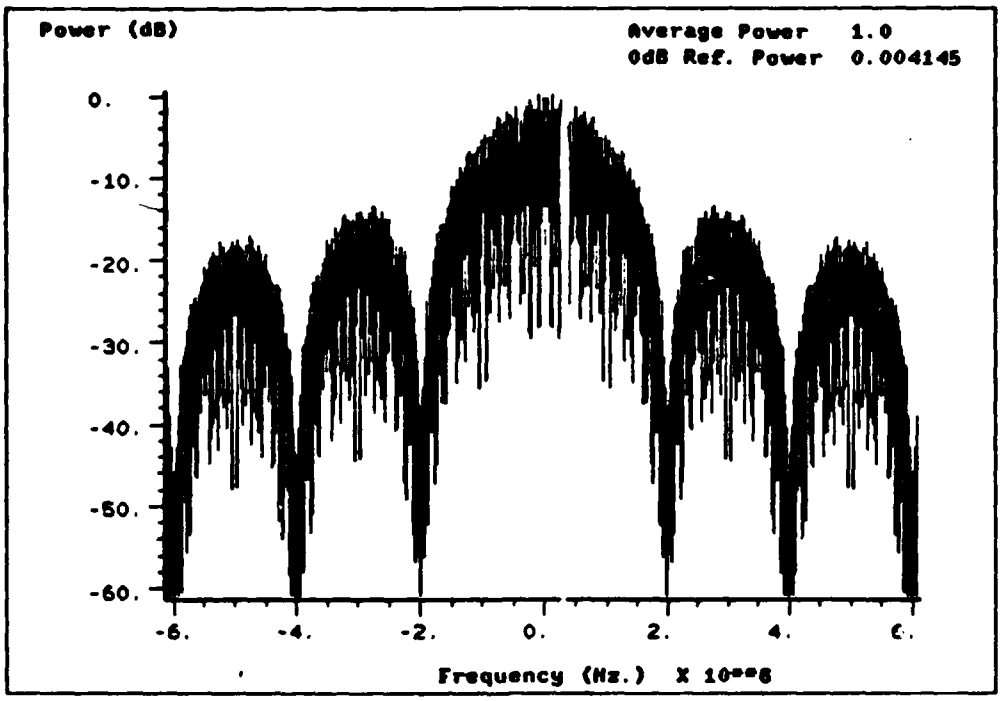

Figure 59. Magnitude Spectrum of the PN Output

QPSK Direct Sequence Transmitter

The transmitter output will be tested to confirm the carrier is properly modulated by the data and PN codes. The test system shown in Figure 60 is simply the transmitter with its output terminated into a sink module. Simulation probes are set to observe the transmitter output as well as the data and PN code inputs.

In order to present reasonable detail of the sinusoidal output, the sampling frequency is set for sixteen samples per carrier period. The carrier frequency is set at 4 MHz throughout the validations. The length of the simulation is influenced by the data rate. The STOP TIME is set to observe at least one data bit. Simulation parameters are given in Table 13.

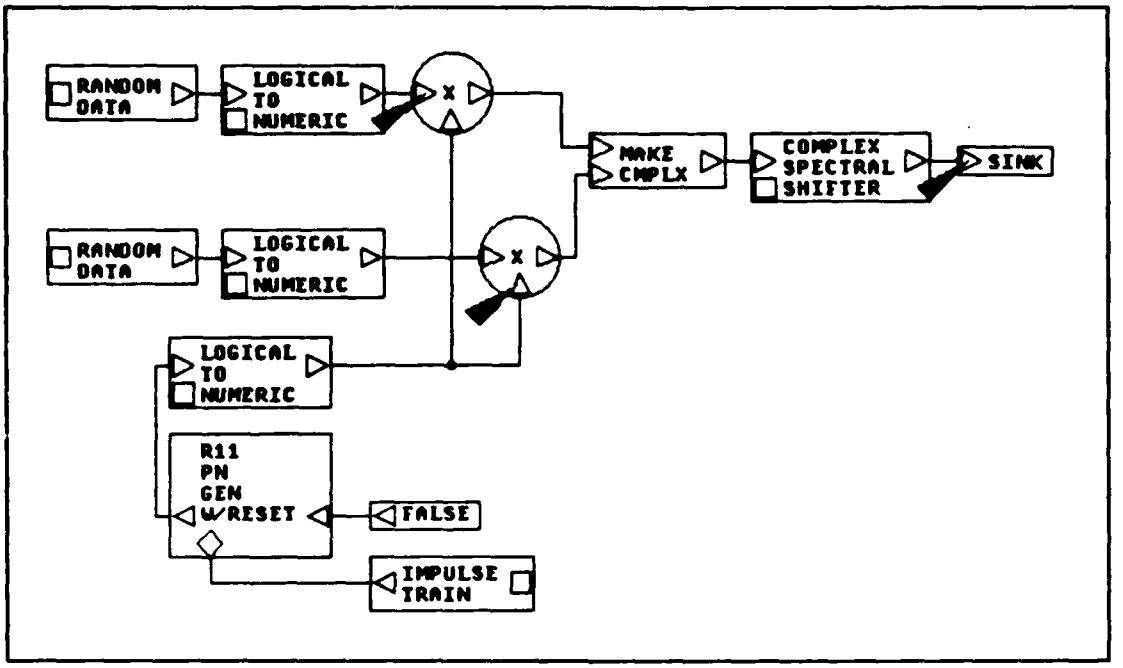

Figure 60. Transmitter Test System

Table 13. Transmitter Validation Parameters

STOP-TIME = 8.4999996E-4
DT = 1.5625e-8
CARRIER FREQUENCY (HZ) = 4.0e6
CHIP RATE (HZ) = 2.0e6
DATA RATE(HZ) = 1200

The transmitter output shown in Figure 61. The plot is overlayed with the PN code over the same interval shown in Figure 62. Carrier phase reversals occur coincident with the the PN code transitions. Over this time interval, a data bit transition also occurs. The phase reversal due to this transition is shown with an overlay of the data output in Figure 63.

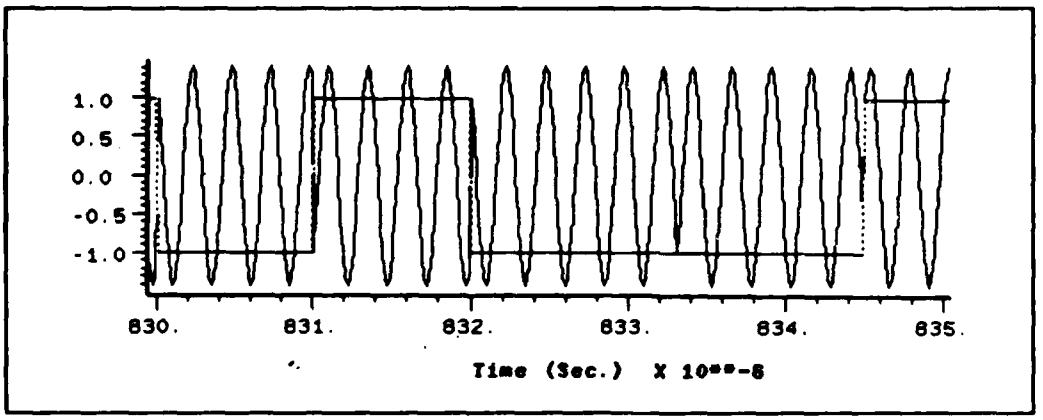

Figure 61. Transmitter Output

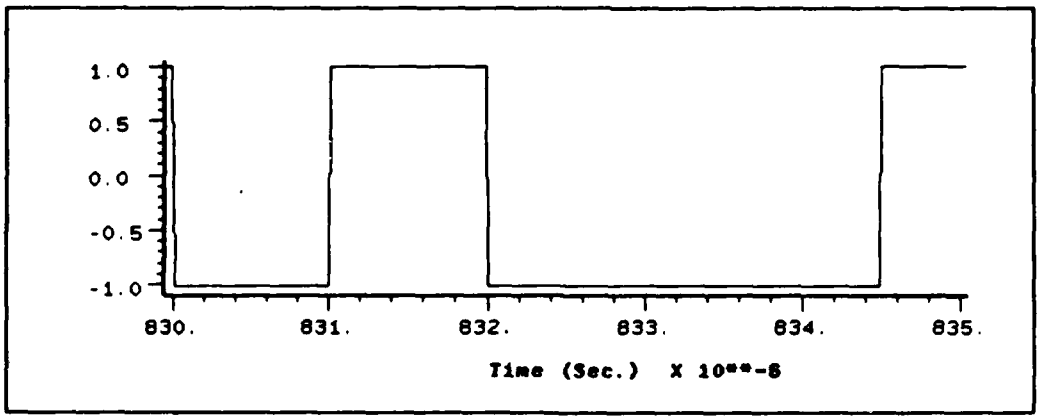

Figure 62. PN Code Output

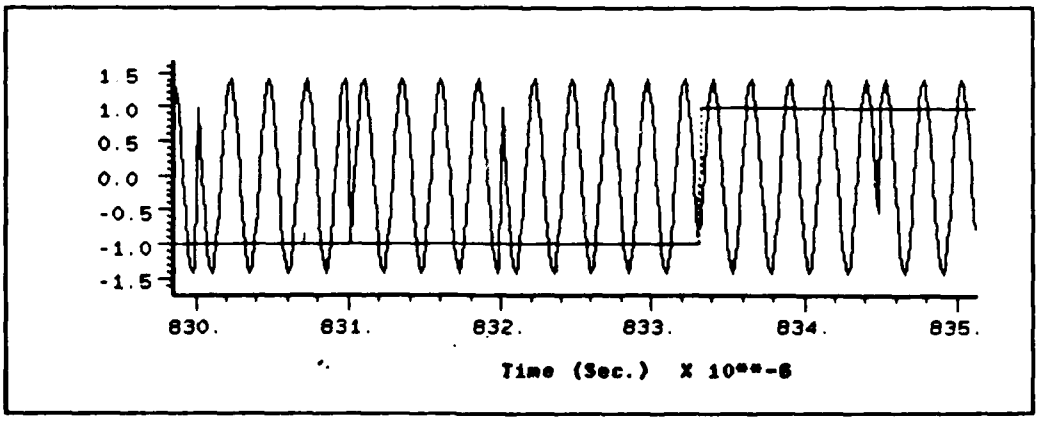

Figure 63. Transmitter Output

And finally, the magnitude spectrum of the transmitter output is shown in Figure 64. The spectrum is identical to that of the PN code except shifted by the value of the carrier frequency.

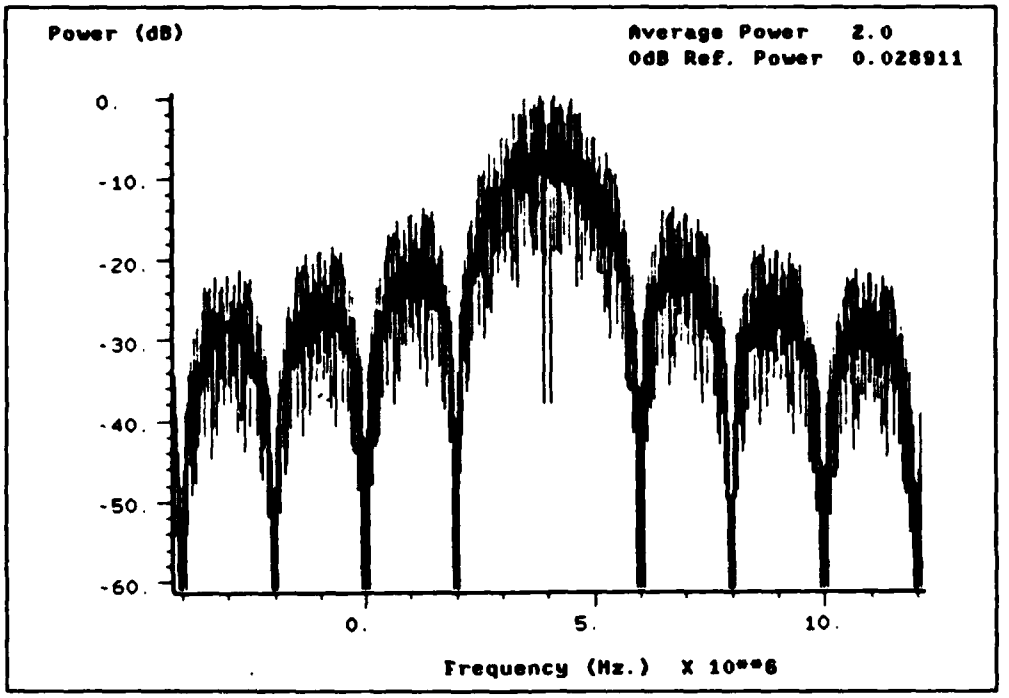

Figure 64. Magnitude Spectrum of the Transmitter Output

Matched Filter Channel

The matched filter channel is tested to confirm expected values for the matched filter, envelope detector, and accumulator output signals. The results for a matched filter length equal to 128 stages are given; however, additional simulations also confirmed outputs for matched filter lengths equal to 64, 256, 512, and 1024 stages.

The test system is the Single-User System shown previously in Figure 39. Probes are placed at the outputs of

the matched filter, envelope detector, and accumulator modules. The validation simulations were run without noise and set to run through three full PN code periods. The first period is dedicated to loading the matched filter reference sequence. The simulation parameters are given in Table 14 and the output of the matched filter at the end of the second PN code period is shown in Figure 65.

Table 14. Matched Filter Validation Parameters

STOP-TIME = 3.1E-3
DT = 6.25e-8
SNR (DB) = 10
NOISE ON-TIME = 3.1E-3
ACCUMULATOR THRESHOLD = 16000
OF MF STAGES = 128
DATA RATE(HZ) = 1200
CHIP RATE (HZ) = 2.0e6
CARRIER FREQUENCY (HZ) = 4.0e6

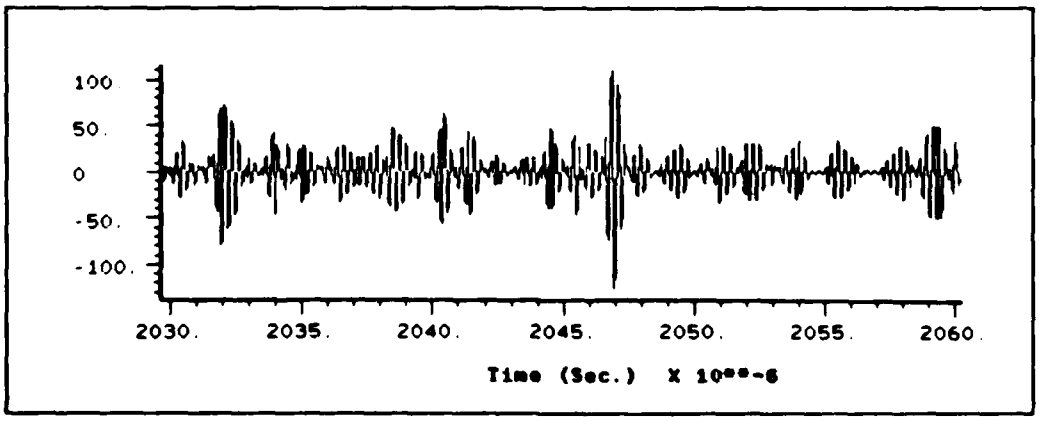

Figure 65. Matched Filter Output (Length = 128)

Figure 65 confirms that the expected amplitude of the main correlation peak is equal to the length of the filter. The output of the matched filter is envelope-detected through a

square-law device and a low-pass filter. The expected amplitude of the main correlation peak is the square of the matched filter length or $(128)^2 = 16,384$. The output of the envelope detector is shown in Figure 66.

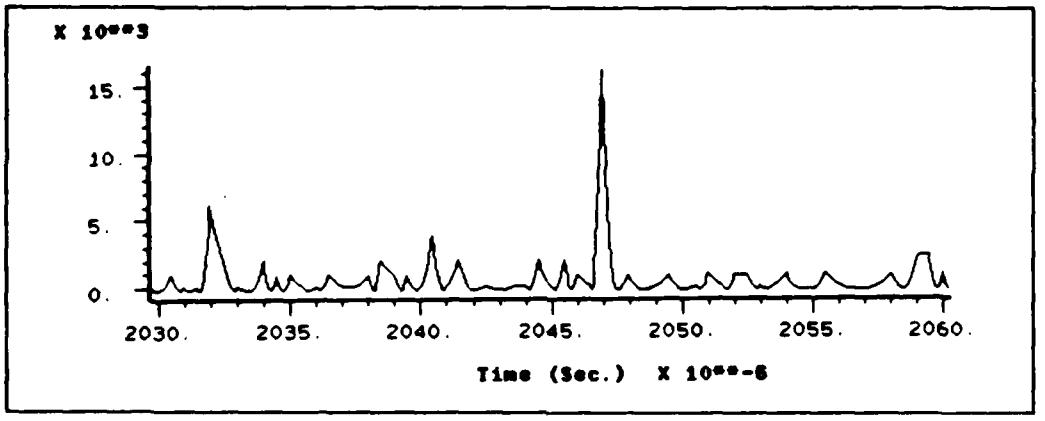

Figure 66. Envelope Detector Output

The output of the Accumulator is shown in Figures 67 and 68 for the end of the second and third PN code periods respectively. Note that the accumulated amplitude of the main correlation peak in Figure 68 is twice that shown in Figure 67. Also note that the noise due to the partial

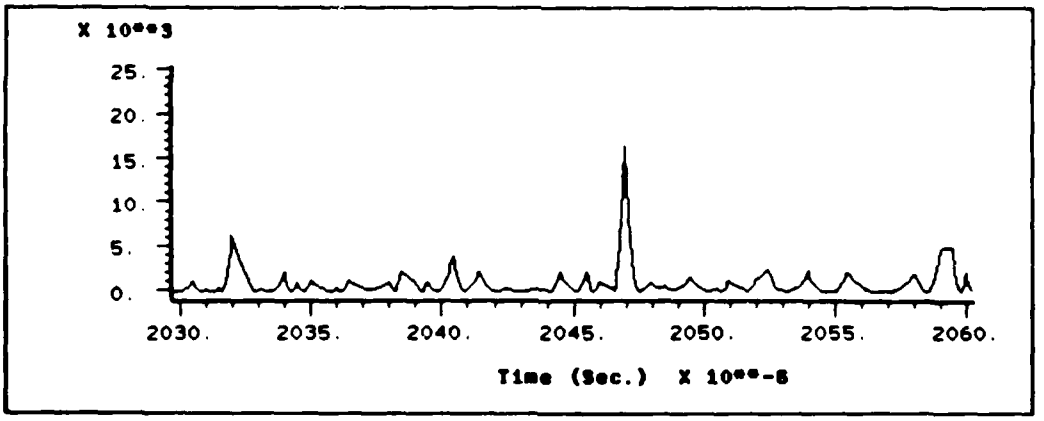

Figure 67. Accumulator Output

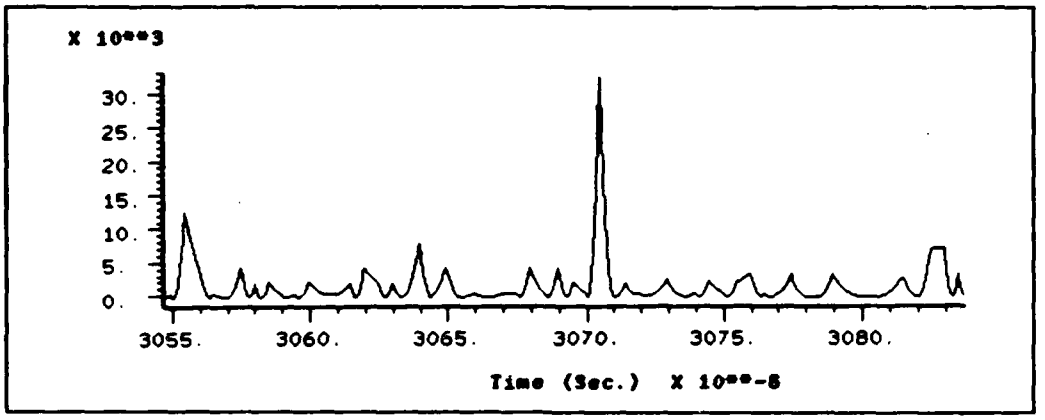

Figure 68. Accumulator Output

autocorrelation of the selected code adds linearly from one period to the next-this noise is not random. Similar results were obtained for matched filter lengths equal to 64, 256, 512, and 1024.

Quadrature Correlator

The Quadrature Correlator serves a specific purpose in the simulation effort. Once the Matched Filter Channel has initiated the Local Reference Generator, it is the correlator output that indicates successful synchronization to the incoming signal. The amplitude of the correlator output signal was determined in Chapter III and is repeated below:

$$Z_c(t) = 2\left[n \cdot R_{PN}(\tau)\right]^2 \qquad (20)$$

where $n = 2047$ is the number of chips in a complete PN code period. When synchronization occurs, $R_{PN}(\tau) = 1$ and $Z_c(t)$ reaches its maximum value of $8.380418 \cdot 10^6$.

The purpose of the validation simulation for the Quadrature Correlator is to determine output amplitudes under various conditions. The test system is shown in Figure 69.

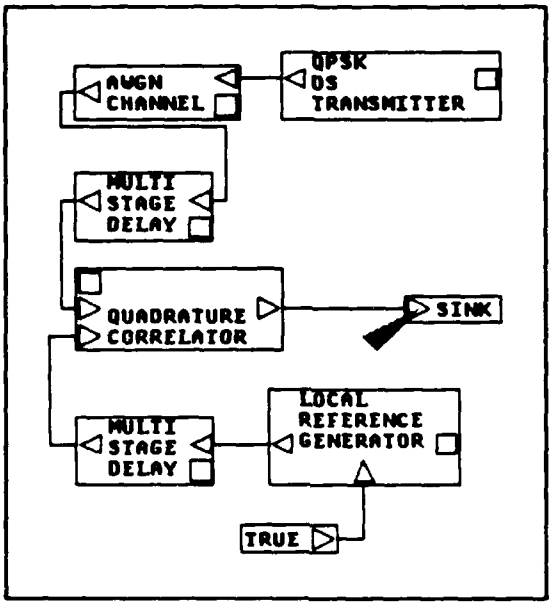

Figure 69. Correlator Output Test System

Simulations will determine output amplitudes for a synchronized correlator and for offsets between the local and incoming codes. The output amplitude for the synchronized correlator varies within a range and will not always match the expected maximum amplitude given in Eq (20). This is attributed to the method of integration used by the simulation model and the phase offsets that occur between the local and incoming carrier frequencies. The simulation model for the integrators use a trapezoidal approximation. The results of the simulations are given in Table 15. While there is an overlap in the output ranges between the offsets,

a clear distinction can be drawn for synchronization within a one-half chip period.

Table 15. Correlator Output Amplitudes

Code Offset (# Chips)	Output Amplitude Range
0	4.20e6 to 8.38e6
1/4	0.35e6 to 3.80e6
1/2	1.90e4 to 1.44e6
1	1.60e3 to 1.60e4
2	1.00e2 to 2.60e3

Bibliography

1. Shanmugan, Sam K. and others. "Block-Oriented Systems Simulator (BOSS)," 1986 IEEE Military Communications Conference, 3: 36.1.1-36.1.10 (October 1986).

2. Jeruchim, Michel C. and others. "Guest Editorial on Computer-Aided Modeling, Analysis, and Design of Communication Links: Introduction and Issue Overview," IEEE Journal on Selected Areas in Communications, Vol. 6, No.1: 1-4 (January 1988).

3. Smirnov, N.I. "Channel for Rapid Synchronization of a Multiple-Address System with Code Separation," Electrosvyaz': 67-75 (Publication of the A.S. Popov Society of Electronics and Communication Engineers of the USSR, June 1973).

4. BOSS (Block Oriented Systems Simulator) User's Manual, Version: ST*AR 1.1. ST*AR Corporation, Lawrence KA, 1986.

5. Palmer, Larry C. "Computer Modeling and Simulation of Communications Satellite Channels," IEEE Journal on Selected Areas in Communications, 2: 89-102 (January 1984).

6. Shanmugan, Sam K. and Victor S. Frost. "Simulation of Spread-Spectrum Systems Using ICCSM," IEEE Global Telecommunications Conference 1983, 3: 1612-1617 (December 1983).

7. Jeruchim, Michel C. "Techniques for Estimating the Bit Error Rate in the Simulation of Digital Communication Systems," IEEE Journal on Selected Areas in Communications, 2: 153-170 (January 1984).

8. Modestino, James W. and Kurt R. Matis. "Interactive Simulation of Digital Communication Systems," IEEE Journal on Selected Areas of Communications, 2: 51-76 (January 1984).

9. Shanmugan, Sam K. "Communication Systems Simulation, Review," IEEE International Conference on Systems, Man and Cybernetics 1983, 3: 323-326 (October 1983).

10. Pickholtz, R.L. et al. "Theory of Spread Spectrum Spectrum Communications - A Tutorial," IEEE Transactions on Communications, Vol.Com-30, No.5: 855-884 (May 1982).

11. Simon, M.K. et al. Spread Spectrum Communications, Vol. III. Rockville, MD: Computer Science Press, 1985.

12. Baier, W.P., M. Pandit, and H. Grammuller. "Combined Acquisition and Fine Synchronization System for Spread Spectrum Receivers Using a Tapped Delay Line Correlator," Proceedings AGARD Conference, No.230: 5.9.1-5.9.7 (1977).

13. Dixon, Robert C. Spread Spectrum Systems. New York: John Wiley and Sons, 1984.

14. Eichinger, B.O., R. Finsterer, and M. Kowatsch. "Convolver-Aided Synchronization in a Direct Sequence Spread Spectrum Communication System," Proceedings of IEEE 1986 Ultrasonics Symposium: 157-161.

15. Holmes, Jack K. Coherent Spread Spectrum Systems. New York: John Wiley and Sons, 1982.

16. Whalen, Anthony D. Detection of Signals in Noise. Florida: Academic Press Inc., 1971

17. Bhargava, V.K. et al. Digital Communications by Satellite. New York: John Wiley and Sons, 1981.

18. Oetting, John. "The Selection of Non-Repeating PN Codes for Code Division Multiple Access," 1985 IEEE Military Communications Conference, Vol. 3: 580-585.

19. Pachares, James. "A Table of Bias Levels Useful in Radar Detection Problems," IRE Transactions on Information Theory, Vol. IT-4: 38-45 (March 1958).

20. Eichinger, B.O. and M. Kowatsch. "Combined Matched Filter/Serial Search Acquisition Concept for Direct Sequence Systems," 1987 IEEE Military Communications Conference: 13.3.1-13.3.6.

21. Baier, W.P., K. Dostert, and M. Pandit. "A Novel Spread Spectrum Receiver Synchronization Scheme Using a SAW-Tapped Delay Line," IEEE Transactions on Communications: 1037-1047 (May 1982).

22. K. Dostert and M. Pandit. "Performance of a SAW -Tapped Delay Line in an Improved Synchronizing Circuit," IEEE Transactions on Communications, Vol. COM-30, No.1: 219-222 (January 1982).

VITA

Captain Fernando A. Morgan was born on [redacted] He graduated from Lakenheath American Highschool in 1971. In February 1976, he joined the United States Air Force and was trained as an Air Traffic Control Radar Technician. In 1981 he attended the University of Arizona under the Airman Education and Commissioning Program and received the degree of Bachelor of Science in Electrical Engineering. Upon graduation in December 1983, he attended Officer Training School and received his commission in March 1984. Following an assignment to the Directorate of Acquisition Logistics, Headquarters Air Force Communications Command, he entered the School of Engineering, Air Force Institute of Technology, in June 1987.

[redacted]

UNCLASSIFIED
SECURITY CLASSIFICATION OF THIS PAGE

REPORT DOCUMENTATION PAGE

Form Approved
OMB No. 0704-0188

1a. REPORT SECURITY CLASSIFICATION UNCLASSIFIED	1b. RESTRICTIVE MARKINGS
2a. SECURITY CLASSIFICATION AUTHORITY	3. DISTRIBUTION / AVAILABILITY OF REPORT Approved for public release; distribution unlimited.
2b. DECLASSIFICATION / DOWNGRADING SCHEDULE	
4. PERFORMING ORGANIZATION REPORT NUMBER(S) AFIT/GE/ENG/88D-31	5. MONITORING ORGANIZATION REPORT NUMBER(S)
6a. NAME OF PERFORMING ORGANIZATION School of Engineering 6b. OFFICE SYMBOL (If applicable) AFIT/ENG	7a. NAME OF MONITORING ORGANIZATION
6c. ADDRESS (City, State, and ZIP Code) Air Force Institute of Technology (AU) Wright-Patterson AFB, Ohio 54533-6583	7b. ADDRESS (City, State, and ZIP Code)
8a. NAME OF FUNDING / SPONSORING ORGANIZATION 8b. OFFICE SYMBOL (If applicable)	9. PROCUREMENT INSTRUMENT IDENTIFICATION NUMBER
8c. ADDRESS (City, State, and ZIP Code)	10. SOURCE OF FUNDING NUMBERS PROGRAM ELEMENT NO. / PROJECT NO. / TASK NO / WORK UNIT ACCESSION NO.
11. TITLE (Include Security Classification) See Box 19	
12. PERSONAL AUTHOR(S) Fernando A. Morgan, B.S.E.E., Capt, USAF	
13a. TYPE OF REPORT MS Thesis 13b. TIME COVERED FROM _____ TO _____ 14. DATE OF REPORT (Year, Month, Day) 1988 December 15. PAGE COUNT 116	
16. SUPPLEMENTARY NOTATION	

17. COSATI CODES			18. SUBJECT TERMS (Continue on reverse if necessary and identify by block number)
FIELD	GROUP	SUB-GROUP	Communication and Radio Systems, Spread Spectrum, Simulation, Block Oriented Systems Simulator (BOSS)
17	04	01	

19. ABSTRACT (Continue on reverse if necessary and identify by block number)

Title: ANALYSIS AND SIMULATION OF A PSEUDONOISE SYNCHRONIZATION SYSTEM

Thesis Chairman: Glenn E. Prescott, Major, USAF
Assistant Professor of Electrical Engineering

Approved for public release in accordance with AFR 190-1
12 Jan 1989

20. DISTRIBUTION / AVAILABILITY OF ABSTRACT ☒ UNCLASSIFIED/UNLIMITED ☐ SAME AS RPT. ☐ DTIC USERS	21. ABSTRACT SECURITY CLASSIFICATION UNCLASSIFIED
22a. NAME OF RESPONSIBLE INDIVIDUAL Glenn E. Prescott, Major, USAF	22b. TELEPHONE (Include Area Code) (513)255-3576 22c. OFFICE SYMBOL AFIT/ENG

DD Form 1473, JUN 86 *Previous editions are obsolete.*

SECURITY CLASSIFICATION OF THIS PAGE
UNCLASSIFIED

This study investigates the performance characteristics of a synchronization system that uses an auxiliary matched filter channel to speed acquisition time. Attention is focused on initial acquisition. The investigation takes the following approach: (1) Perform a quantitative analysis to characterize mean acquisition time under varying conditions of matched filter length, noise levels, and number of users in the system. (2) Build and validate a simulation model of the synchronization system using the Block Oriented Systems Simulator (BOSS). (3) Test the matched filter channel against the analytic expectations for false alarm performance via the simulation model.

The quantitative results indicate that the matched filter channel improves acquisition time. For signal-to-noise ratios above 0dB and a particular matched filter length, the mean acquisition time was directly a function of the number of users in the system. Mean acquisition time was significantly improved for signal-to-noise ratios above 0dB. As signal-to-noise ratios decrease below 0dB, thermal noise becomes the dominant influence. For signal-to-noise ratios below -18dB, mean acquisition time is a function of the noise level-irrespective of the number of users. Mean acquisition time asymptotically approaches a doubling in time for each 1.5dB decrease in the signal-to-noise ratio.

The simulation results confirmed the analytic expectations for false alarm performance of the matched filter channel. Exceptions were noted due to the high partial autocorrelation characteristics of the selected synchronization code. The Block Oriented Systems Simulator provided a highly flexible simulation environment. The successful static tests prove suitability of the model to accurately simulate dynamic applications of the system.